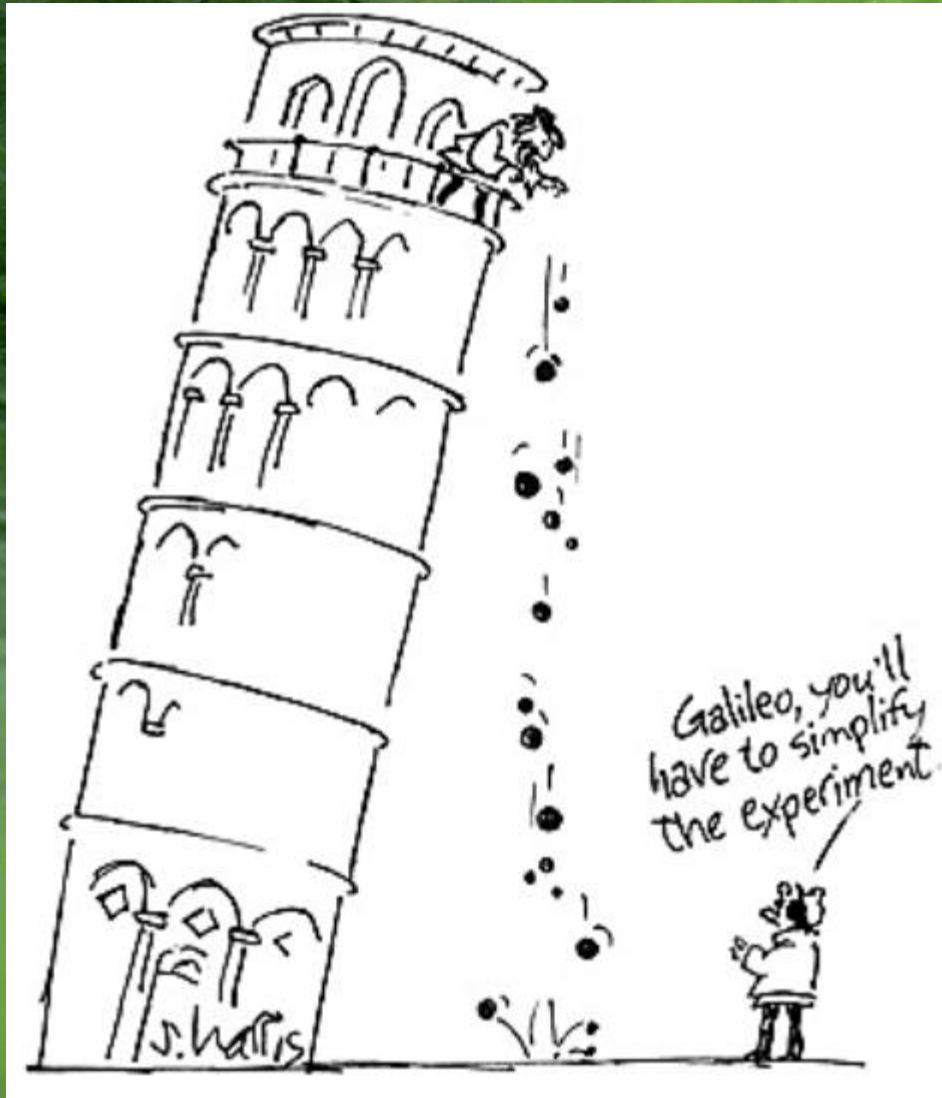


# Electric and Magnetic fields



Faculty of Physics UW

Jacek.Szczytko@fuw.edu.pl

# Homogenous magnetic field

The Landau gauge solution

$$\left\{ \frac{1}{2m} [\hat{p} - q \vec{A}(\vec{r}, t)]^2 + q\varphi(\vec{r}, t) + U(\vec{r}, t) \right\} \psi(\vec{r}, t) = i\hbar \frac{d}{dt} \psi(\vec{r}, t)$$

**Landau gauge:** magnetic field  $\vec{B} = (0, 0, B_z) \Rightarrow B_z = \frac{\partial A_y}{\partial x} - \frac{\partial A_x}{\partial y}$  (unfortunately distinguishes direction)

$$\vec{A} = [0, B_z x, 0] \text{ czyli } A_y = B_z x \stackrel{\text{def}}{=} Bx \quad q = -e$$

We assume that in a plane  $xy$  there is no other potential

$$\left\{ \frac{1}{2m} \left[ -\hbar^2 \frac{\partial^2}{\partial x^2} + \left( -i\hbar \frac{\partial}{\partial y} + eBx \right)^2 - \hbar^2 \frac{\partial^2}{\partial z^2} \right] + U(z) \right\} \psi(\vec{r}) = E\psi(\vec{r})$$

Which gives: 
$$\left[ -\frac{\hbar^2}{2m} \nabla^2 - \frac{ie\hbar}{m} Bx \frac{\partial}{\partial y} + \frac{(eBx)^2}{2m} + U(z) \right] \psi(\vec{r}) = E\psi(\vec{r})$$

The evidence of the Lorentz force

Parabolic potential!

# Homogenous magnetic field

$$\left[ -\frac{\hbar^2}{2m} \nabla^2 - \frac{ie\hbar}{m} Bx \frac{\partial}{\partial y} + \frac{(eBx)^2}{2m} + U(z) \right] \psi(\vec{r}) = E\psi(\vec{r})$$

Vector potential does not depend on  $y$ , we can assume the function of the form:

$$\psi(\vec{r}) = w(z)u(x) \exp(ik_y y)$$

$$\left[ -\frac{\hbar^2}{2m} \frac{d^2}{dx^2} + \frac{1}{2} m \omega_c^2 \left( x + \frac{\hbar k_y}{eB} \right)^2 \right] u(x) = \varepsilon u(x)$$

$$\omega_c = \left| \frac{eB}{m} \right|$$

$$R_c = \frac{v}{\omega_c} = \frac{\sqrt{2mE}}{|eB|}$$

Cyclotron frequency

Cyclotron radius (*gyroradius*)

$k_y$  wave vector. What interesting in  $\varepsilon$  THERE IS NO  $k_y$ .

The parabolic potential of the form of  $x_k = -\hbar k_y / eB$

# Homogenous magnetic field

$$\left[ -\frac{\hbar^2}{2m} \nabla^2 - \frac{ie\hbar}{m} Bx \frac{\partial}{\partial y} + \frac{(eBx)^2}{2m} + U(z) \right] \psi(\vec{r}) = E\psi(\vec{r})$$

Vector potential does not depend on  $y$ , we can assume the function of the form:

$$\psi(\vec{r}) = w(z)u(x) \exp(ik_y y)$$

$$\left[ -\frac{\hbar^2}{2m} \frac{d^2}{dx^2} + \frac{1}{2} m \omega_c^2 \left( x + \frac{\hbar k_y}{eB} \right)^2 \right] u(x) = \varepsilon u(x) \quad \omega_c = \left| \frac{eB}{m} \right| \quad R_c = \frac{v}{\omega_c} = \frac{\sqrt{2mE}}{|eB|}$$

Magnetic length:  $l_B = \sqrt{\frac{\hbar}{m\omega_c}} = \sqrt{\frac{\hbar}{|eB|}}$  does not depend on mass  $m$ , but ONLY on magnetic field  $B$ !

The typical value for  $B = 1.0$  T is  $l_B = 26$  nm.

Solutions  $\varepsilon_{nk} = \left( n - \frac{1}{2} \right) \hbar \omega_c$  (does not depend on  $k_y$ ).

$$\phi_{nk}(x, y) \propto H_{n-1} \left( \frac{x - x_k}{l_B} \right) \exp \left[ -\frac{(x - x_k)^2}{2l_B^2} \right] \exp(ik_y y)$$

$n = 1, 2, 3 \dots$  they are subsequent **Landau levels**.

# Homogenous magnetic field

## The 2D case:

Solutions  $\varepsilon_{nk} = \left(n - \frac{1}{2}\right) \hbar\omega_c + E_n$  (does not depend on  $k_y$ ;  $E_n$ - is any 2D energy).

$$\phi_{nk}(x, y) \propto H_{n-1}\left(\frac{x - x_k}{l_B}\right) \exp\left[-\frac{(x - x_k)^2}{2l_B^2}\right] \exp(ik_y y) \quad n = 1, 2, 3 \dots$$

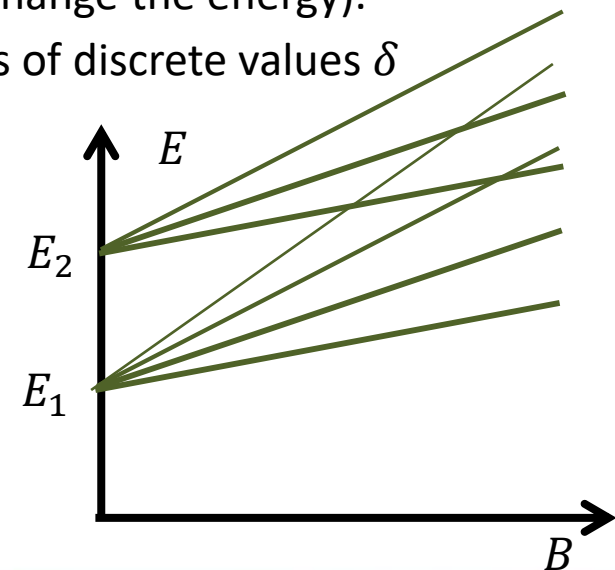
Wave functions are the functions of the oscillator (along  $x$ , of the order of  $l_B/\sqrt{2}$ ) and travelling waves (along  $y$ ) – weird, right? Why?

The energy does not depend on  $k$  vector – states of different  $k$  have the same energy, so they are degenerated (therefore any combination of them does not change the energy).

The density of states is reduced from the constant  $\frac{m}{\pi\hbar^2}$  to a series of discrete values  $\delta$  given by the equation of  $\varepsilon_{nk}$  - they are called **Landau levels**.

Full energy (including binding potential in  $z$  direction):

$$E = E_z + \varepsilon_{nk} = E_z + \left(n - \frac{1}{2}\right) \hbar\omega_c$$
$$n = 1, 2, 3 \dots$$





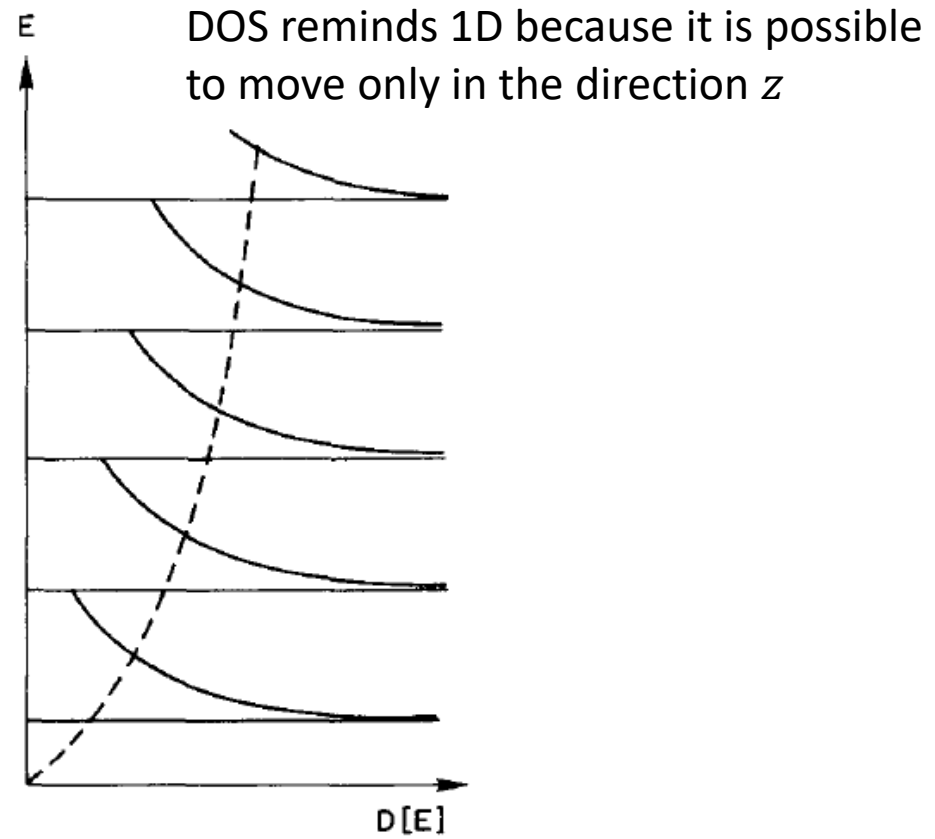
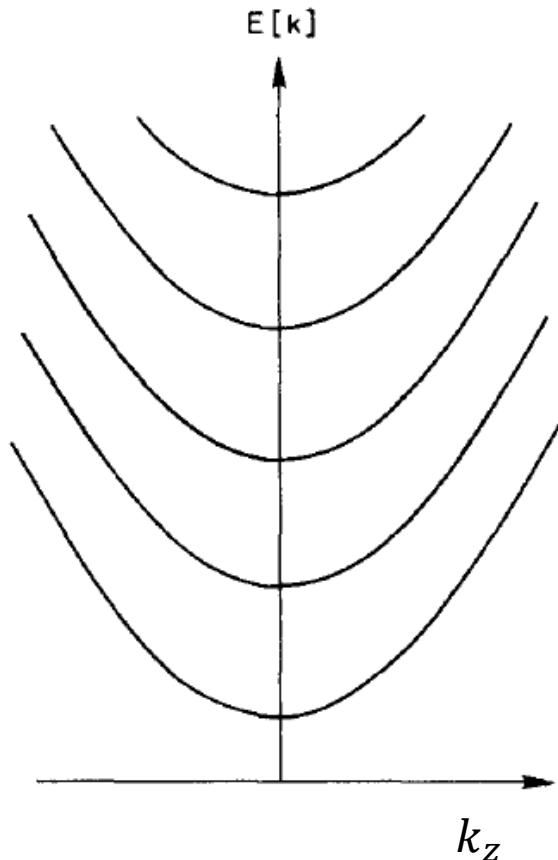
# Homogenous magnetic field

The 3D case (no  $U(z)$  potential)

Solution:

$$\varepsilon_{nk} = \left(n - \frac{1}{2}\right) \hbar\omega_c + \frac{\hbar^2 k_z^2}{2m^*}$$

$n = 1, 2, 3 \dots$  are subsequent Landau levels.



<http://www2.warwick.ac.uk/fac/sci/physics/current/postgraduate/regs/mpags/ex5/mag/>

# Homogenous magnetic field

The solution in the symmetric gauge:

$$\left\{ \frac{1}{2m} [\hat{p} - q \vec{A}(\vec{r}, t)]^2 + q\phi(\vec{r}, t) + U(\vec{r}, t) \right\} \psi(\vec{r}, t) = i\hbar \frac{d}{dt} \psi(\vec{r}, t)$$

**The symmetric gauge:** field  $\vec{B} = (0, 0, B_z) \Rightarrow A_\theta = \frac{1}{2} Br, A_r = 0, A_z = 0$

$$\left\{ -\frac{\hbar^2}{2m} \left[ \frac{\partial^2}{\partial r^2} + \frac{1}{r} \frac{\partial}{\partial r} + \frac{1}{r^2} \frac{\partial^2}{\partial \theta^2} \right] - \frac{i\hbar e B}{m} \frac{\partial}{\partial \theta} + \frac{e^2 B^2 r^2}{8m} + U(z) \right\} \psi(r, \theta, z) = E\psi(r, \theta, z)$$

This time a rotation angle  $\theta$  is the invariant, which can be associated with angular momentum and the function in the form of  $\exp(il\theta)$

$$\varepsilon_{nl} = \left( n + \frac{1}{2}l + \frac{1}{2}|l| - \frac{1}{2} \right) \hbar\omega_c \quad n = 1, 2, 3 \dots \quad l = 0, \pm 1, \pm 2, \pm 3 \dots$$

$$\phi_{nk}(r, \theta) \propto \exp(il\theta) \exp\left[-\frac{r^2}{4l_B^2}\right] r^{|l|} L_{n-1}^{(|l|)}\left(\frac{r^2}{2l_B^2}\right)$$

The symmetrical potential also has its drawbacks - where is the origin of ALL cyclotron orbits?

What are the solutions with negative sign?

Associate Laguerre polynomial

# Homogenous magnetic field

In a magnetic field, we cannot forget about spin!

Electron spin:  $\mu_B = \frac{e\hbar}{2m_0}$  (Bohr magneton = magnitude of the magnetic moment of the electron on the orbit of the total angular momentum  $1\hbar$ )

$$H' = \mu_B \vec{B} \underline{g} \hat{S}$$

In general g-factor may be the tensor

In the case of free electron  $g = 2,0023 \dots$ , but in the solid state it may have very different values (eg.  $g = -0.44$  in GaAs and  $g = +0.4$  in  $\text{Al}_{0.3}\text{Ga}_{0.7}\text{As}$ ).



# Homogenous magnetic field

**We return to the Landau gauge:**

Solutions  $\varepsilon_{nk} = \left(n - \frac{1}{2}\right) \hbar\omega_c + E_n$  (does not depend on  $k_y$ ;  $E_n$ - is any 2D energy).

$$\phi_{nk}(x, y) \propto H_{n-1}\left(\frac{x - x_k}{l_B}\right) \exp\left[-\frac{(x - x_k)^2}{2l_B^2}\right] \exp(ik_y y) \quad n = 1, 2, 3 \dots$$

**Question:** for a given  $n$  (i.e. Landau level) how many different states  $\phi_{nk}(x, y)$  of the same energy there are – i.e. what is the degeneration of the Landau levels?

Let's calculate how many different functions of quantum numbers  $k_y$  (only  $k_y$  counts, because in Landau gauge  $x_k$  depends only on  $k_y$ ) – similar considerations can be worked out in an arbitrary gauge.

# Homogenous magnetic field

**We return to the Landau gauge:**

Solutions  $\varepsilon_{nk} = \left(n - \frac{1}{2}\right) \hbar\omega_c + E_n$  (does not depend on  $k_y$ ;  $E_n$  - is any 2D energy).

$$\phi_{nk}(x, y) \propto H_{n-1}\left(\frac{x - x_k}{l_B}\right) \exp\left[-\frac{(x - x_k)^2}{2l_B^2}\right] \exp(ik_y y) \quad n = 1, 2, 3 \dots$$

**Question:** for a given  $n$  (i.e. Landau level) how many different states  $\phi_{nk}(x, y)$  of the same energy there are – i.e. what is the degeneration of the Landau levels?

Let's calculate how many different functions of quantum numbers  $k_y$  (only  $k_y$  counts, because in Landau gauge  $x_k$  depends only on  $k_y$ ) – similar considerations can be worked out in an arbitrary gauge.

What is the number of states per one level? The sample  $S = L_x \times L_y$ , in the Landau gauge for  $y$  coordinate we have plane wave condition  $k = (2\pi/L_y)n_y$  (where  $n_y$  is an integer number).

**How many states of different  $n_y$  there are?**

For  $x$  coordinate the wavefunction is centered in  $x_k = -\frac{\hbar k}{eB} = -(2\pi\hbar n_y/eBL_y)$ .

If  $n_y$  is too large then  $x_k$  can be outside the sample – no harmonic force, no harmonic solution.

# Landau levels

The solution of the Schrödinger equation in a magnetic field gives a discrete spectrum.

What is the number of states per one level? The sample  $S = L_x \times L_y$ , in the Landau gauge for  $y$  coordinate we have plane wave condition  $k = (2\pi/L_y)n_y$  (where  $n_y$  is an integer number).

For  $x$  coordinate the wavefunction is centered in  $x_k = -\frac{\hbar k}{eB} = -(2\pi\hbar n_y/eBL_y)$ .

The condition for  $x_k$  to be in the sample (rather than outside):

$$-L_x < \frac{2\pi\hbar n_y}{eBL_y} < 0 \quad \text{czyli} \quad 0 < n_y < \frac{eB}{h} L_x L_y = n_B S \quad (\text{the absolute value})$$

There is no factor 2 associated with the degeneracy of the spin (because spin in the magnetic field is not degenerated)

The dimension of  $n_B = \frac{eB}{h}$  is "amount" per unit area

$n_B = \frac{eB}{h}$  The degeneration of Landau levels – is the number of allowed states for each of the Landau level per unit area – **it increases with increasing field  $B$**

# Landau levels


The solution of the Schrödinger equation in a magnetic field gives a discrete spectrum.

What is the number of states per one level? The sample  $S = L_x \times L_y$ , in the Landau gauge for  $y$  coordinate we have plane wave condition  $k = (2\pi/L_y)n_y$  (where  $n_y$  is an integer number).

For  $x$  coordinate the wavefunction is centered in  $x_k = -\frac{\hbar k}{eB} = -(2\pi\hbar n_y/eBL_y)$ .

The condition for  $x_k$  to be in the sample (rather than outside):

$$-L_x < \frac{2\pi\hbar n_y}{eBL_y} < 0 \quad \text{czyli} \quad 0 < n_y < \frac{eB}{h} L_x L_y = n_B S = \frac{e}{h} BS = \frac{\Phi}{\Phi_0}$$

flux  $\Phi_0 = \frac{h}{e} = 4.135667516 \times 10^{-15} \text{ Wb} \quad [\text{Wb}] = [\text{T m}^2]$  

The magnetic flux quantum (pol. *flukson*) (In a superconductor  $h/2e$ , so this is not a „quantum”)

$\Phi = BS$  the total magnetic flux in the sample  $S = L_x \times L_y$

$$0 < n_y \Phi_0 < \Phi$$

The amount of allowed states is related to the amount of magnetic flux quanta passing through the sample!

# Local density of states

The density of states (in general) can be defined as:

$$N(E) = \sum_n \delta(E - \varepsilon_n)$$

After integration

$$\int_{E_1}^{E_2} N(E) dE = \int_{E_1}^{E_2} \sum_n \delta(E - \varepsilon_n) dE = \sum_n \int_{E_1}^{E_2} \delta(E - \varepsilon_n) dE$$

For instance:

$$N^{1D}(E) = \sum_k \delta(E - \varepsilon(k)) = \int \frac{1}{E'(k)} \delta(k - k') 2 dk = \frac{1}{\pi} \sqrt{\frac{2m}{E}}$$

$$N^{2D}(E) = \sum_k \delta(E - \varepsilon(k)) = \int \frac{1}{E'(k)} \delta(k - k') 2\pi k dk = \frac{m}{\pi \hbar^2}$$

$$N^{3D}(E) = \sum_k \delta(E - \varepsilon(k)) = \int \frac{1}{E'(k)} \delta(k - k') 4\pi k^2 dk = \frac{1}{2\pi^2} \left(\frac{2m}{\hbar^2}\right)^{3/2} \sqrt{E}$$

On exercises



# Landau levels

$$N^{2D}(E) = \frac{m}{\pi\hbar^2}$$

Broadening of levels due to the scattering  $\Gamma = \hbar/\tau_i$

$\tau_i$  this is single-particle (or quantum) lifetime – this is NOT the same time, which we discussed with Drude model (transport lifetime)

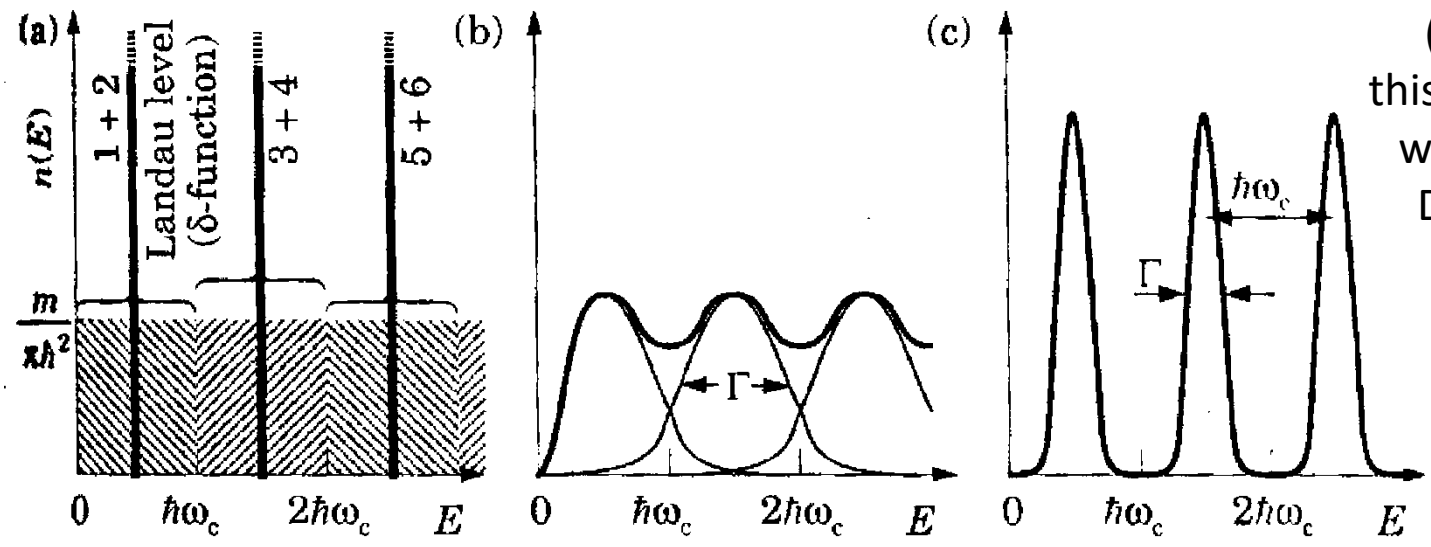


**FIGURE 6.7.** Density of states in a magnetic field, neglecting spin splitting. (a) The states in each range  $\hbar\omega_c$  are squeezed into a  $\delta$ -function Landau level. (b) Landau levels have a non-zero width  $\Gamma$  in a more realistic picture and overlap if  $\hbar\omega_c < \Gamma$ . (c) The levels become distinct when  $\hbar\omega_c > \Gamma$ .

Counting 2 spins: 
$$2n_B = \frac{2eB}{h} = \frac{2m\omega_c}{2\pi\hbar} = \frac{m}{\pi\hbar^2} \hbar\omega_c$$

Each of the states on the Landau level occupies an area  $\frac{h}{eB} = 2\pi l_B^2$

$$l_B = \sqrt{\frac{\hbar}{m\omega_c}} = \sqrt{\frac{\hbar}{|eB|}}$$

# Landau levels

$n_B = \frac{eB}{h}$  The degeneration of Landau levels – is the number of allowed states for each of the Landau level per unit area – **it increases with increasing field  $B$**

The carrier concentration in 2D:  $n_{2D}$  – on how many Landau levels these carriers can be hold?

Filling factor  $\nu$  (*współczynnik wypełnienia*) – usually this is not an integer

$$\nu = \frac{n_{2D}}{n_B} = \frac{hn_{2D}}{eB} = \frac{\Phi_0 n_{2D}}{B} = 2\pi l_B^2 n_{2D} \quad (\text{taking into account the spin degeneracy})$$

Increasing the magnetic field we are successively filling the Landau levels. You can completely fill  $n$ -th level ( $\nu = n$ ) and then  $B_n = hn_{2D}/en$ , until we reach  $n = 1$ , i.e. all electrons are at the same Landau level (ie. the *quantum limit*).

For  $\nu < 1$  interesting things happens (which'll be right back!)

# Landau levels

$n_B = \frac{eB}{h}$  The degeneration of Landau levels – is the number of allowed states for each of the Landau level per unit area – **it increases with increasing field  $B$**

The carrier concentration in 2D:  $n_{2D}$  – on how many Landau levels these carriers can be hold?

Filling factor  $\nu$  (*współczynnik wypełnienia*) – usually this is not an integer

$$\nu = \frac{n_{2D}}{n_B} = \frac{hn_{2D}}{eB} = \frac{\Phi_0 n_{2D}}{B} = 2\pi l_B^2 n_{2D} \quad (\text{taking into account the spin degeneracy})$$

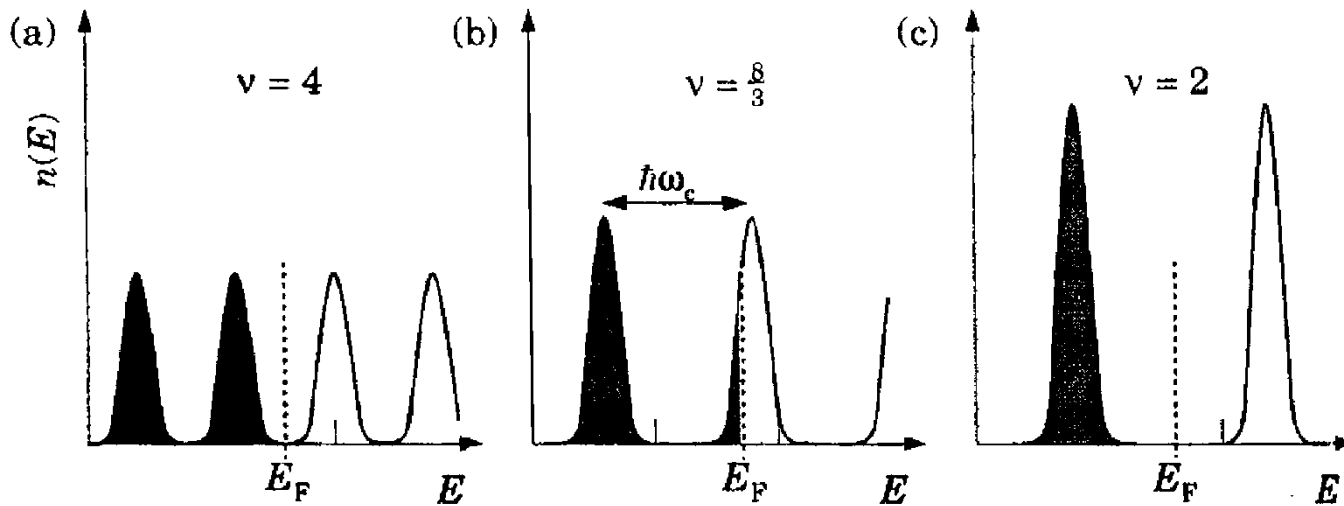


**FIGURE 6.8.** Occupation of Landau levels in a magnetic field neglecting the spin splitting, showing how the Fermi level moves to maintain a constant density of electrons. The fields are in the ratio 2 : 3 : 4 and give  $\nu = 4$ ,  $\frac{8}{3}$ , and 2.

# Landau levels

The Fermi level lies **between** Landau levels - there is no DOS, change of  $E_F$  does not change DOS –incompressible states (*stany nieściśliwe*)

The Fermi level lies **inside** the Landau level – large DOS, change of  $E_F$  strongly affects the DOS – *compressible states* (*stany ściśliwe*)

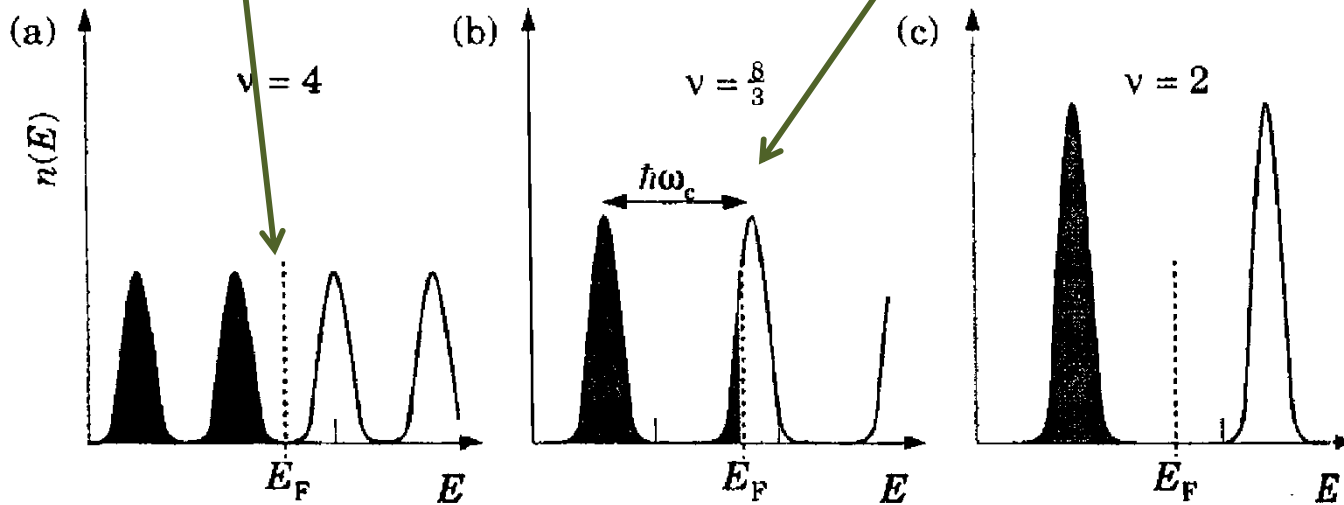


**FIGURE 6.8.** Occupation of Landau levels in a magnetic field neglecting the spin splitting, showing how the Fermi level moves to maintain a constant density of electrons. The fields are in the ratio 2 : 3 : 4 and give  $\nu = 4, \frac{8}{3},$  and 2.

# Landau levels

The Fermi level in the magnetic field:

$$\nu = \frac{n_{2D}}{n_B} = \frac{hn_{2D}}{eB} = \frac{\Phi_0 n_{2D}}{B} = 2\pi l_B^2 n_{2D}$$

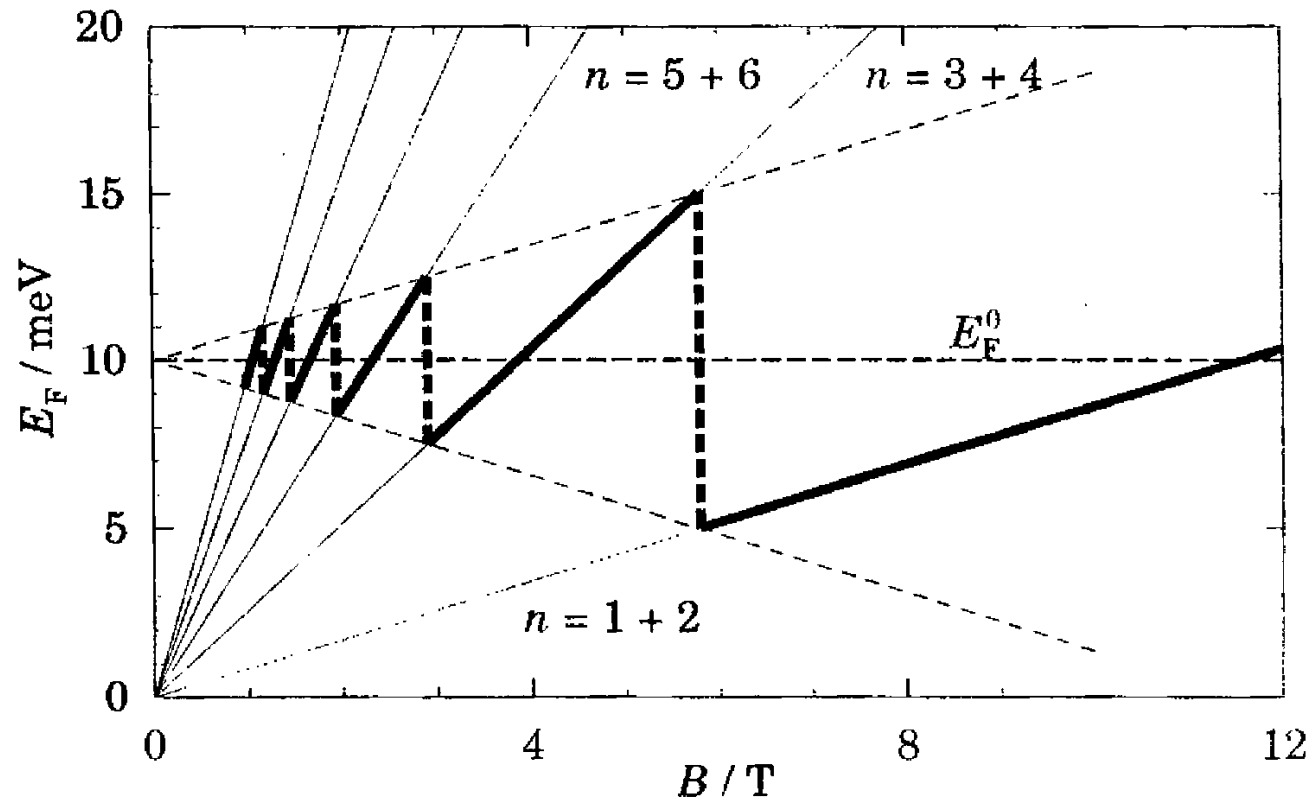


**FIGURE 6.9.** Variation of the Fermi level as a function of magnetic field for a two-dimensional electron gas in GaAs with  $E_F^0 = 10$  meV before the field was applied. Spin splitting is neglected. The fan of thin lines shows the Landau levels, while the discontinuous thick line is  $E_F$ .



# Landau levels

The Fermi level in the magnetic field:

$$\nu = \frac{n_{2D}}{n_B} = \frac{hn_{2D}}{eB} = \frac{\Phi_0 n_{2D}}{B} = 2\pi l_B^2 n_{2D}$$

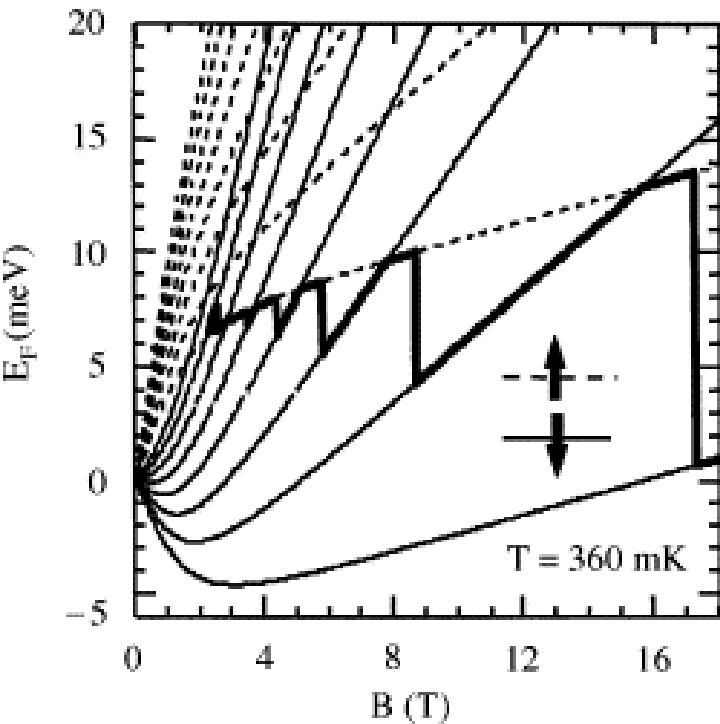


Fig. 16. Landau level fan diagram for the magnetic 2DEG sample described in [Fig. 15](#). Solid (dashed) lines correspond to spin-down (spin-up) states. The dark solid line shows the variation of the Fermi energy with magnetic field. Parameters used in this calculation are:  $E_F=7$  meV at  $B=0$ , and  $T=360$  mK. The spin-splitting parameters used are obtained by fitting the magneto-optical data in [Fig. 3](#):  $T_0=2.1$  K and a saturation conduction band spin splitting of 12.9 meV.

*Spin dynamics and quantum transport in magnetic semiconductor quantum structures*

D.D Awschalom, N. Samarth, *Journal of Magnetism and Magnetic Materials* **200** (1999) 130-147

# Shubnikov-de Haas effect

## Shubnikov-de Haas effect

### 9.4.1 Types of quantum oscillation

As the electronic density of states at  $E_F$  determines most of a metal's properties, virtually all properties will exhibit quantum oscillations in a magnetic field. Examples include<sup>7</sup>

- oscillations of the magnetisation (the de Haas–van Alphen effect);
- oscillations of the magnetoresistance (the Shubnikov–de Haas effect);
- oscillations of the sample length;
- oscillations of the sample temperature;
- oscillations in the ultrasonic attenuation;
- oscillations in the Peltier effect and thermoelectric voltage;
- oscillations in the thermal conductivity.

---

<sup>6</sup>However, open orbits do lead to a very interesting quantum phenomenon which has recently been observed in high-frequency experiments; see A. Ardavan *et al.*, *Phys. Rev. B* **60**, 15500 (1999); *Phys. Rev. Lett.* **81**, 713 (1998).

<sup>7</sup>Some pictures of typical data are shown in *Solid State Physics*, by N.W Ashcroft and N.D. Mermin (Holt, Rinehart and Winston, New York 1976) pages 266-268.

# Shubnikov-de Haas effect

## Shubnikov-de Haas effect

Density of states oscillates - falls to 0 for  $\nu = n$  and is highest for  $\nu \approx n + \frac{1}{2}$  - the easiest measurement is the magnetoresistance  $R_{xx}$ .

Oscillations depend on the ratio of the Fermi energy  $E_F$  to the cyclotron frequency  $\hbar\omega_c = eB/m^*$ . Oscillations are periodic in  $1/B$ .

$$\nu = \frac{n_{2D}}{n_B} = \frac{\hbar n_{2D}}{eB} = \frac{\Phi_0 n_{2D}}{B} = 2\pi l_B^2 n_{2D}$$

From SdH we can determine the effective mass  $m^*$  and quantum time  $\tau_q$ . The amplitude of oscillation is given by

$$\Delta\rho_{SdH} = 4\rho_0\delta \cos(4\pi\nu) \frac{\xi(T)}{\sinh(\xi(T))} \exp\left(-\frac{\pi}{\omega_c\tau_q}\right)$$

$$\xi(T) = 2\pi^2 kT / \hbar\omega_c$$

Temperature dependence gives  $m^*$ , damping  $\tau_q$ .

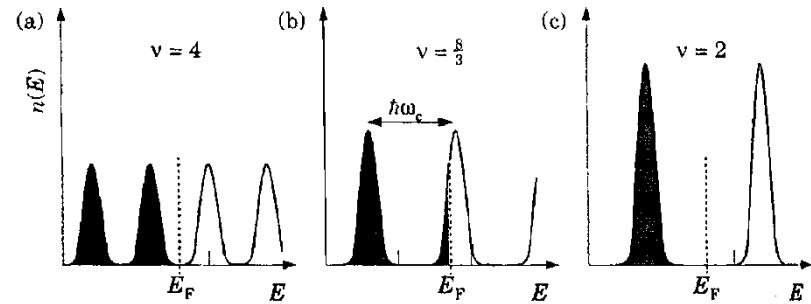
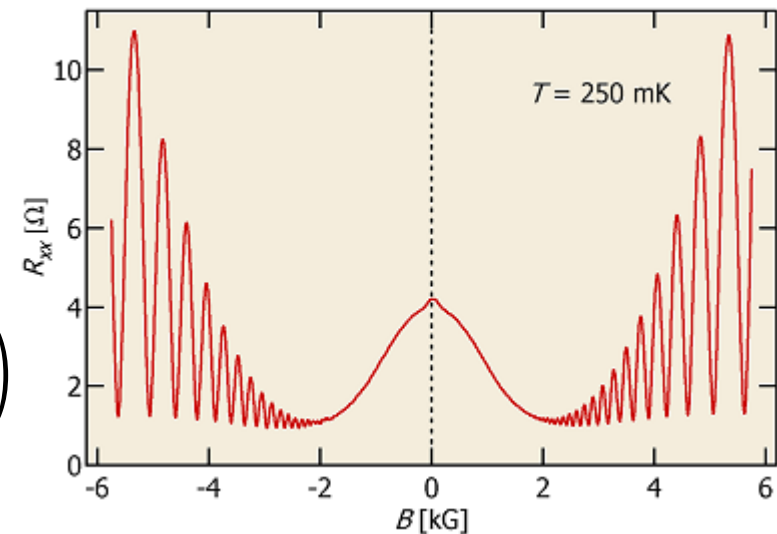


FIGURE 6.8. Occupation of Landau levels in a magnetic field neglecting the spin splitting, showing how the Fermi level moves to maintain a constant density of electrons. The fields are in the ratio 2 : 3 : 4 and give  $\nu = 4, \frac{8}{3},$  and 2.



<http://groups.physics.umn.edu/zudovlab/content/sdho.htm>

# Shubnikov-de Haas effect

## Shubnikov-de Haas effect

Density of states oscillates - falls to 0 for  $\nu = n$  and is highest for  $\nu \approx n + \frac{1}{2}$  - the easiest measurement is the magnetoresistance  $R_{xx}$ .

Oscillations depend on the ratio of the Fermi energy  $E_F$  to the cyclotron frequency  $\hbar\omega_c = eB/m^*$ .

Oscillations are periodic in  $1/B$ .

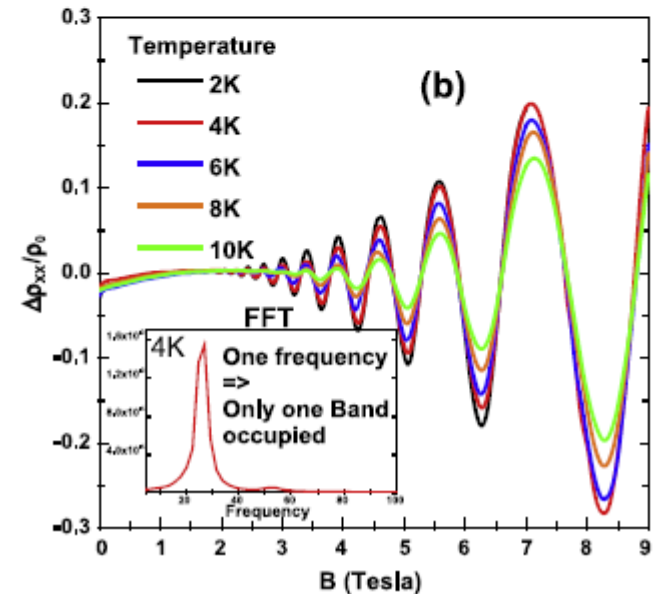
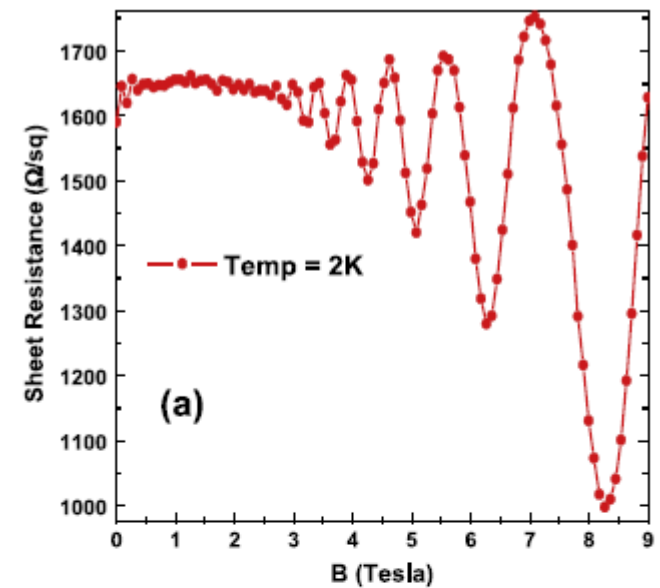
$$\nu = \frac{n_{2D}}{n_B} = \frac{\hbar n_{2D}}{eB} = \frac{\Phi_0 n_{2D}}{B} = 2\pi l_B^2 n_{2D}$$

From SdH we can determine the effective mass  $m^*$  and quantum time  $\tau_q$ . The amplitude of oscillation is given by

$$\Delta\rho_{SdH} = 4\rho_0\delta \cos(4\pi\nu) \frac{\xi(T)}{\sinh(\xi(T))} \exp\left(-\frac{\pi}{\omega_c\tau_q}\right)$$

$$\xi(T) = 2\pi^2 kT / \hbar\omega_c$$

Temperature dependence gives  $m^*$ , damping  $\tau_q$ .

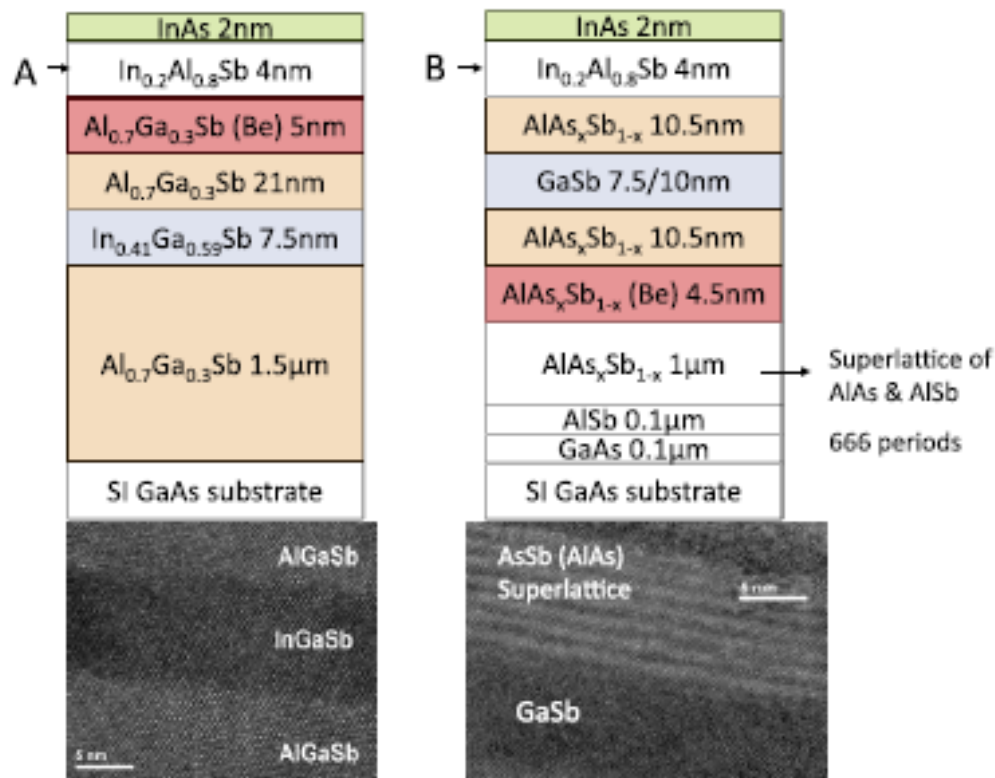


A. Nainani et al. Solid-State Electronics 62 (2011) 138–141

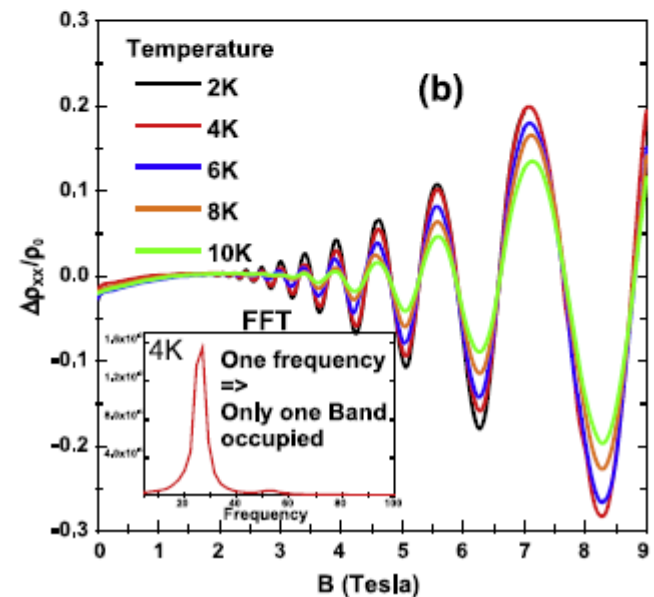
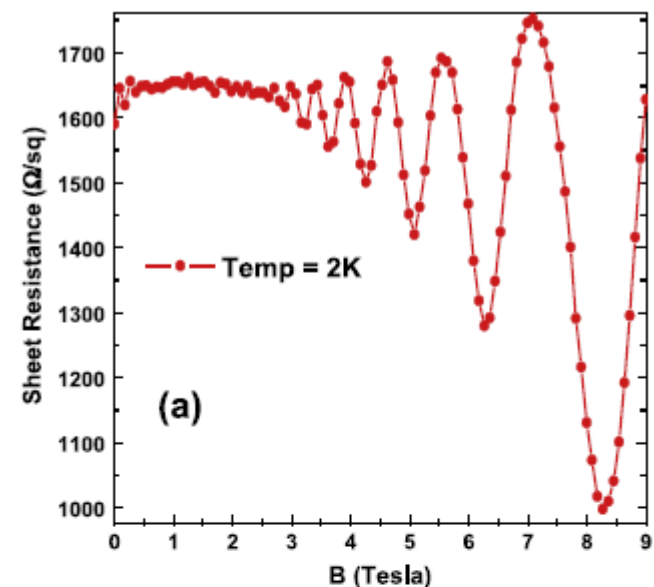


# Shubnikov-de Haas effect

## Shubnikov-de Haas effect



**Fig. 1.** Cross-section showing the layer details in a quantum well heterostructure with (A)  $\text{In}_x\text{Ga}_{1-x}\text{Sb}$  and (B) GaSb channel. The  $\text{AlAs}_x\text{Sb}_{1-x}$  layers are composed of AlSb/AlAs short-period superlattices. Also shown are high resolution TEM images around the channel region.





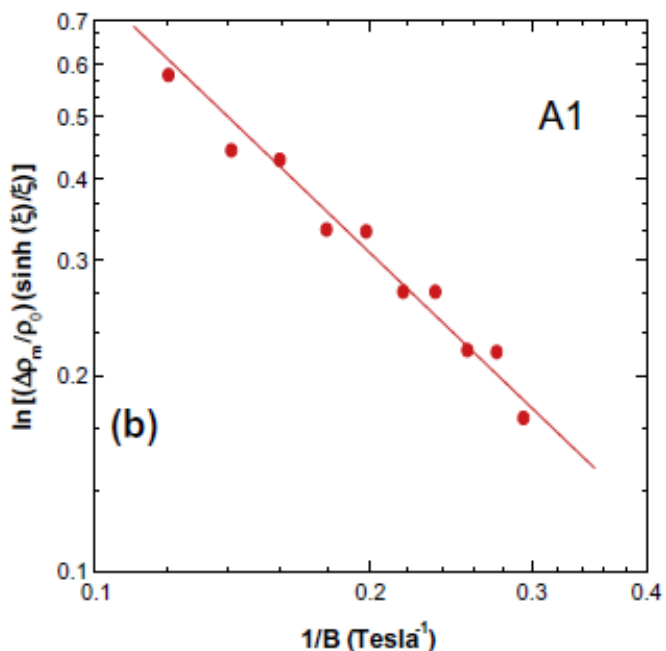
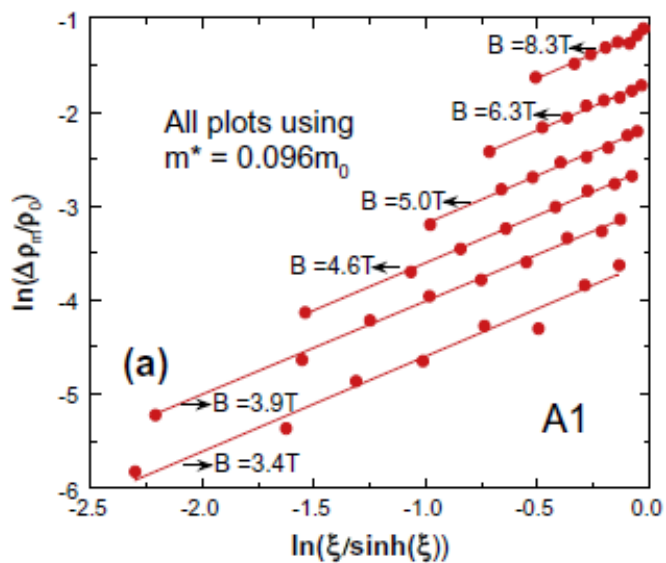
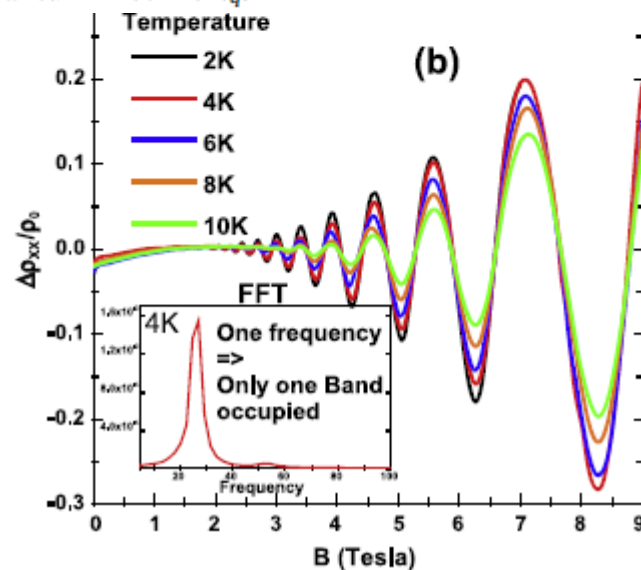
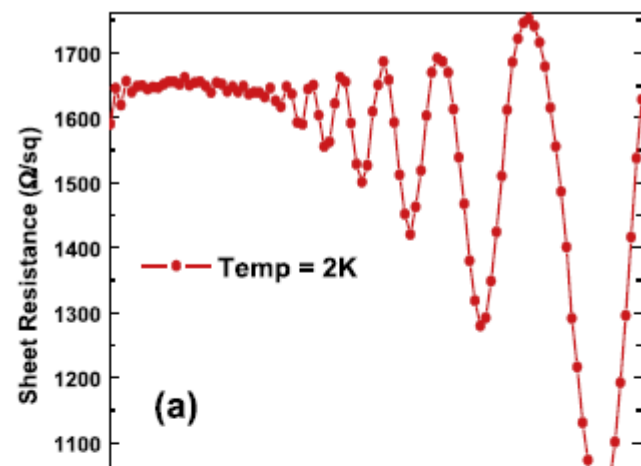


Fig. 3. (a) Effective hole mass is calculated using the temperature dependence of the oscillations as the value for which a gradient of unity is obtained in the plot of  $\ln\left(\frac{\Delta\rho_p}{\rho_0}\right)$ , vs.  $\ln\left(\frac{\xi}{\sinh\xi}\right)$ . (b) Dingle plot: Slope of line is  $-\pi\alpha/\mu$  where  $\alpha$  is the ratio  $\tau/\tau_q$  of the transport time  $\tau$  to the quantum lifetime  $\tau_q$ .

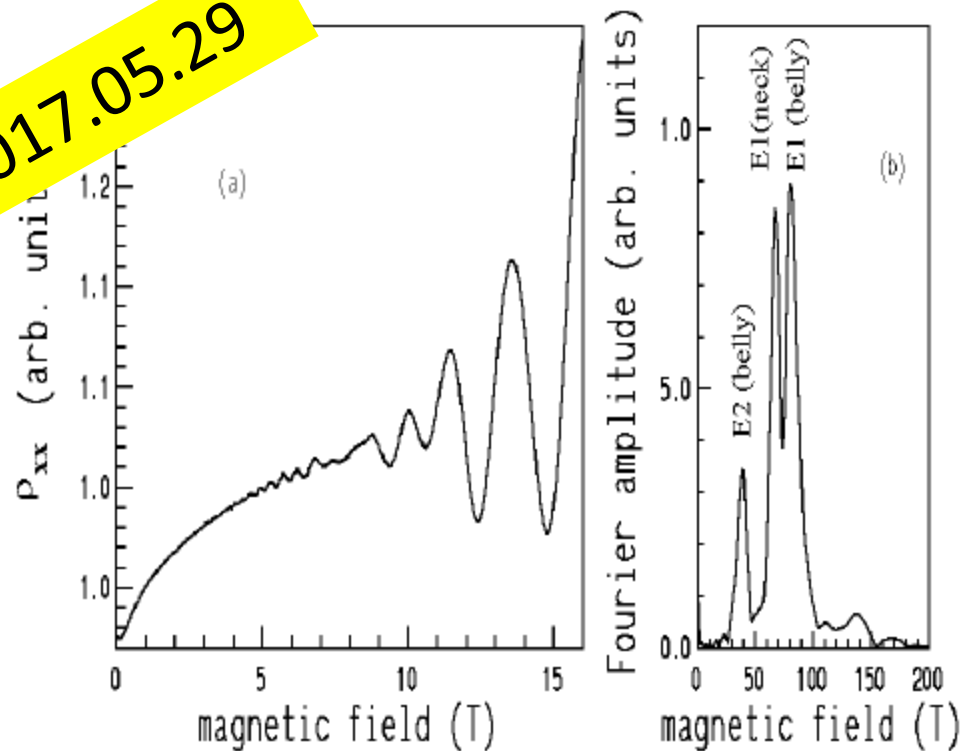
$$\xi(T) = 2\pi^2 T / \omega_c$$



# Shubnikov-de Haas effect

Shubnikov-de Haas effect

Tutaj 2017.05.29



15 period multiple quantum well structure composed of a 50Å thick lattice matched InGaAs quantum well and a 50Å thick InP barrier.

Figure 1. Shubnikov-de Haas oscillations (a) and its Fourier transform (b) measured at 4.2K for sample No.326.

Henriques et al. Brazil. J. of Phys. 29, 707 (1999)

# Shubnikov-de Haas effect

## Shubnikov-de Haas effect

Density of states oscillates - falls to 0 for  $\nu = n$  and is highest for  $\nu \approx n + \frac{1}{2}$  - the easiest measurement is the magnetoresistance  $R_{xx}$ .

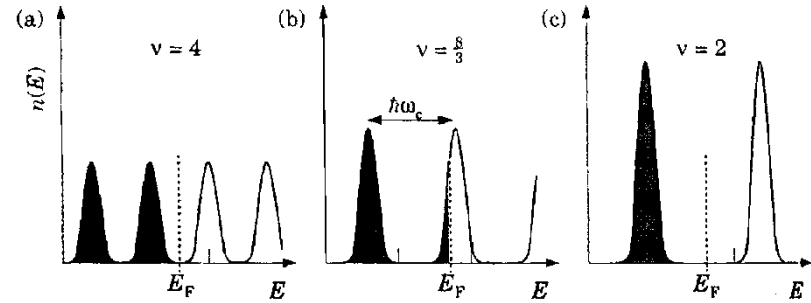
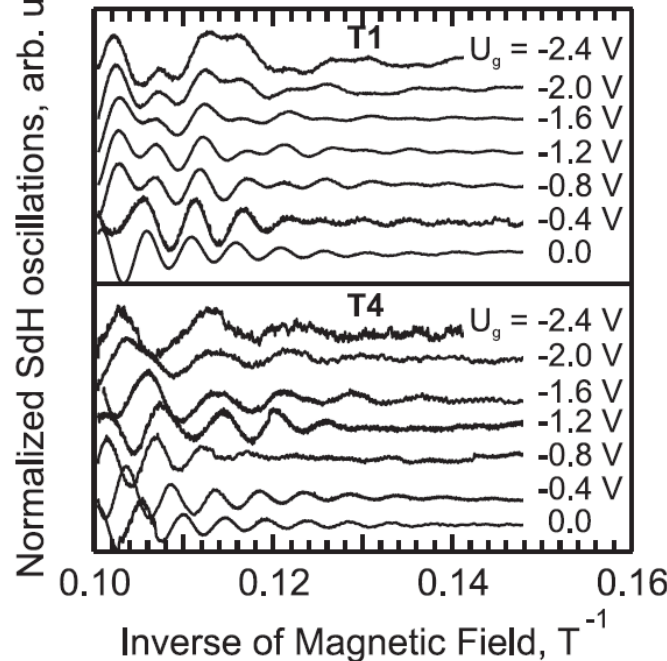
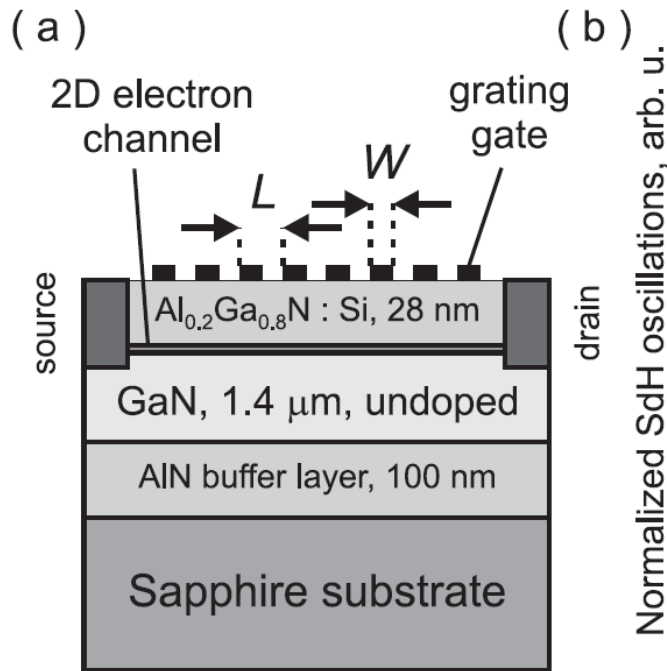


FIGURE 6.8. Occupation of Landau levels in a magnetic field neglecting the spin splitting, showing how the Fermi level moves to maintain a constant density of electrons. The fields are in the ratio 2 : 3 : 4 and give  $\nu = 4, \frac{8}{3},$  and 2.



K. Nogajewski et al.,  
Appl. Phys. Lett. 99, 213501 (2011)

# Shubnikov-de Haas effect

## Shubnikov-de Haas effect

Density of states oscillates - falls to 0 for  $\nu = n$  and is highest for  $\nu \approx n + \frac{1}{2}$  - the easiest measurement is the magnetoresistance  $R_{xx}$ .

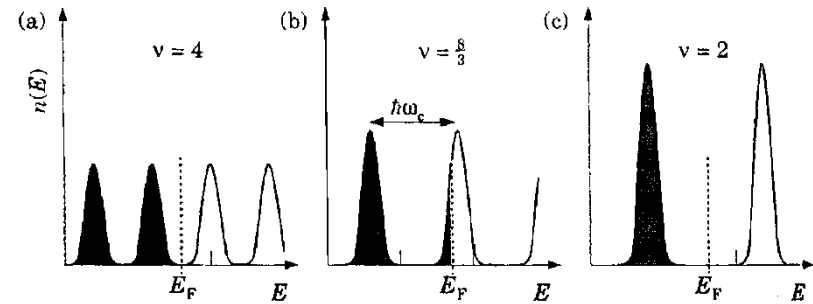


FIGURE 6.8. Occupation of Landau levels in a magnetic field neglecting the spin splitting, showing how the Fermi level moves to maintain a constant density of electrons. The fields are in the ratio

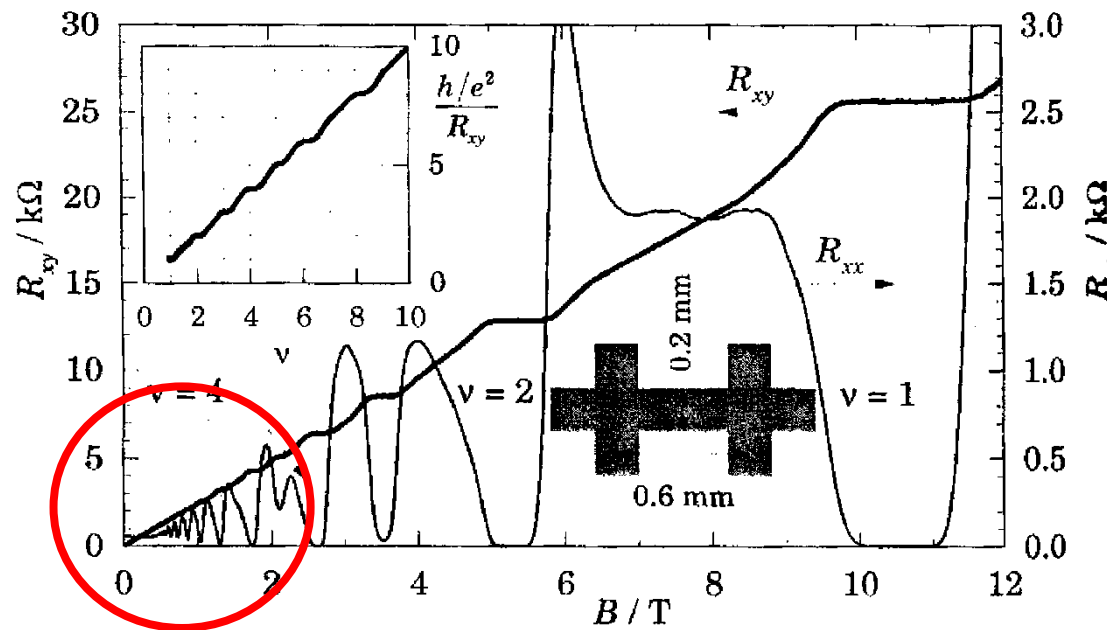
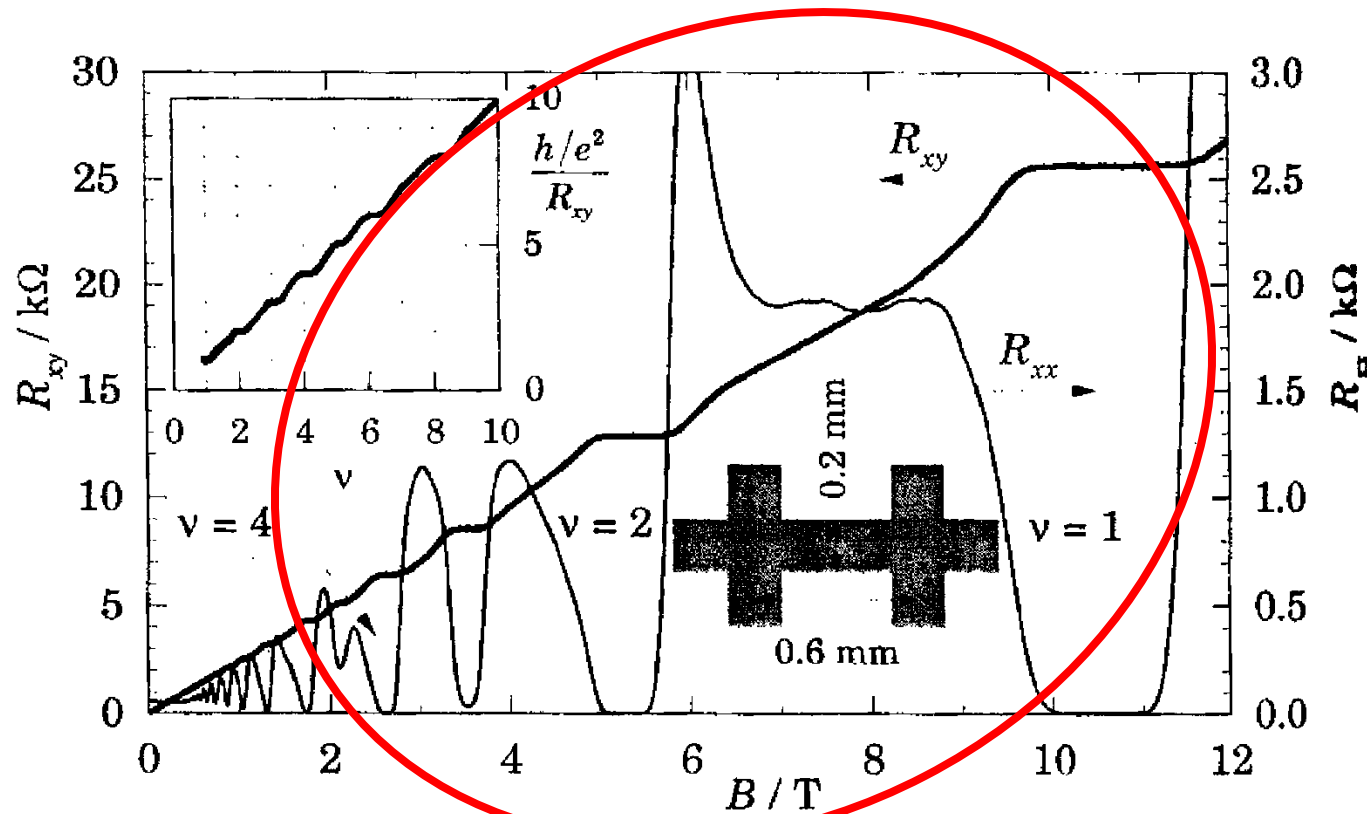


FIGURE 6.10. Longitudinal and transverse (Hall) resistivity,  $R_{xx}$  and  $R_{xy}$ , of a two-dimensional electron gas of density  $n_{2D} = 2.6 \times 10^{15} \text{ nm}^{-2}$  as a function of magnetic field. The measurements were made at  $T = 1.13 \text{ K}$ . The inset shows  $1/R_{xx}$  divided by the quantum unit of conductance  $e^2/h$  as a function of the filling factor  $\nu$ . [Data kindly supplied by Dr A. R. Long, University of Glasgow.]

# Integer Quantum Hall Effect (IQHE)

Integer Quantum Hall effect (IQHE) – for 2D gas: if the Fermi level is located in localized states the Hall resistance (*opór hallowski*) is quantized

$$R_H = \frac{1}{\nu} \frac{h}{e^2}$$



**FIGURE 6.10.** Longitudinal and transverse (Hall) resistivity,  $R_{xx}$  and  $R_{xy}$ , of a two-dimensional electron gas of density  $n_{2D} = 2.6 \times 10^{15} \text{ nm}^{-2}$  as a function of magnetic field. The measurements were made at  $T = 1.13 \text{ K}$ . The inset shows  $1/R_{xx}$  divided by the quantum unit of conductance  $e^2/h$  as a function of the filling factor  $\nu$ . [Data kindly supplied by Dr A. R. Long, University of Glasgow.]



# Quantum dots

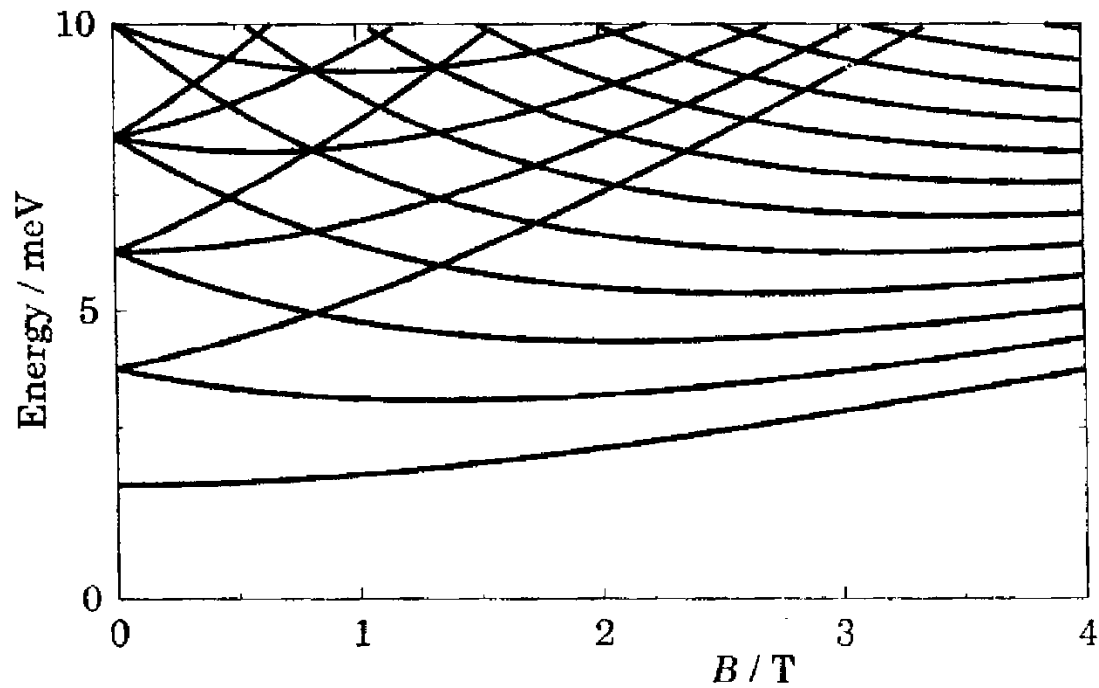


**FIGURE 6.16.** Energy levels in a magnetic field of a GaAs dot with a parabolic confining potential giving  $\hbar\omega_0 = 2$  meV.

# Harmonic potential 2D

$$E_n^x = \hbar\omega_0 \left( n_x + \frac{1}{2} \right) \text{ in the } x\text{-direction and the same in } y$$

$$E_n^y = \hbar\omega_0 \left( n_y + \frac{1}{2} \right)$$

$$E_n = E_n^x + E_n^y = \hbar\omega_0(N + 1)$$

Degeneracy?

$$N = n_x + n_y$$

2D disk shaped dot

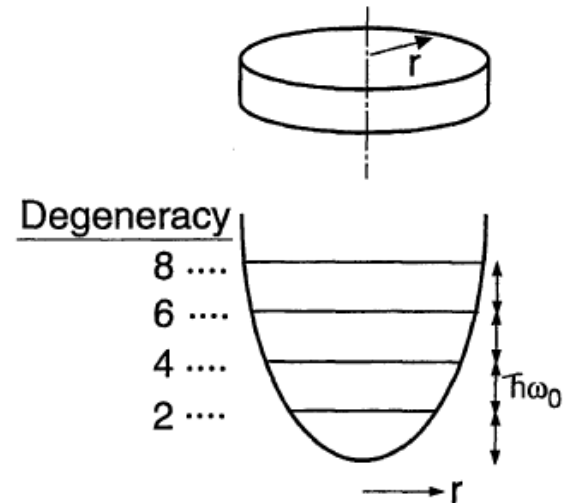


Fig. 5. Schematic model for the vertical dot with a harmonic lateral potential. The single-particle states are laterally confined into discrete equidistant 0D levels whose degeneracies are 2, 4, 6, 8, ... including spin degeneracy from the lowest level.

Jpn. J. Appl. Phys. Vol. 36 (1997) pp. 3917-3923  
Part 1, No. 6B, June 1997

**Reminder**

# Harmonic potential 2D

$$E_n^x = \hbar\omega_0 \left( n_x + \frac{1}{2} \right) \text{ in the } x\text{-direction and the same in } y$$

$$E_n^y = \hbar\omega_0 \left( n_y + \frac{1}{2} \right)$$

$$E_n = E_n^x + E_n^y = \hbar\omega_0(N + 1)$$

Degeneracy?

$$N = n_x + n_y$$

$$g_N = N + 1$$

$N$	$(n_x, n_y)$
0	(0,0)
1	(1,0) (0,1)
2	(2,0) (1,1) (0,2)
3	(3,0) (2,1) (1,2) (0,3)

2D disk shaped dot

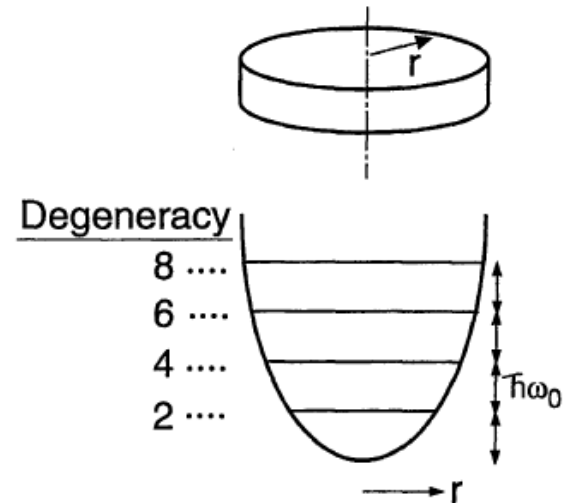
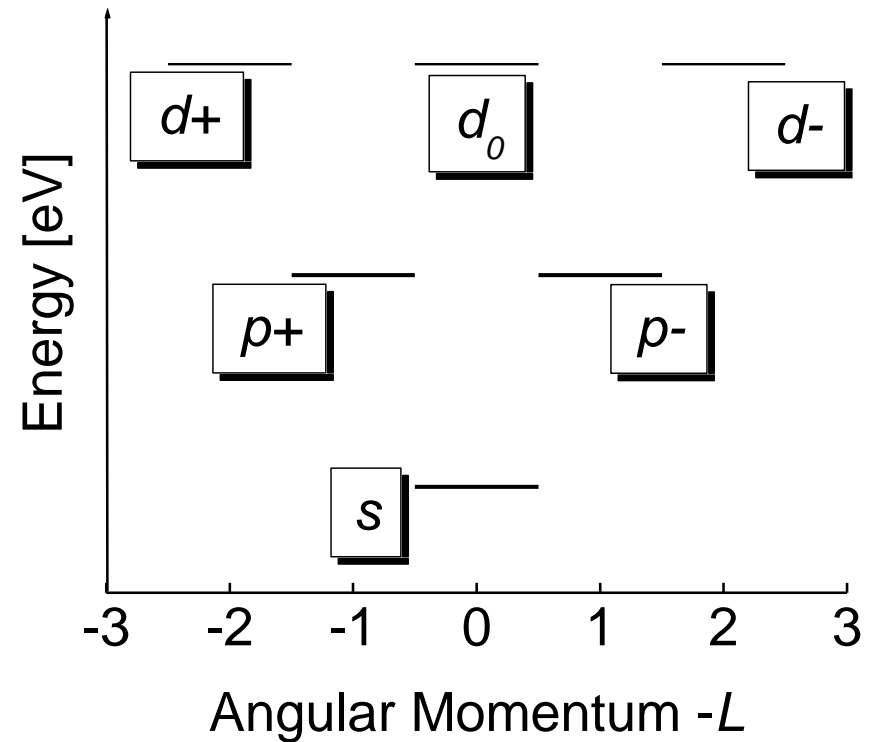
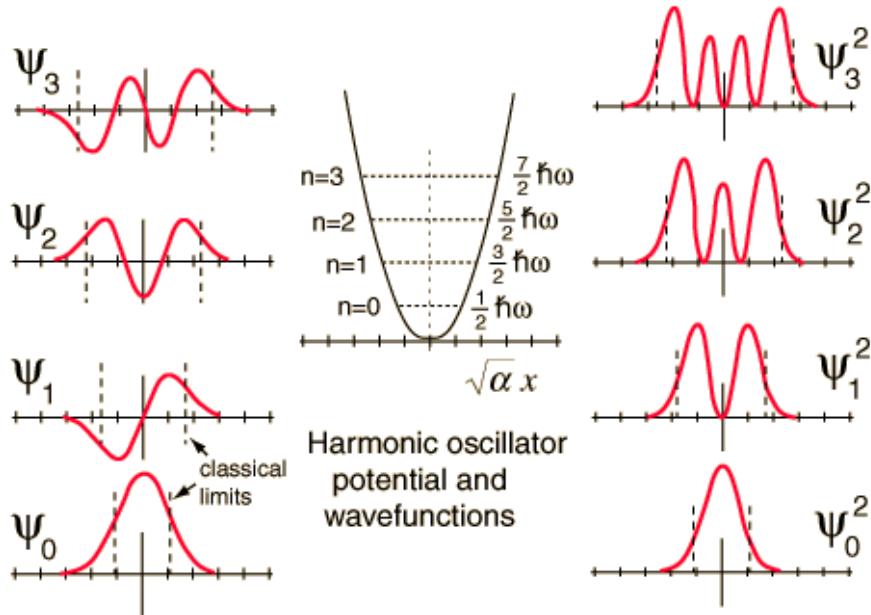


Fig. 5. Schematic model for the vertical dot with a harmonic lateral potential. The single-particle states are laterally confined into discrete equidistant 0D levels whose degeneracies are 2, 4, 6, 8, ... including spin degeneracy from the lowest level.

Jpn. J. Appl. Phys. Vol. 36 (1997) pp. 3917-3923  
Part 1, No. 6B, June 1997

# Harmonic potential 2D



$$n, m = 0, 1, 2, \dots$$

$$L = n - m \text{ (elektron)}$$

Reminder

# Homogenous magnetic field

The solution in the symmetric gauge:

$$\left\{ \frac{1}{2m} [\hat{p} - q \vec{A}(\vec{r}, t)]^2 + q\phi(\vec{r}, t) + U(\vec{r}, t) \right\} \psi(\vec{r}, t) = i\hbar \frac{d}{dt} \psi(\vec{r}, t)$$

**The symmetric gauge:** field  $\vec{B} = (0, 0, B_z) \Rightarrow A_\theta = \frac{1}{2}Br, A_r = 0, A_z = 0$

$$\left\{ -\frac{\hbar^2}{2m} \left[ \frac{\partial^2}{\partial r^2} + \frac{1}{r} \frac{\partial}{\partial r} + \frac{1}{r^2} \frac{\partial^2}{\partial \theta^2} \right] - \frac{i\hbar e B}{m} \frac{\partial}{\partial \theta} + \frac{e^2 B^2 r^2}{8m} + U(z) \right\} \psi(r, \theta, z) = E\psi(r, \theta, z)$$

This time a rotation angle  $\theta$  is the invariant, which can be associated with angular momentum and the function in the form of  $\exp(il\theta)$

$$\varepsilon_{nl} = \left( n + \frac{1}{2}l + \frac{1}{2}|l| - \frac{1}{2} \right) \hbar\omega_c \quad n = 1, 2, 3 \dots \quad l = 0, \pm 1, \pm 2, \pm 3 \dots$$

$$\phi_{nk}(r, \theta) \propto \exp(il\theta) \exp \left[ -\frac{r^2}{4l_B^2} \right] r^{|l|} L_{n-1}^{(|l|)} \left( \frac{r^2}{2l_B^2} \right)$$

The symmetrical potential also has its drawbacks - where is the origin of ALL cyclotron orbits?

What are the solutions with negative sign?

Associate Laguerre polynomial



# Quantum dots

$$E_{nl} = (2n + |l| - 1) \sqrt{(\hbar\omega_0)^2 + \left(\frac{1}{2}\hbar\omega_c\right)^2} + \left(\frac{1}{2}\hbar\omega_c\right) l$$
$$n = 1, 2, 3 \dots \quad l = 0, \pm 1, \pm 2, \pm 3 \dots$$

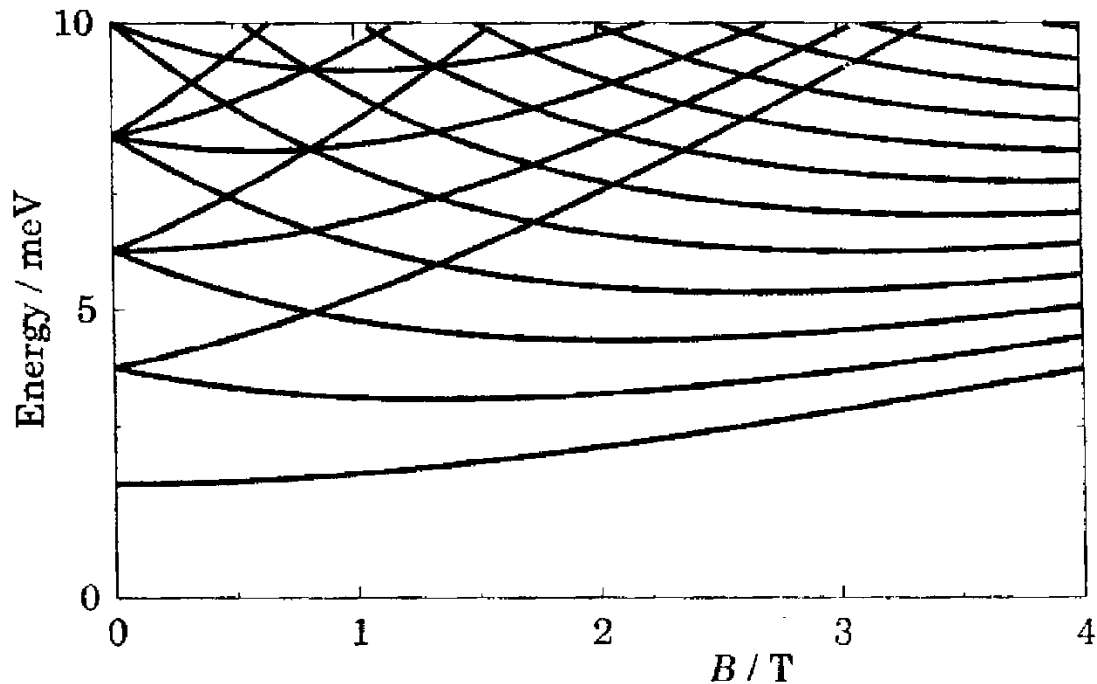
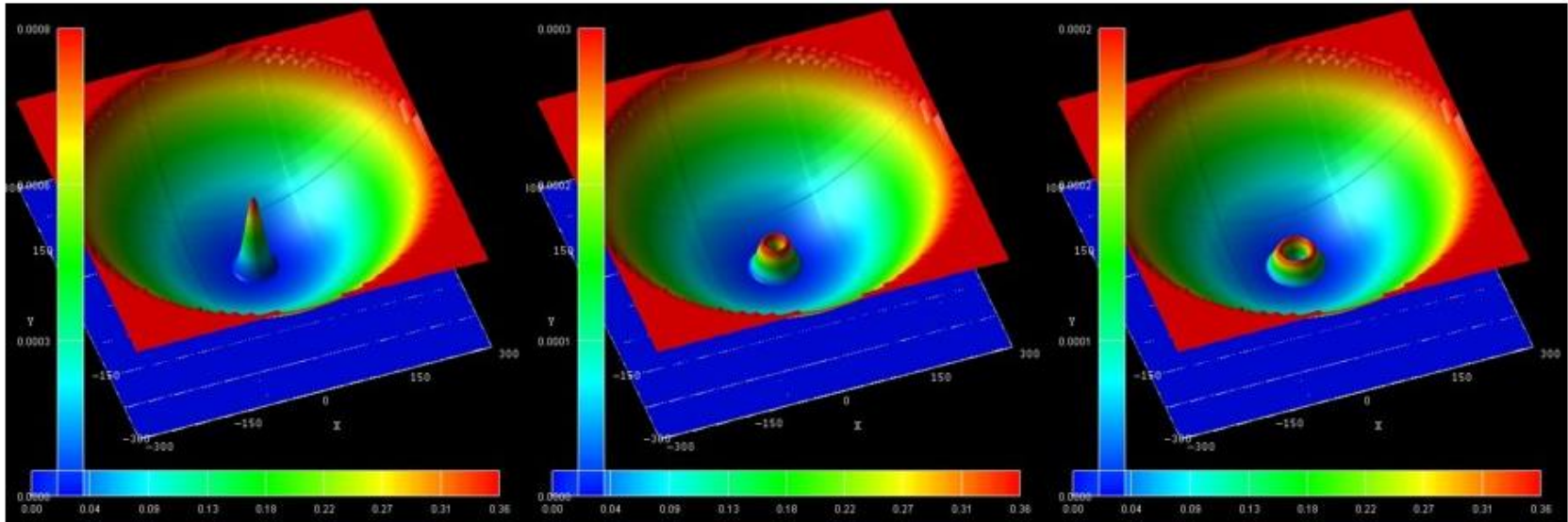


**FIGURE 6.16.** Energy levels in a magnetic field of a GaAs dot with a parabolic confining potential giving  $\hbar\omega_0 = 2$  meV.

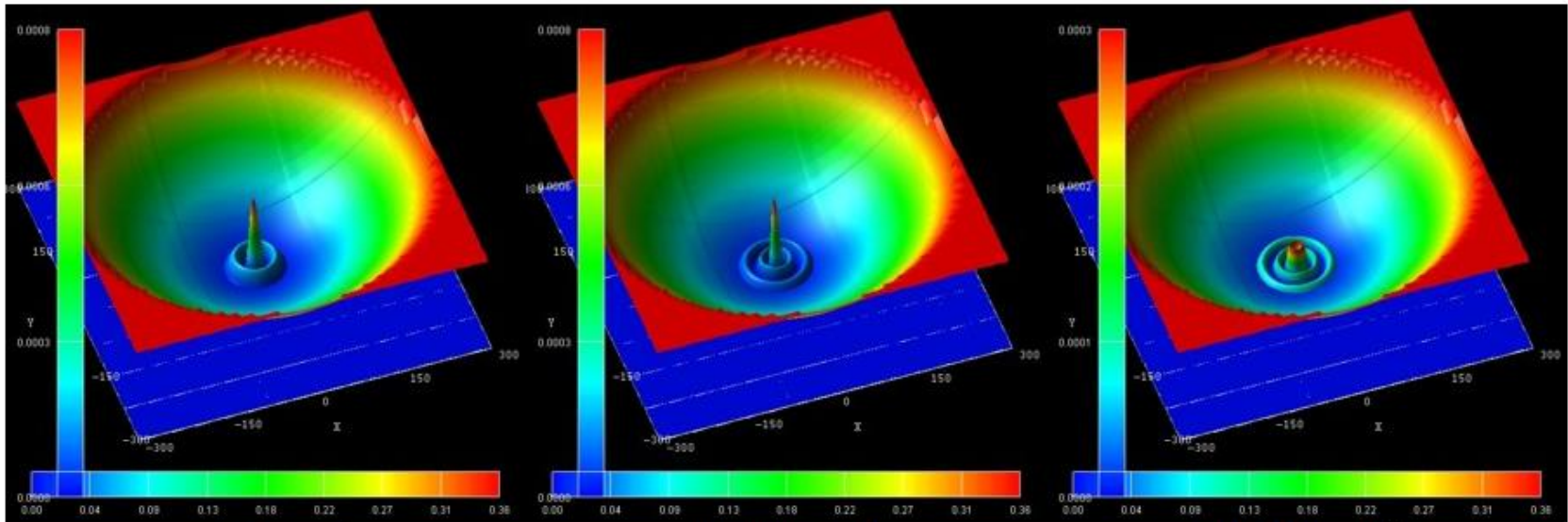
# Kropki kwantowe



$(n,l) = (0,0)$  (1<sup>st</sup>)

$(n,l) = (0,1)$  (2<sup>nd</sup>)

$(n,l) = (0,2)$  (4<sup>th</sup>)



$(n,l) = (1,0)$  (5<sup>th</sup>)

$(n,l) = (2,0)$  (13<sup>th</sup>)

$(n,l) = (2,2)$  (18<sup>th</sup>)

# Quantum dots

Phys. Scr. T149 (2012) 014056 (4pp)

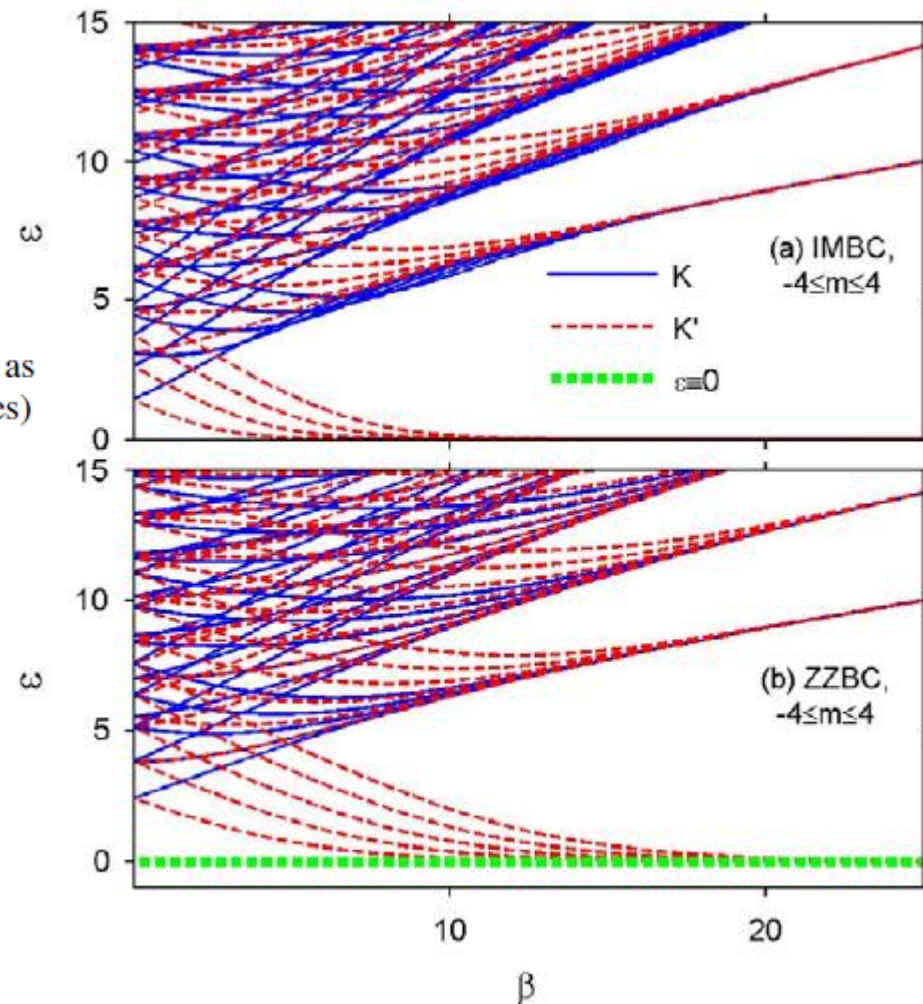
doi:10.1088/0031-8949/2012/T149/014056

Fock-Darwin spectrum

## Interband optical absorption in a circular graphene quantum dot

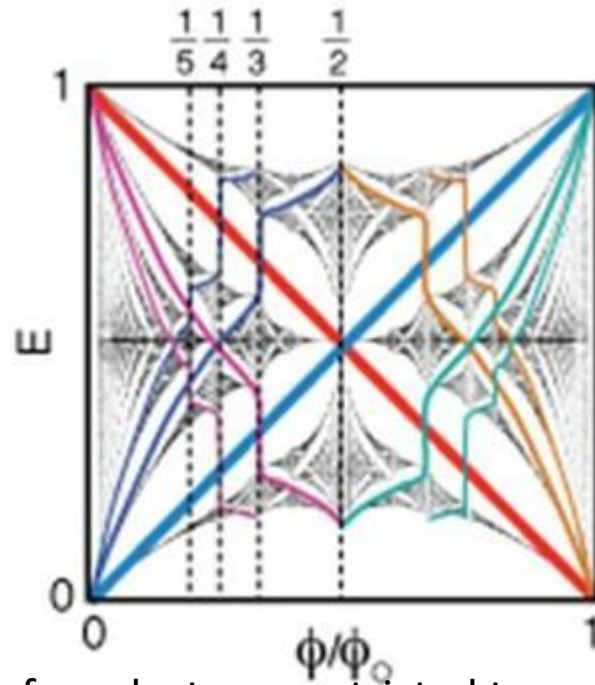
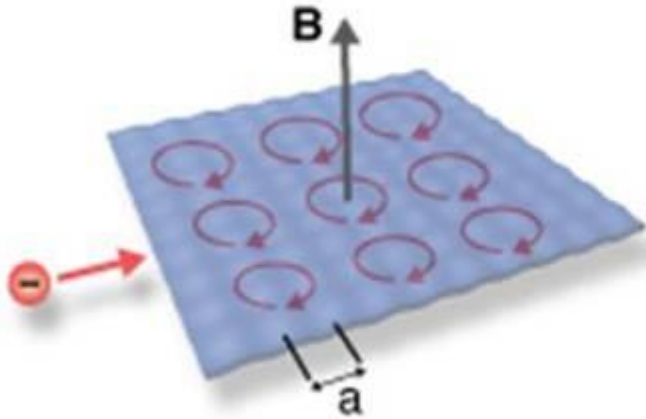
M Grujić<sup>1</sup>, M Zarenia<sup>2</sup>, M Tadić<sup>1</sup> and F M Peeters<sup>2</sup>

**Figure 1.** The electron states of a circular graphene quantum dot as a function of external magnetic field  $\beta$  for the  $K$  (blue solid curves) and  $K'$  (red dashed curves) valleys with  $R = 70$  nm for (a) the IMBC and (b) the ZZBC. The green dashed line in panel (b) displays zero-energy level for the case of ZZBC.



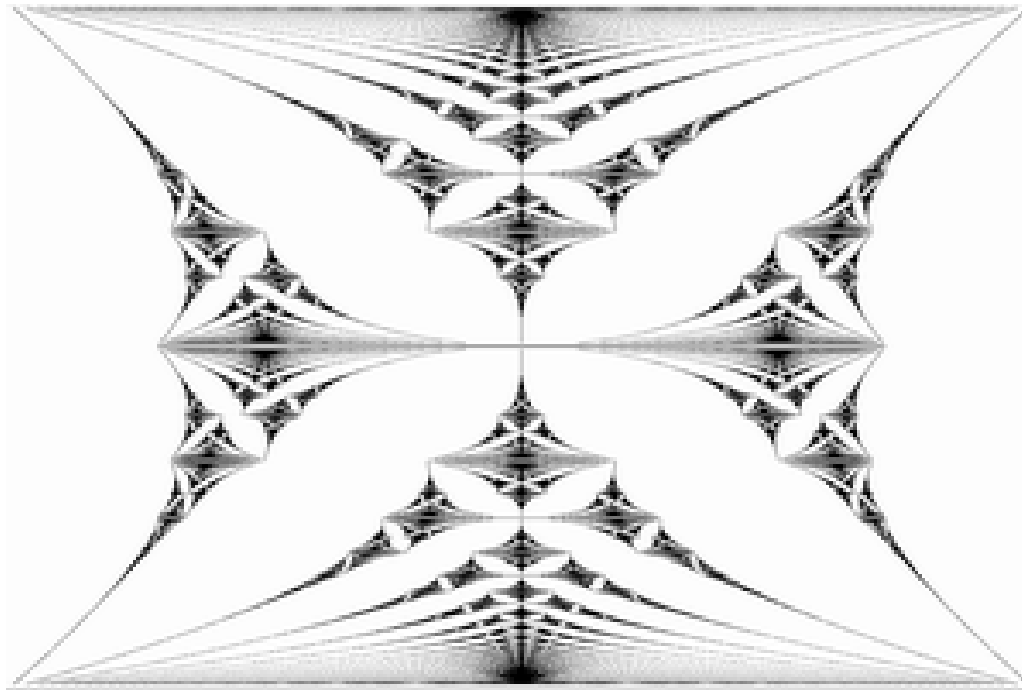


# Hofstadter butterfly



The Hofstadter butterfly is the energy spectrum of an electron, restricted to move in two-dimensional periodic potential under the influence of a perpendicular magnetic field. The horizontal axis is the energy and the vertical axis is the magnetic flux through the unit cell of the periodic potential. The flux is a dimensionless number when measured in quantum flux units (will call it  $a$ ). It is an example of a fractal energy spectrum. When the flux parameter  $a$  is rational and equal to  $p/q$  with  $p$  and  $q$  relatively prime, the spectrum consists of  $q$  non-overlapping energy bands, and therefore  $q+1$  energy gaps (gaps number  $0$  and  $q$  are the regions below and above the spectrum accordingly). When  $a$  is irrational, the spectrum is a cantor set.

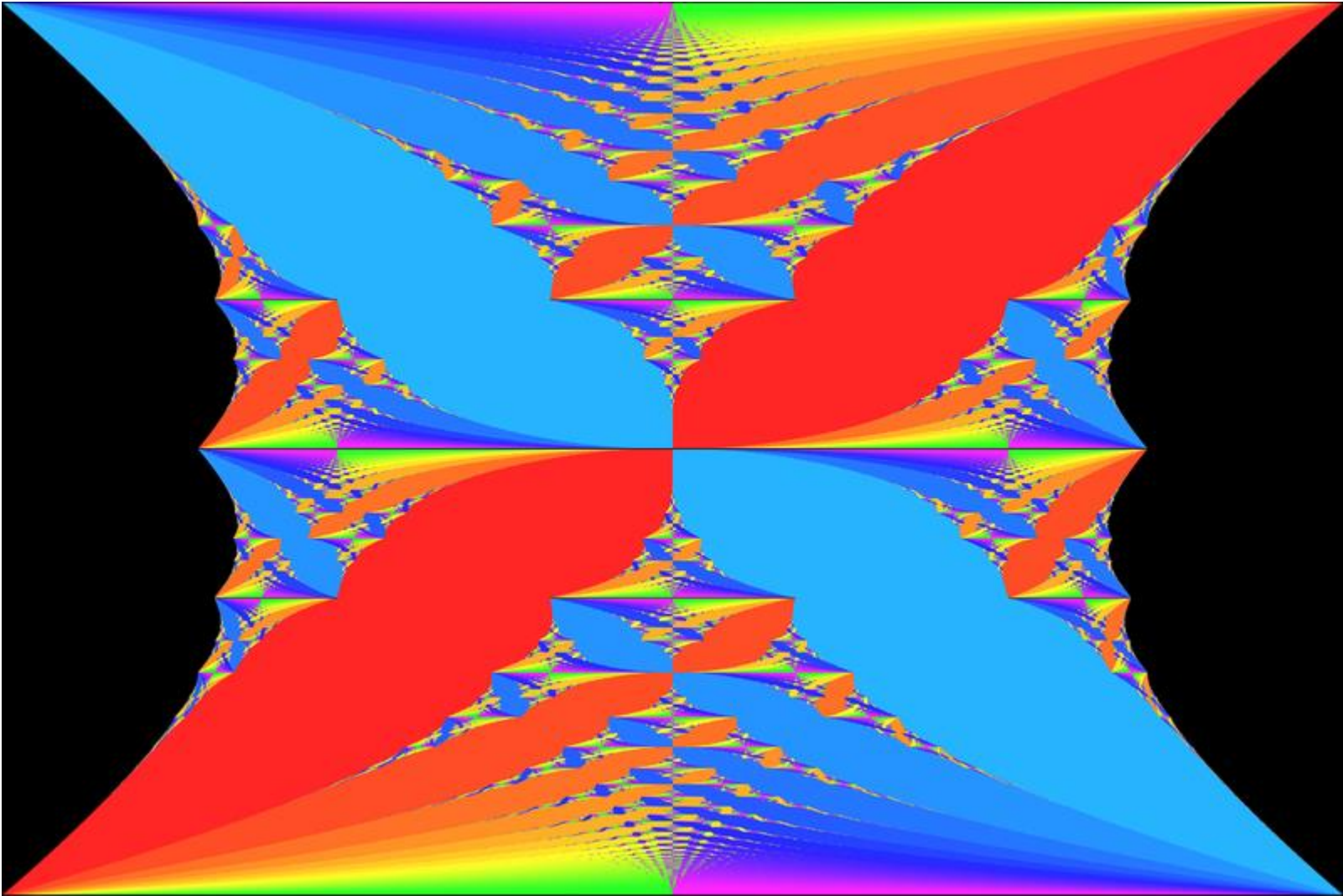
# Hofstadter butterfly



The Hofstadter butterfly is the energy spectrum of an electron, restricted to move in two-dimensional periodic potential under the influence of a perpendicular magnetic field. The horizontal axis is the energy and the vertical axis is the magnetic flux through the unit cell of the periodic potential. The flux is a dimensionless number when measured in quantum flux units (will call it  $\alpha$ ). It is an example of a fractal energy spectrum. When the flux parameter  $\alpha$  is rational and equal to  $p/q$  with  $p$  and  $q$  relatively prime, the spectrum consists of  $q$  non-overlapping energy bands, and therefore  $q+1$  energy gaps (gaps number  $0$  and  $q$  are the regions below and above the spectrum accordingly). When  $\alpha$  is irrational, the spectrum is a cantor set.

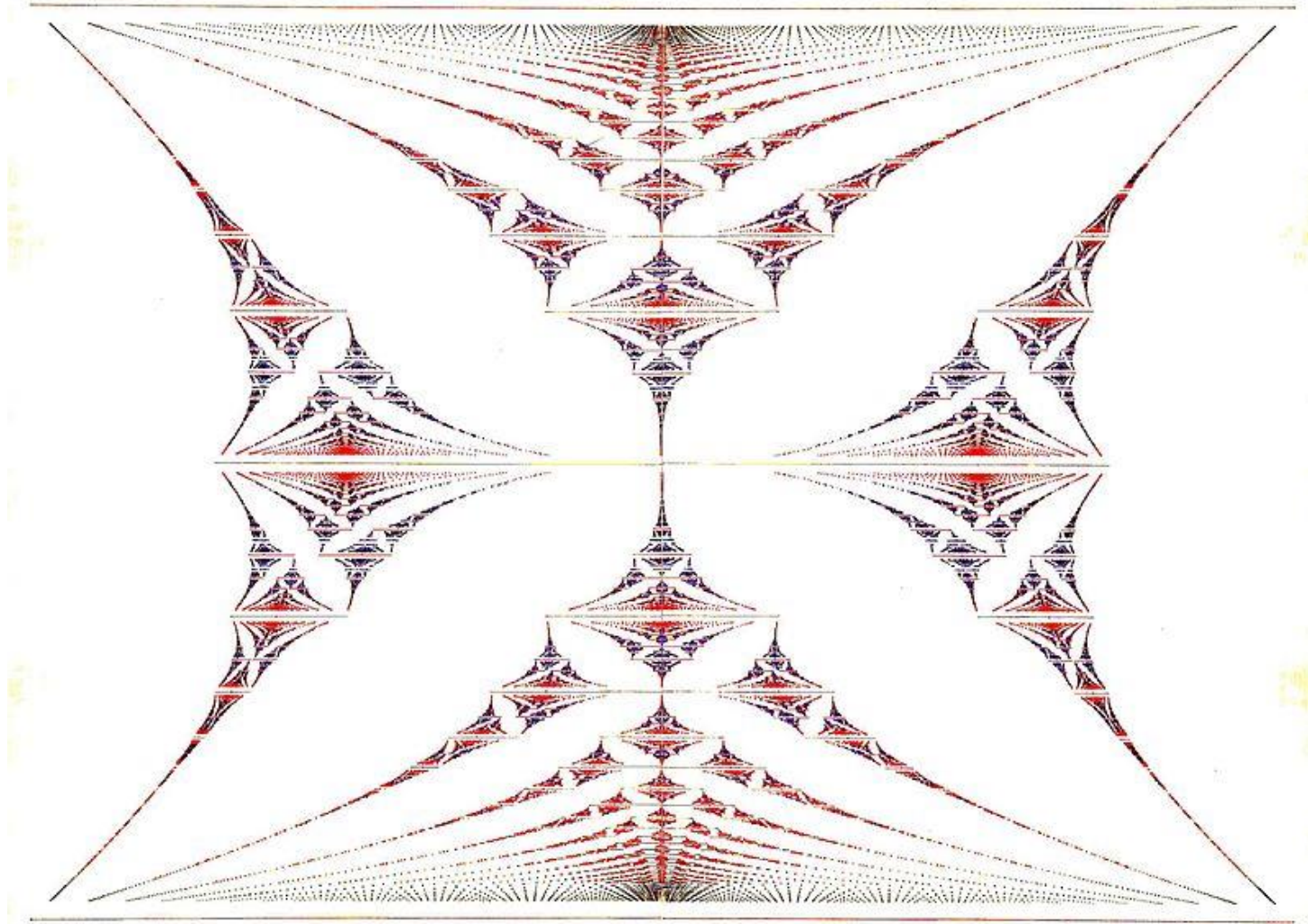


# Hofstadter's butterfly



[http://en.wikipedia.org/wiki/Hofstadter%27s\\_butterfy](http://en.wikipedia.org/wiki/Hofstadter%27s_butterfy)

# Hofstadter's butterfly



[http://en.wikipedia.org/wiki/Hofstadter%27s\\_butterfy](http://en.wikipedia.org/wiki/Hofstadter%27s_butterfy)



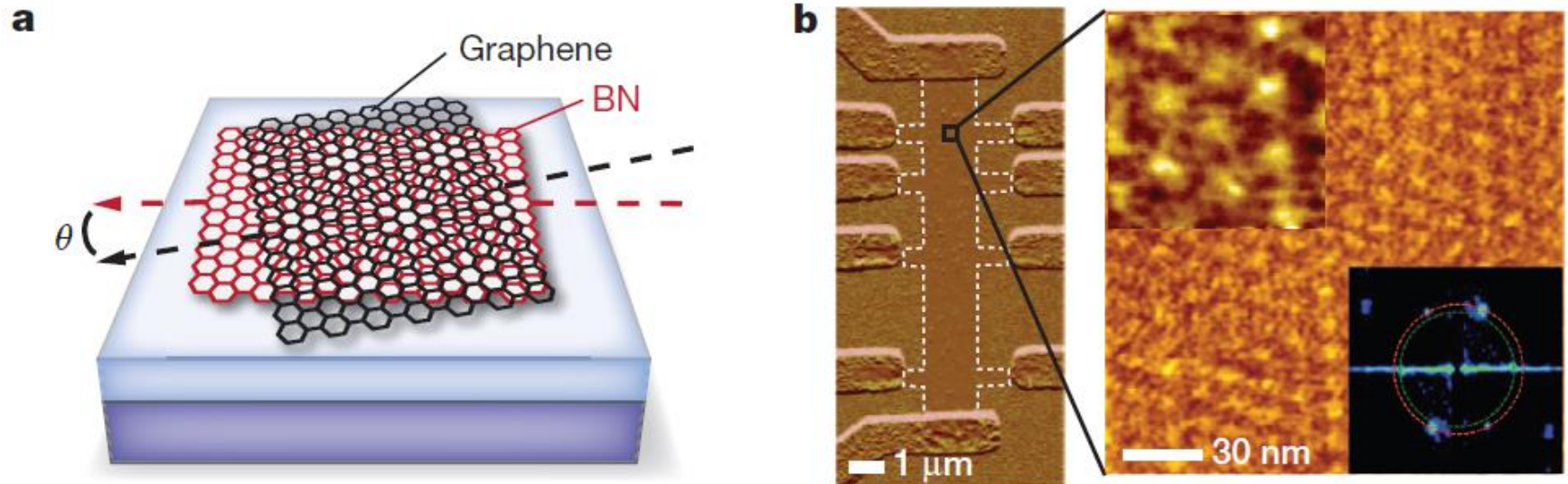
# Hofstadter's butterfly

## LETTER

doi:10.1038/nature12186

### Hofstadter's butterfly and the fractal quantum Hall effect in moiré superlattices

C. R. Dean<sup>1</sup>, L. Wang<sup>2</sup>, P. Maher<sup>3</sup>, C. Forsythe<sup>3</sup>, F. Ghahari<sup>3</sup>, Y. Gao<sup>2</sup>, J. Katoch<sup>4</sup>, M. Ishigami<sup>4</sup>, P. Moon<sup>5</sup>, M. Koshino<sup>5</sup>, T. Taniguchi<sup>6</sup>, K. Watanabe<sup>6</sup>, K. L. Shepard<sup>7</sup>, J. Hone<sup>2</sup> & P. Kim<sup>3</sup>



# Hofstadter's butterfly

Figure 3 | Fractal gaps. a, Landau fan diagrams similar to those in Fig. 2 but measured from a separate device. Here the zero-field satellite peak position indicates a moiré period of 11.6 nm, indicating that the superlattice unit cell was approximately 1.5 times smaller in this device than in the one used in Fig. 2. Significantly more structure is observed here than in Fig. 2. b, Bottom: the

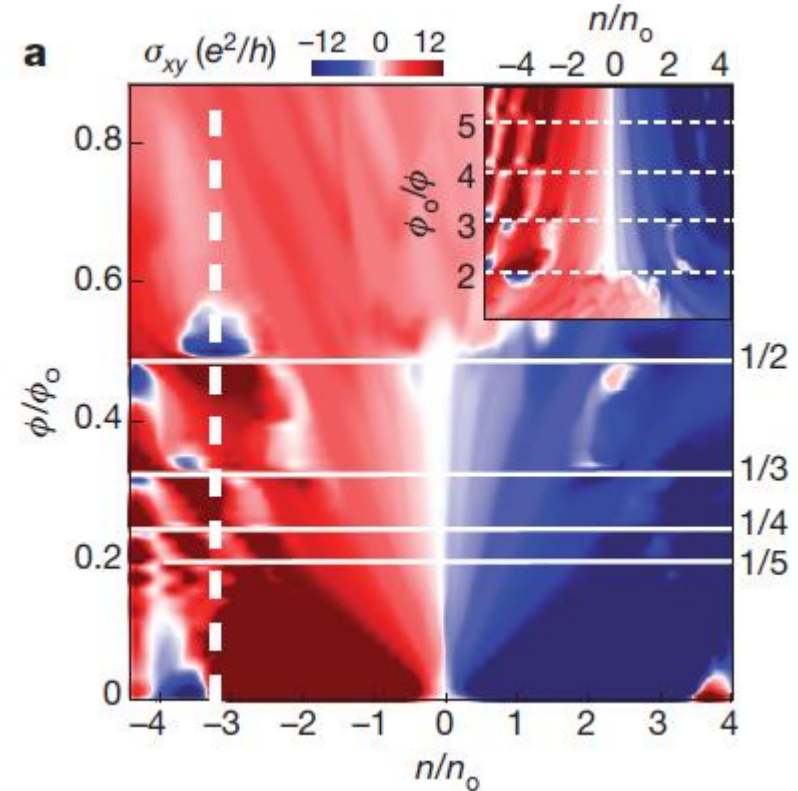
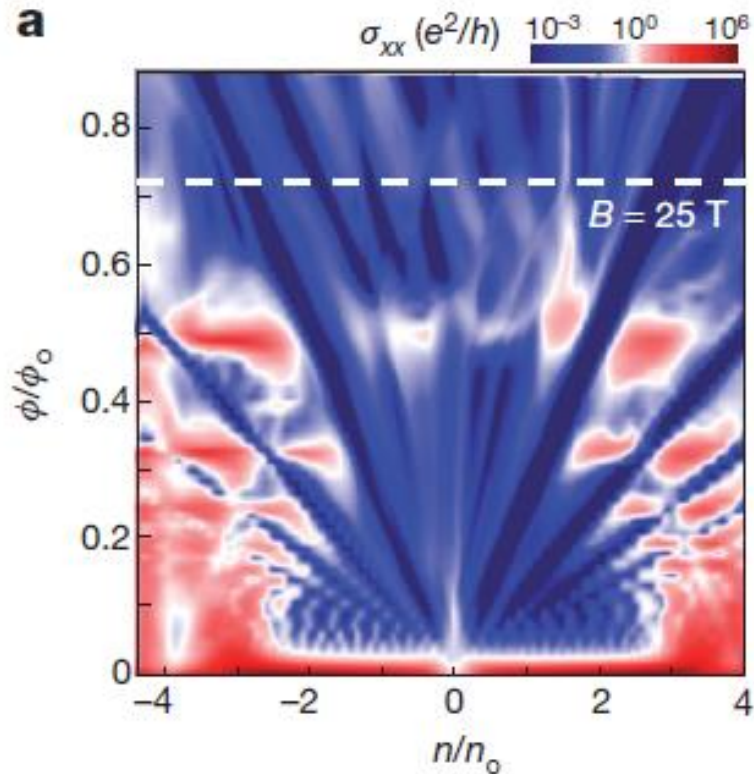


Figure 4 | Recursive structure. a,  $R_{xy}$  Wannier diagram for the device used in Fig. 3. White solid lines label  $\phi/\phi_0$  values corresponding to the pure cases,  $\phi/\phi_0 = 1/m$ . Inset: data replotted against  $\phi_0/\phi$ , illustrating that the main experimental features exhibit a  $1/B$  periodicity. b, Longitudinal conductivity,

# Shubnikov-de Haas effect

## Shubnikov-de Haas effect

Density of states oscillates - falls to 0 for  $\nu = n$  and is highest for  $\nu \approx n + \frac{1}{2}$  - the easiest measurement is the magnetoresistance  $R_{xx}$ .

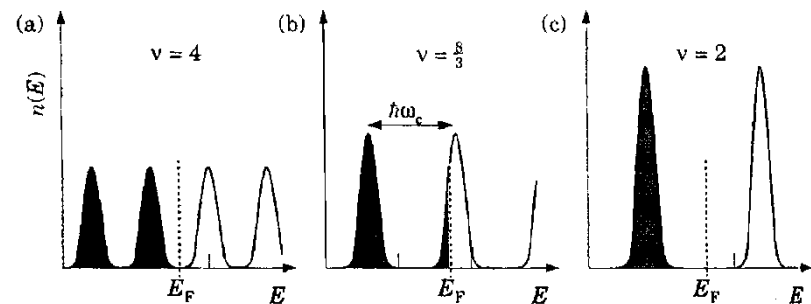


FIGURE 6.8. Occupation of Landau levels in a magnetic field neglecting the spin splitting, showing how the Fermi level moves to maintain a constant density of electrons. The fields are in the ratio

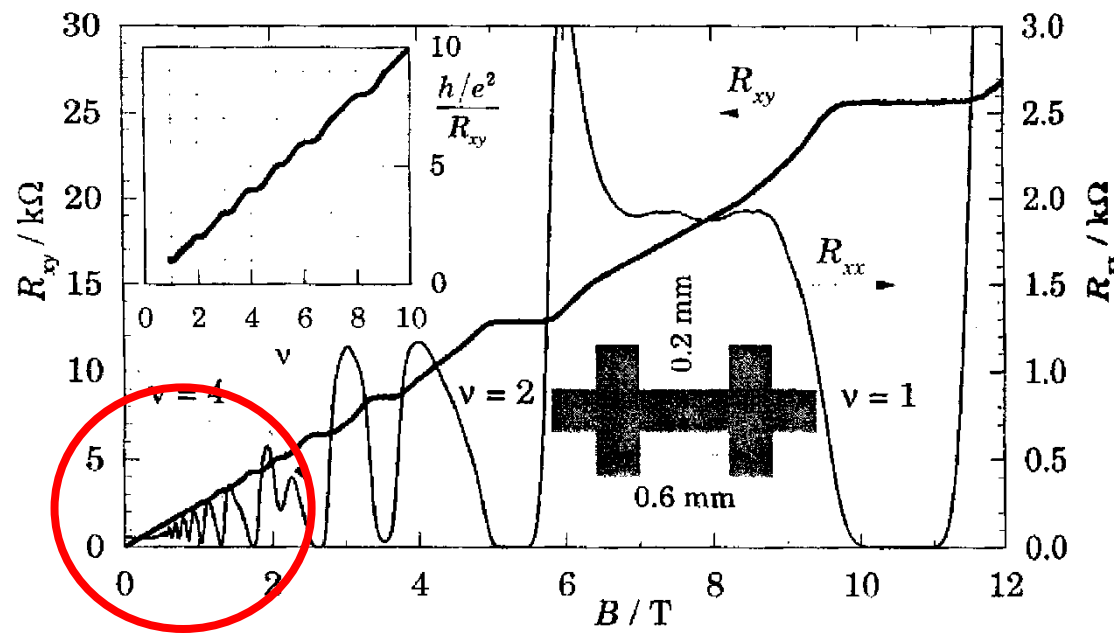


FIGURE 6.10. Longitudinal and transverse (Hall) resistivity,  $R_{xx}$  and  $R_{xy}$ , of a two-dimensional electron gas of density  $n_{2D} = 2.6 \times 10^{15} \text{ nm}^{-2}$  as a function of magnetic field. The measurements were made at  $T = 1.13 \text{ K}$ . The inset shows  $1/R_{xx}$  divided by the quantum unit of conductance  $e^2/h$  as a function of the filling factor  $\nu$ . [Data kindly supplied by Dr A. R. Long, University of Glasgow.]



# Integer Quantum Hall Effect (IQHE)

Integer Quantum Hall effect (IQHE) – for 2D gas: if the Fermi level is located in localized states the Hall resistance (*opór hallowski*) is quantized

$$R_H = \frac{1}{\nu} \frac{h}{e^2}$$

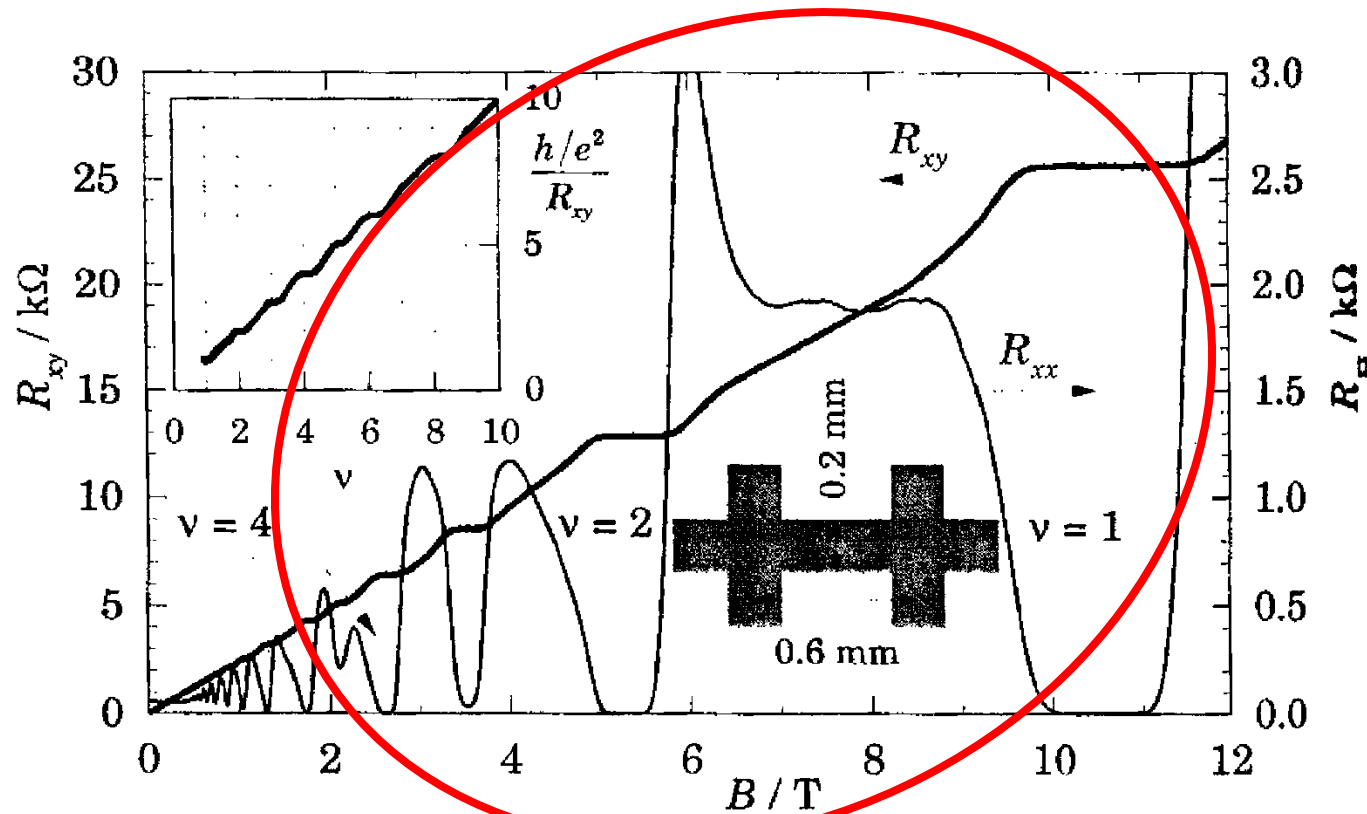


**FIGURE 6.10.** Longitudinal and transverse (Hall) resistivity,  $R_{xx}$  and  $R_{xy}$ , of a two-dimensional electron gas of density  $n_{2D} = 2.6 \times 10^{15} \text{ nm}^{-2}$  as a function of magnetic field. The measurements were made at  $T = 1.13 \text{ K}$ . The inset shows  $1/R_{xx}$  divided by the quantum unit of conductance  $e^2/h$  as a function of the filling factor  $\nu$ . [Data kindly supplied by Dr A. R. Long, University of Glasgow.]

# Integer Quantum Hall Effect (IQHE)

Integer Quantum Hall effect (IQHE) – for 2D gas: if the Fermi level is located in localized states the Hall resistance (*opór hallowski*) is quantized

$$R_H = \frac{1}{\nu} \frac{h}{e^2}$$

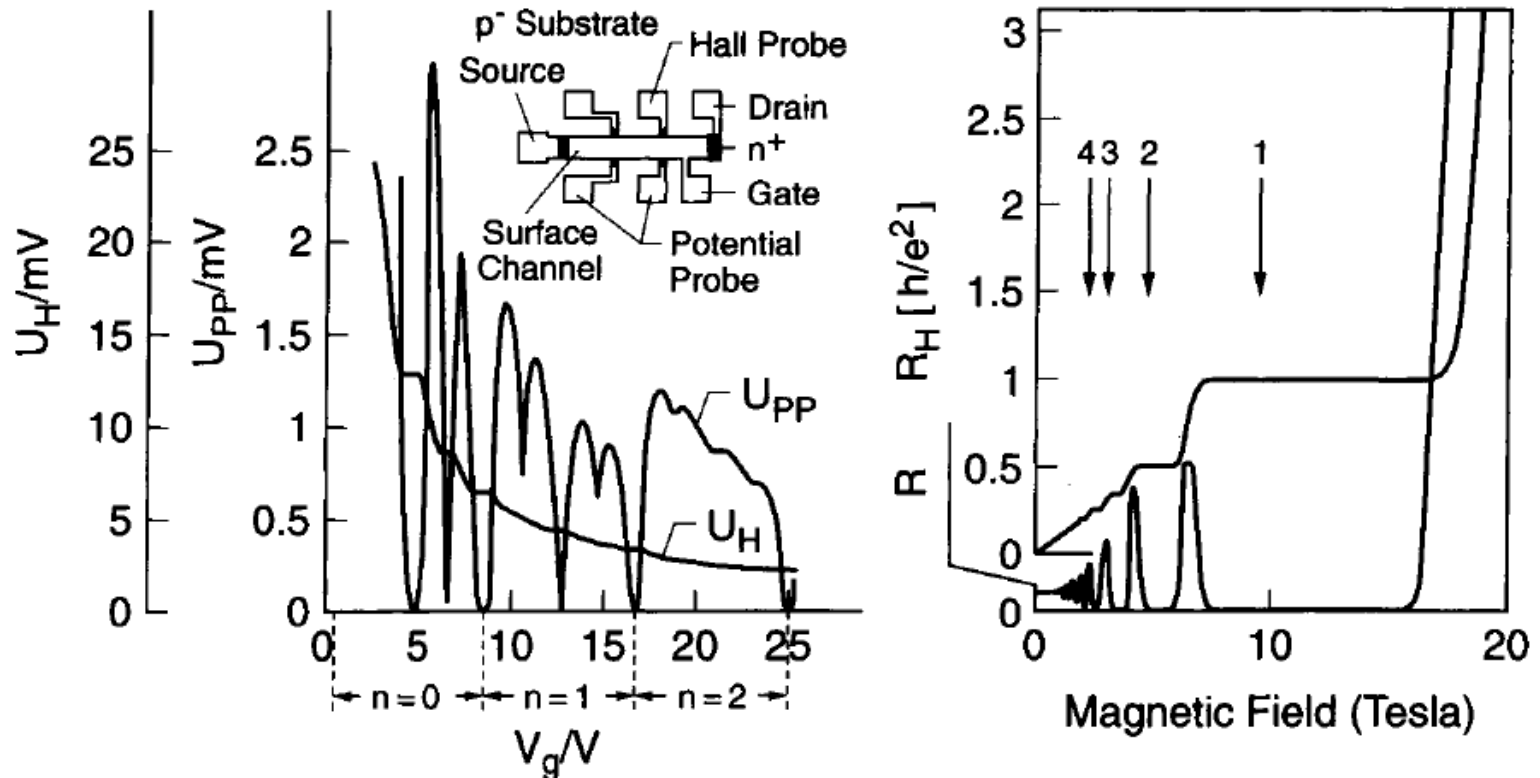


Figure 7. Left panel: original data of the discovery of the integral quantum Hall effect (IQHE) by Klaus von Klitzing in 1980 in the two-dimensional electron system of a silicon MOSFET transistor. Instead of a smooth curve he observed plateaus in the Hall voltage ( $U_H$ ) and found concomitant deep minima in the magneto-resistance ( $U_{PP}$ ). The horizontal axis represents gate voltage ( $V_G$ ) which varies the carrier density,  $n$ . The right panel shows equivalent data taken on a two-dimensional electron system in GaAs/AlGaAs. Since these data are plotted versus magnetic field they can directly be compared to Edwin Hall's data of Fig. 6. Rather than the linear dependence of the Hall resistance on magnetic field of Fig. 6, these data show wide plateaus in  $R_H$  and in addition deep minima in  $R$ .

Stromer, Nobel Lecture

# Conductivity tensor

Conductivity  $\sigma = n e \mu$

current density:  $\vec{j} = \sigma \vec{E}$  - generally  $\sigma$  can be a tensor:

$$\vec{j}_x = q n \vec{v}_x \text{ and } \vec{v}_x = \frac{q\tau}{m} \vec{E}_x = \mu \vec{E}_x$$

In general e.g.  $j_x = \sigma_{xx} E_x$  and  $j_y = \sigma_{yx} E_x$  etc.

Drude model with magnetic field:

$$m^* \left\{ \frac{d\vec{v}}{dt} + \frac{\vec{v}}{\tau} \right\} = q\vec{E} + q\vec{v} \times \vec{B}$$

$\tau$  – momentum relaxation time (*scattering time*)

$$m^* \left\{ \frac{dv_x}{dt} + \frac{v_x}{\tau} \right\} = qE_x + qv_y B$$

$$m^* \left\{ \frac{dv_y}{dt} + \frac{v_y}{\tau} \right\} = qE_y - qv_x B$$

# Hall effect

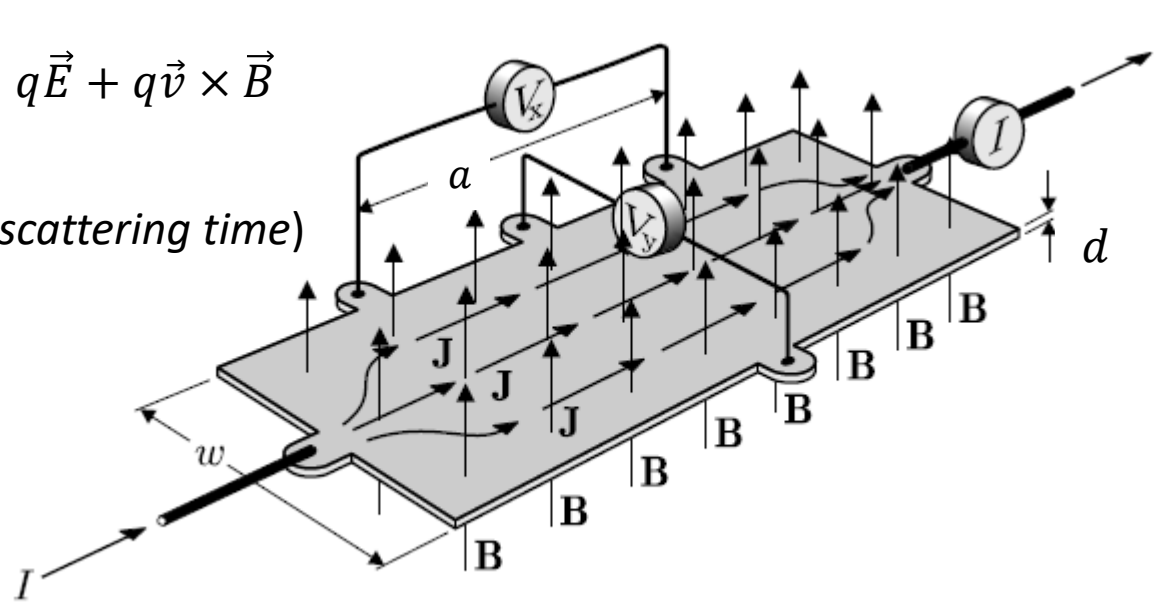
Lorentz force:  $\vec{F} = q\vec{v} \times \vec{B}$

Drude model:  $m^* \left\{ \frac{d\vec{v}}{dt} + \frac{\vec{v}}{\tau} \right\} = q\vec{E} + q\vec{v} \times \vec{B}$

$\tau$  – momentum relaxation time (*scattering time*)

$$m^* \left\{ \frac{dv_x}{dt} + \frac{v_x}{\tau} \right\} = qE_x + qv_y B$$

$$m^* \left\{ \frac{dv_y}{dt} + \frac{v_y}{\tau} \right\} = qE_y - qv_x B$$



We get:

$$v_y \{1 + \omega_c^2 \tau^2\} = \frac{q\tau}{m^*} (E_y - \omega_c \tau E_x)$$

$$\omega_c = \frac{qB}{m^*} \quad \mu = \frac{q\tau}{m^*} \quad j_y = 0 = \sum_i q_i n v_y^i$$

**On exercises**

# Hall effect

Neglecting  $\omega_c^2 \tau^2 \ll 1$  and taking into account conductivity of electrons  $n$  and holes  $p$  :

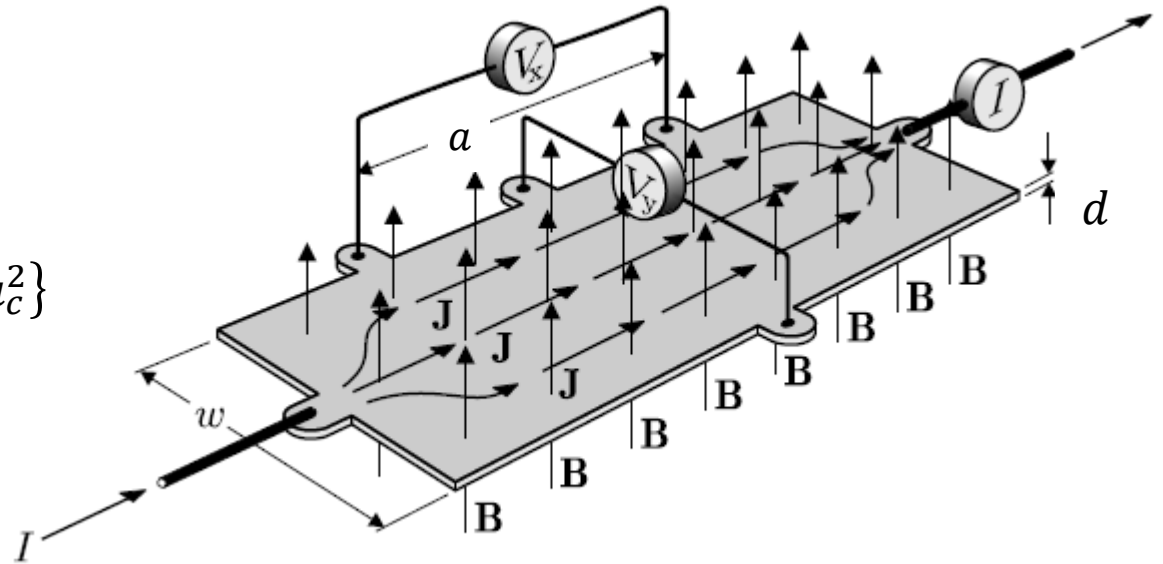
$$j_y = 0 = \sum_i q_i n v_y^i$$

$$E_y \{n\mu_c + p\mu_h\} = E_x B \{p\mu_h^2 - n\mu_c^2\}$$

We get so-called Hall constant:

$$R_H = \frac{E_y}{j_x B} = \frac{1}{|e|} \frac{p\mu_h^2 - n\mu_c^2}{(n\mu_c + p\mu_h)^2}$$

E.g. for  $p = 0$  we get  $R_H = -\frac{1}{en}$



On exercises



# Hall effect

Taking  $\sigma_0 = n e \mu = n e^2 \tau / m$

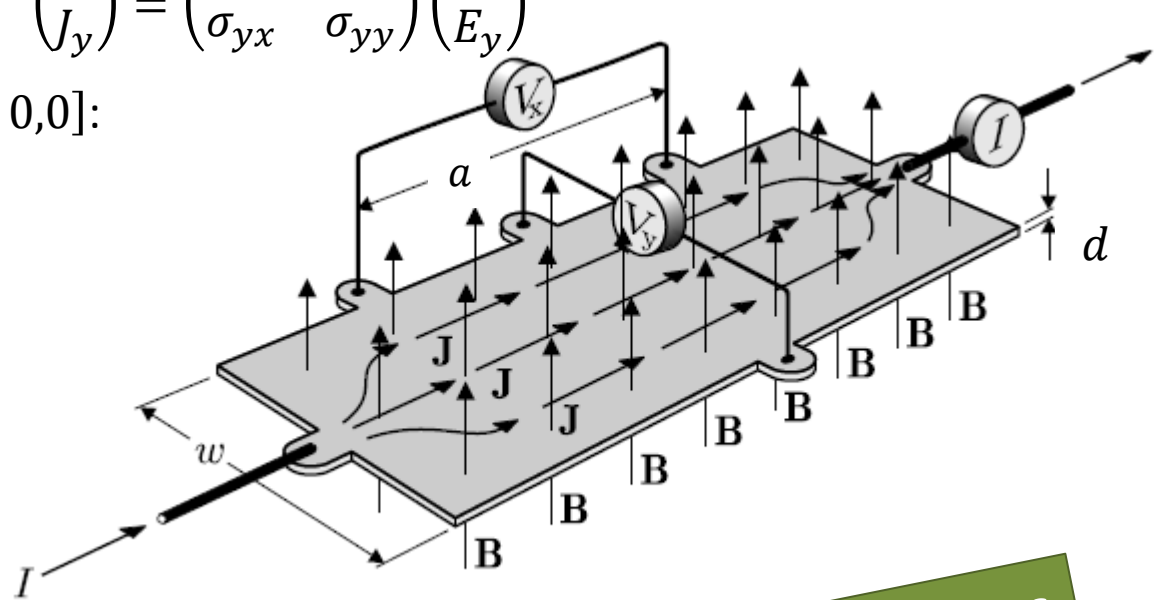
$$\begin{pmatrix} J_x \\ J_y \end{pmatrix} = \begin{pmatrix} \sigma_{xx} & \sigma_{xy} \\ \sigma_{yx} & \sigma_{yy} \end{pmatrix} \begin{pmatrix} E_x \\ E_y \end{pmatrix}$$

In case of the Hall effect  $E = [E_x, 0, 0]$ :

$$j_x = \sigma_{xx} E_x \quad j_y = \sigma_{yx} E_x$$

$$\sigma_{xx} = \frac{\sigma_0}{1 + \omega_c^2 \tau^2}$$

$$\sigma_{yx} = \frac{\sigma_0 \omega_c \tau}{1 + \omega_c^2 \tau^2}$$



On exercises

Conductivity tensor:

$$\sigma = \begin{pmatrix} \sigma_{xx} & -\sigma_{yx} \\ \sigma_{yx} & \sigma_{xx} \end{pmatrix} = \begin{pmatrix} \sigma_L & -\sigma_T \\ \sigma_T & \sigma_L \end{pmatrix} = \frac{\sigma_0}{1 + \omega_c^2 \tau^2} \begin{pmatrix} 1 & \omega_c \tau \\ -\omega_c \tau & 1 \end{pmatrix}$$

Resistivity tensor:

$$\rho = \frac{1}{\sigma_L^2 + \sigma_T^2} \begin{pmatrix} \sigma_L & -\sigma_T \\ \sigma_T & \sigma_L \end{pmatrix} = \frac{1}{\sigma_0} \begin{pmatrix} 1 & -\omega_c \tau \\ \omega_c \tau & 1 \end{pmatrix}$$

# Hall effect

The full conductivity tensor

$$\sigma = ne\mu \begin{pmatrix} \frac{1}{1+s^2} & \frac{-s}{1+s^2} & 0 \\ s & 1 & 0 \\ \frac{1}{1+s^2} & \frac{1}{1+s^2} & 0 \\ 0 & 0 & 1 \end{pmatrix}$$

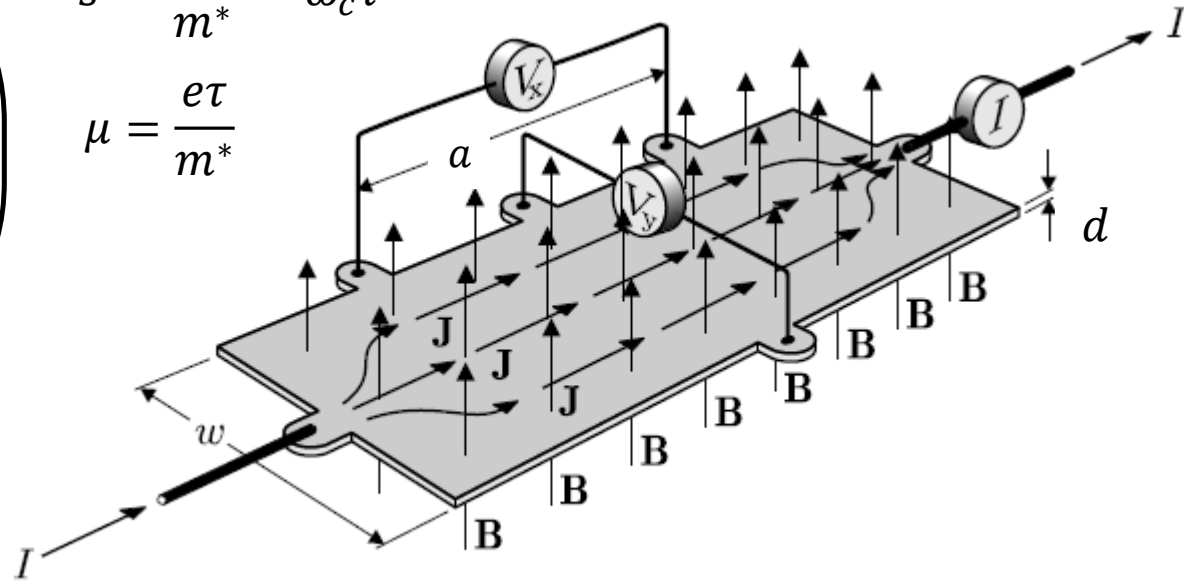
The full resistivity tensor

$$\rho = \sigma^{-1} = \frac{1}{ne\mu} \begin{pmatrix} 1 & s & 0 \\ -s & 1 & 0 \\ 0 & 0 & 1 \end{pmatrix}$$

$$\vec{E} = \rho \vec{j} = \begin{bmatrix} \frac{j_x}{ne\mu} \\ \frac{j_x B}{ne} \\ 0 \end{bmatrix}$$

$$s = \frac{eB\tau}{m^*} = \omega_c \tau$$

$$\mu = \frac{e\tau}{m^*}$$



$$U_{xy} = E_y w = \frac{I_x B}{wd ne} w = \frac{I_x}{dne} B = R_H \frac{I_x B}{d}$$

$$R_H = \frac{1}{ne} \quad \text{Hall constant}$$

# Hall effect

The full conductivity tensor

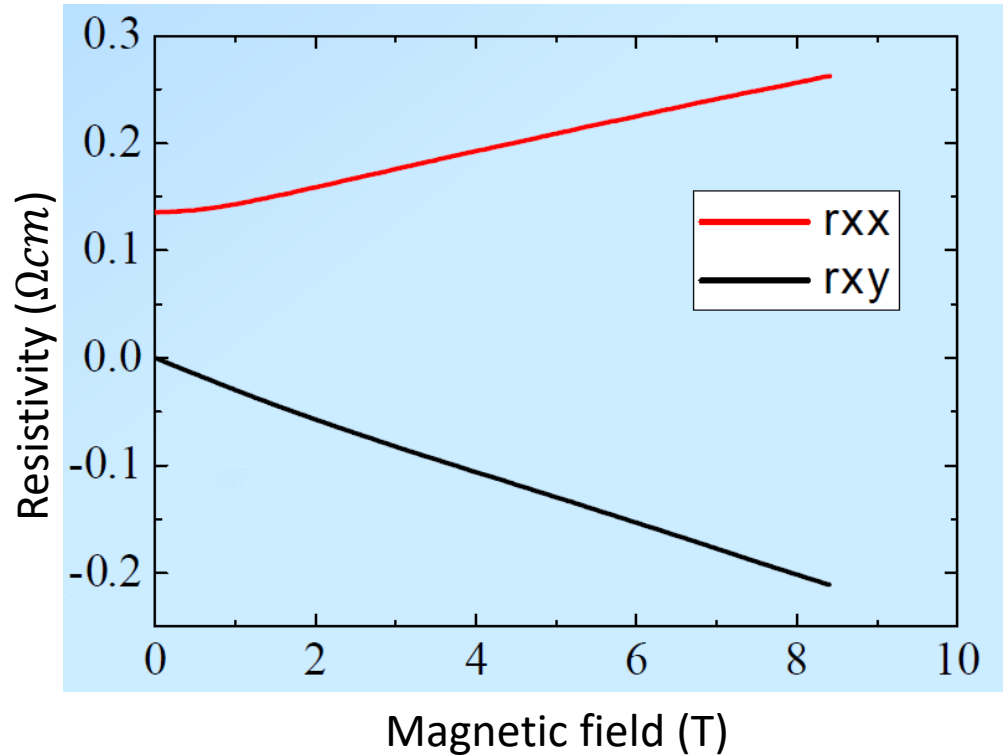
$$\sigma = ne\mu \begin{pmatrix} \frac{1}{1+s^2} & \frac{-s}{1+s^2} & 0 \\ s & 1 & 0 \\ \frac{1}{1+s^2} & \frac{1}{1+s^2} & 0 \\ 0 & 0 & 1 \end{pmatrix}$$

The full resistivity tensor

$$\rho = \sigma^{-1} = \frac{1}{ne\mu} \begin{pmatrix} 1 & s & 0 \\ -s & 1 & 0 \\ 0 & 0 & 1 \end{pmatrix}$$

For the different conductivity channels:

$$\sigma = \sum_i \sigma_i \quad \text{Multi-carrier transport – we analyse the tensor } \sigma$$



# Hall effect

The full conductivity tensor

$$\sigma = ne\mu \begin{pmatrix} \frac{1}{1+s^2} & \frac{-s}{1+s^2} & 0 \\ s & 1 & 0 \\ \frac{1}{1+s^2} & \frac{1}{1+s^2} & 0 \\ 0 & 0 & 1 \end{pmatrix}$$

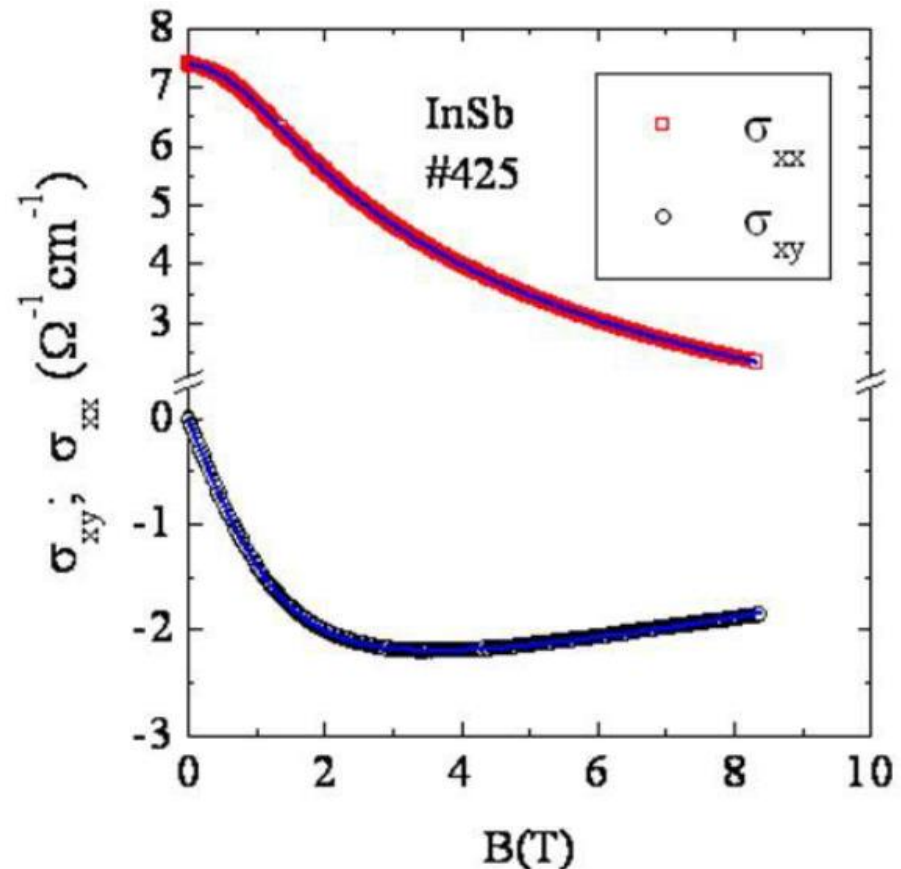
The full resistivity tensor

$$\rho = \sigma^{-1} = \frac{1}{ne\mu} \begin{pmatrix} 1 & s & 0 \\ -s & 1 & 0 \\ 0 & 0 & 1 \end{pmatrix}$$

For the different conductivity channels:

$$\sigma = \sum_i \sigma_i \quad \text{Multi-carrier transport}$$

$$R_H = \frac{1}{ne}$$



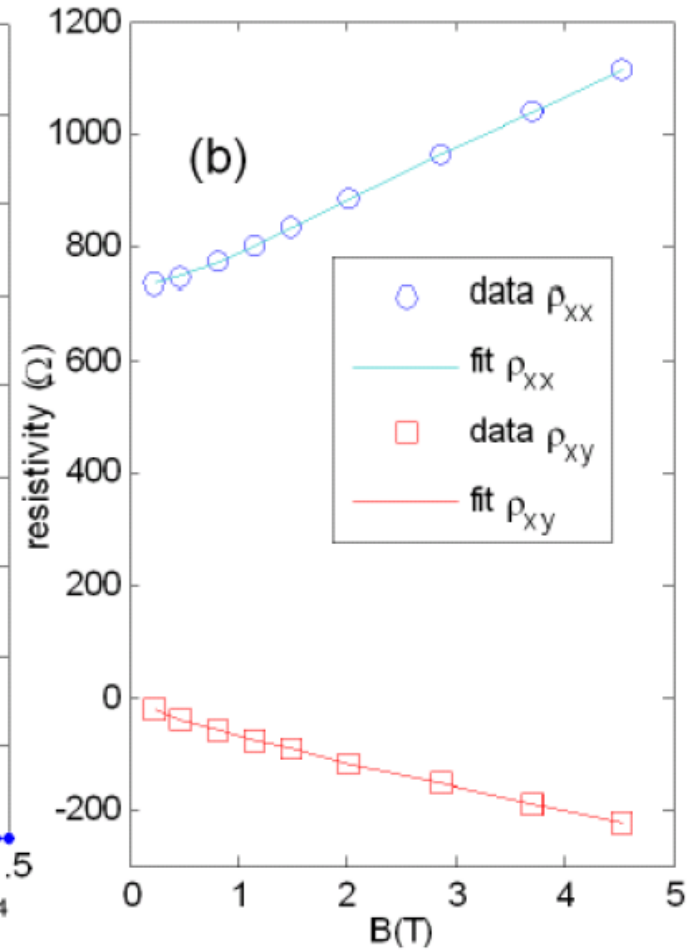
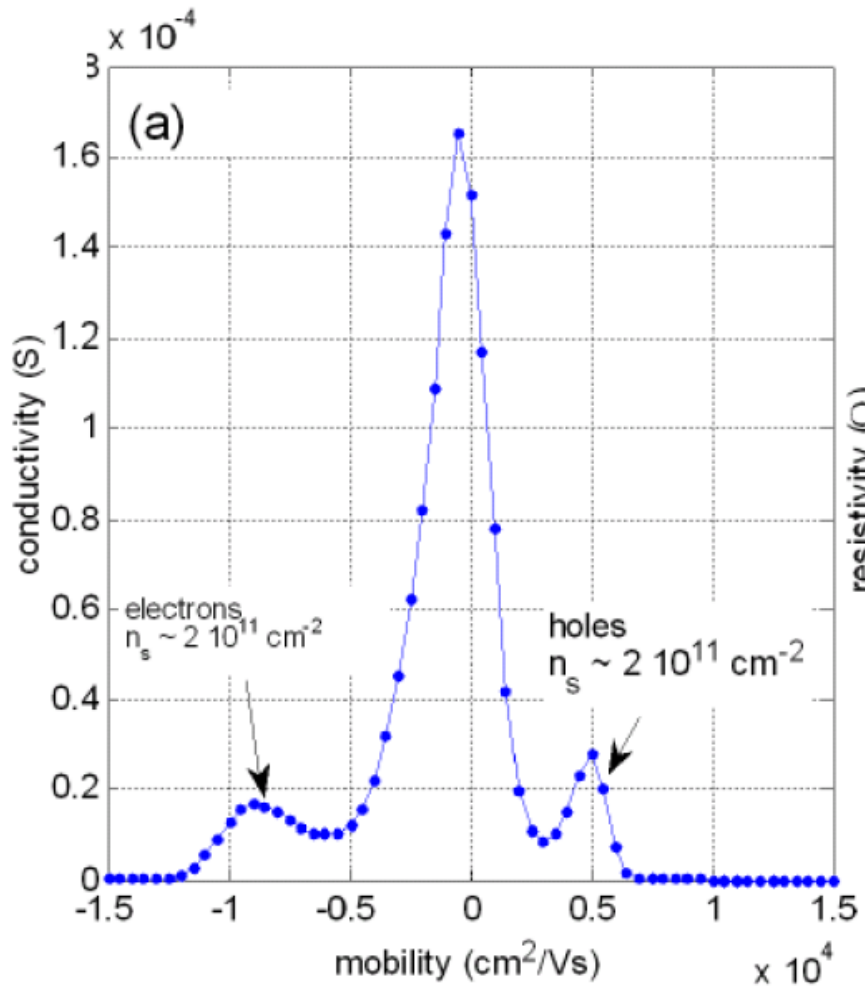
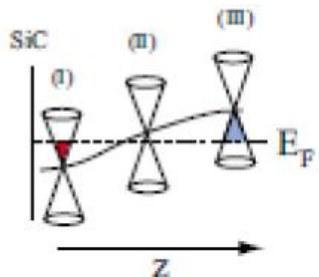
$$n_1 = (1.483 \pm 0.004) 10^{16} \quad \mu_1 = (1361 \pm 5) \text{ cm}^2/\text{Vs}$$

$$n_2 = (4.60 \pm 0.02) 10^{15} \quad \mu_2 = (4622.6 \pm 9.5) \text{ cm}^2/\text{Vs}$$

$$p = (1.77 \pm 0.06) 10^{16} \quad \mu_h = (255 \pm 7) \text{ cm}^2/\text{Vs}$$



# Hall effect



Multi-carrier transport in graphene (M. Gryglas-Borysiewicz)

# Hall effect

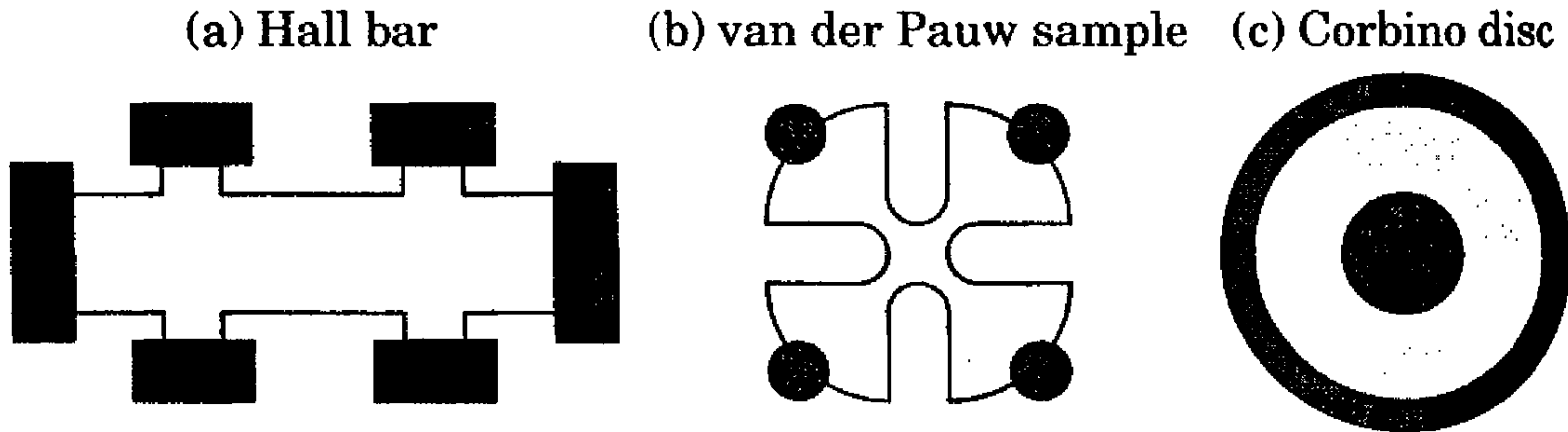


**FIGURE 6.5.** Samples commonly used for measuring the conductivity of semiconductors: (a) Hall bar, (b) van der Pauw sample, and (c) Corbino disc. The dark areas are the contacts for measuring voltage or current, and the light areas are the active regions of the sample.

$$\sigma = ne\mu \begin{pmatrix} \frac{1}{1+s^2} & \frac{-s}{1+s^2} & 0 \\ s & 1 & 0 \\ \frac{1}{1+s^2} & \frac{-s}{1+s^2} & 0 \\ 0 & 0 & 1 \end{pmatrix}$$

$$s = \frac{eB\tau}{m^*} = \omega_c\tau$$

$$\mu = \frac{e\tau}{m^*}$$

# Hall effect

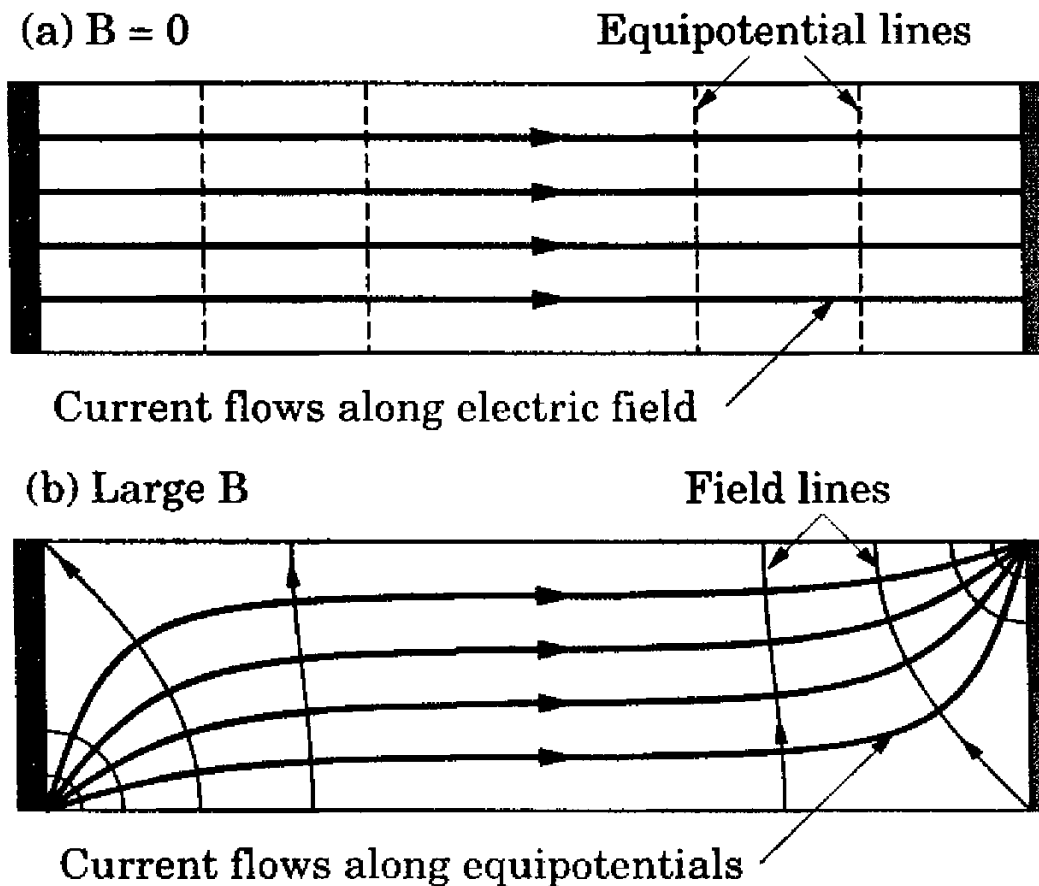


**FIGURE 6.6.** Electric field, current flow, and equipotentials inside a long rectangular sample with contacts across each end. (a) In the absence of an electric field the current is uniform throughout the sample and runs along the electric field. (b) In a strong magnetic field, where  $|\sigma_T| \gg \sigma_L$ , the current runs along equipotentials.

# Shubnikov-de Haas effect

## Shubnikov-de Haas effect

Density of states oscillates - falls to 0 for  $\nu = n$  and is highest for  $\nu \approx n + \frac{1}{2}$  - the easiest measurement is the magnetoresistance  $R_{xx}$ .

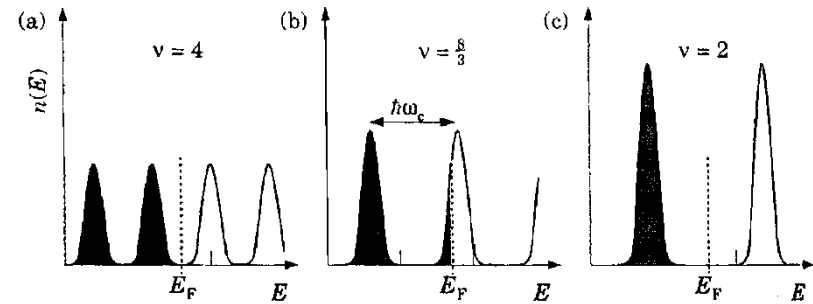


FIGURE 6.8. Occupation of Landau levels in a magnetic field neglecting the spin splitting, showing how the Fermi level moves to maintain a constant density of electrons. The fields are in the ratio

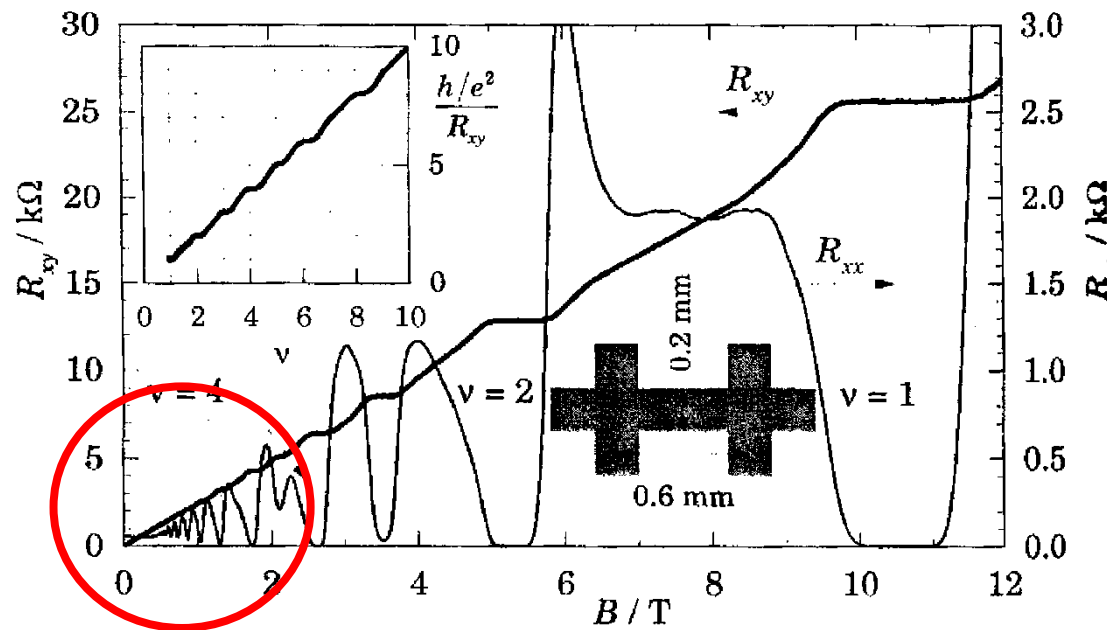


FIGURE 6.10. Longitudinal and transverse (Hall) resistivity,  $R_{xx}$  and  $R_{xy}$ , of a two-dimensional electron gas of density  $n_{2D} = 2.6 \times 10^{15} \text{ nm}^{-2}$  as a function of magnetic field. The measurements were made at  $T = 1.13 \text{ K}$ . The inset shows  $1/R_{xx}$  divided by the quantum unit of conductance  $e^2/h$  as a function of the filling factor  $\nu$ . [Data kindly supplied by Dr A. R. Long, University of Glasgow.]



# Integer Quantum Hall Effect (IQHE)

Integer Quantum Hall effect (IQHE) – for 2D gas: if the Fermi level is located in localized states the Hall resistance (*opór hallowski*) is quantized

$$R_H = \frac{1}{\nu} \frac{h}{e^2}$$

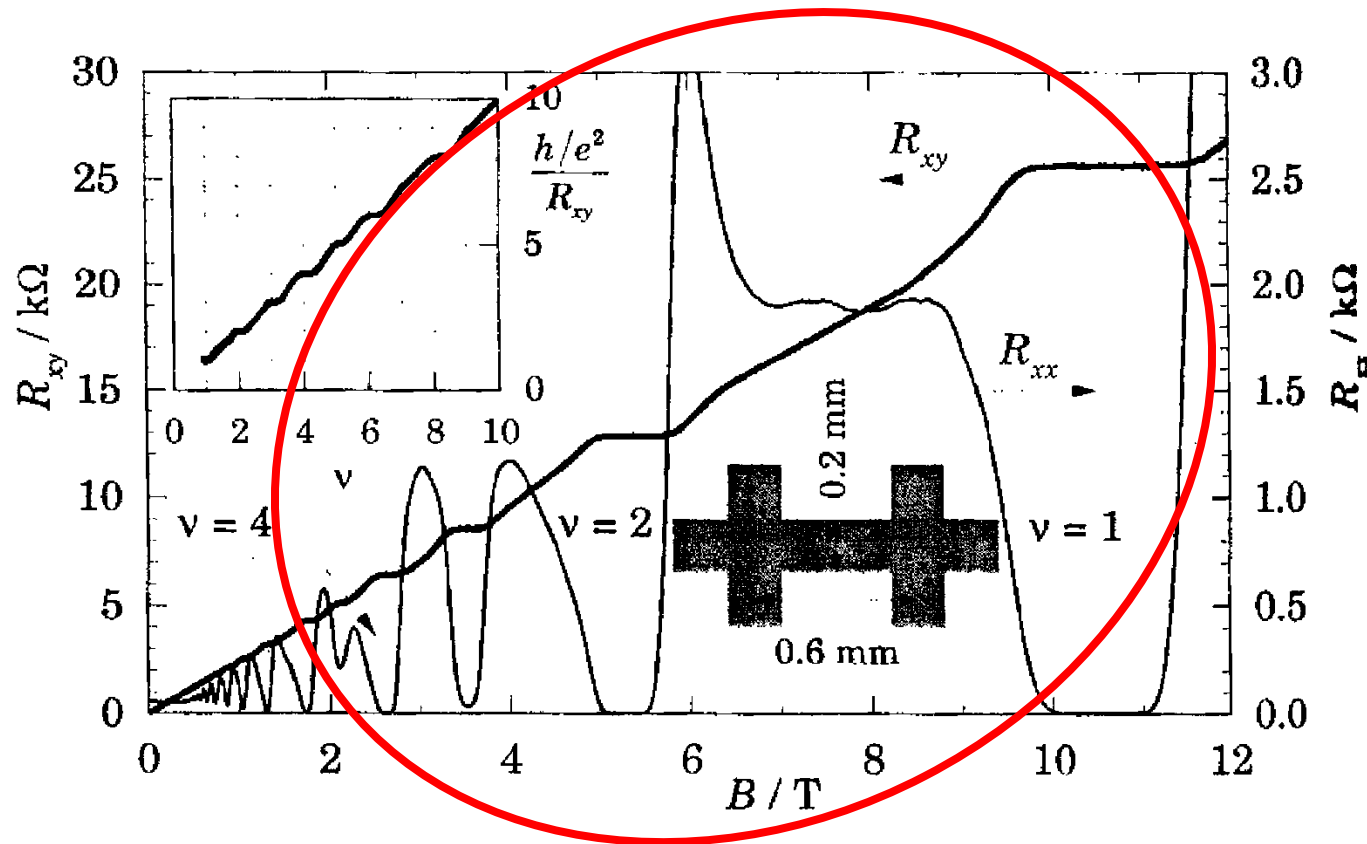


**FIGURE 6.10.** Longitudinal and transverse (Hall) resistivity,  $R_{xx}$  and  $R_{xy}$ , of a two-dimensional electron gas of density  $n_{2D} = 2.6 \times 10^{15} \text{ nm}^{-2}$  as a function of magnetic field. The measurements were made at  $T = 1.13 \text{ K}$ . The inset shows  $1/R_{xx}$  divided by the quantum unit of conductance  $e^2/h$  as a function of the filling factor  $\nu$ . [Data kindly supplied by Dr A. R. Long, University of Glasgow.]

# Integer Quantum Hall Effect (IQHE)

Integer Quantum Hall effect (IQHE) – for 2D gas: if the Fermi level is located in localized states the Hall resistance (*opór hallowski*) is quantized

$$R_H = \frac{1}{\nu} \frac{h}{e^2}$$

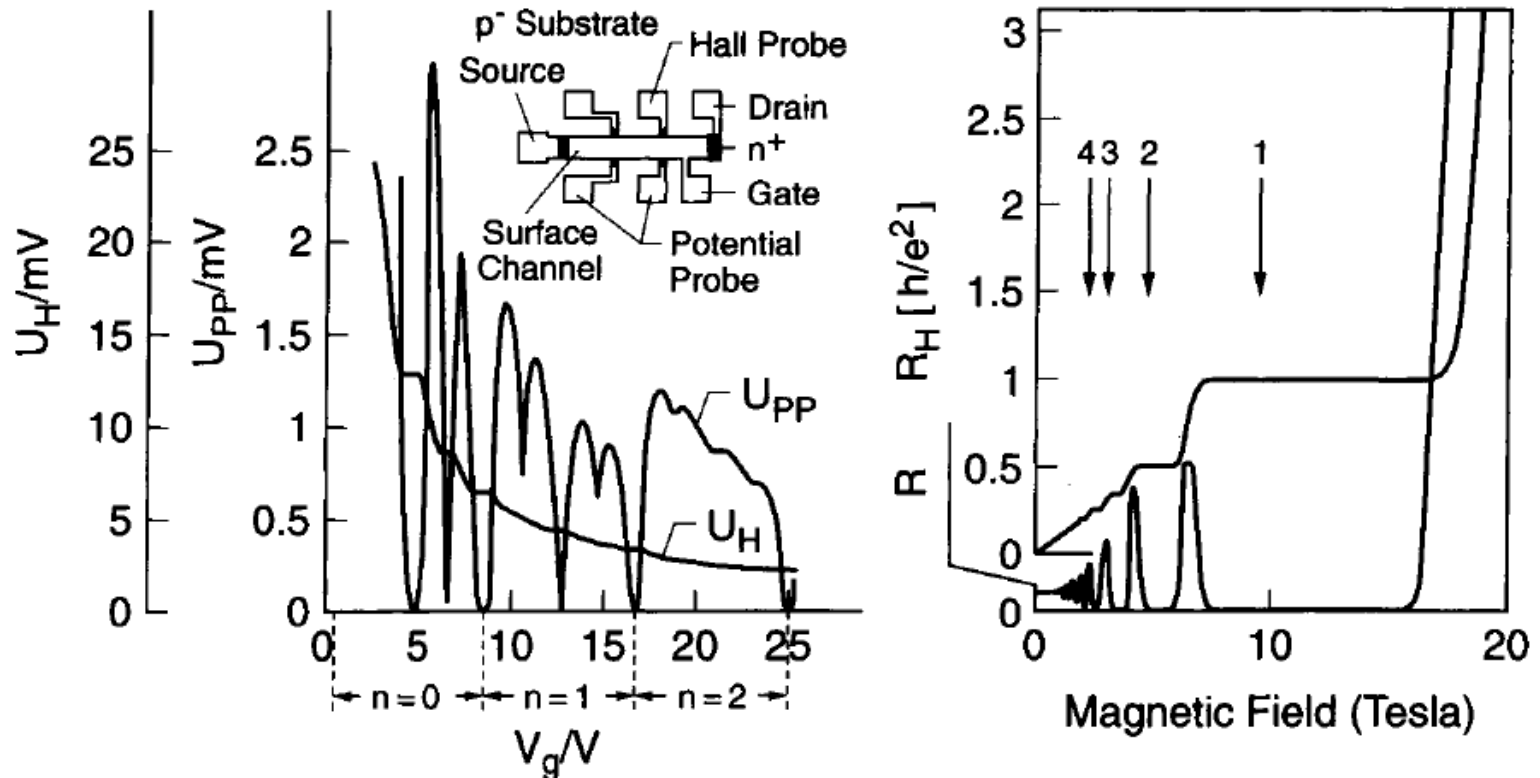


Figure 7. Left panel: original data of the discovery of the integral quantum Hall effect (IQHE) by Klaus von Klitzing in 1980 in the two-dimensional electron system of a silicon MOSFET transistor. Instead of a smooth curve he observed plateaus in the Hall voltage ( $U_H$ ) and found concomitant deep minima in the magneto resistance ( $U_{PP}$ ). The horizontal axis represents gate voltage ( $V_G$ ) which varies the carrier density,  $n$ . The right panel shows equivalent data taken on a two-dimensional electron system in GaAs/AlGaAs. Since these data are plotted versus magnetic field they can directly be compared to Edwin Hall's data of Fig. 6. Rather than the linear dependence of the Hall resistance on magnetic field of Fig. 6, these data show wide plateaus in  $R_H$  and in addition deep minima in  $R$ .

Stromer, Nobel Lecture

# Quantum Hall Effect



The Nobel Prize in Physics 1985  
Klaus von Klitzing

The Nobel Prize in Physics 1985

Nobel Prize Award Ceremony

Klaus von Klitzing



Klaus von Klitzing

The Nobel Prize in Physics 1985 was awarded to Klaus von Klitzing *"for the discovery of the quantized Hall effect"*.

# Quantum Hall Effect



## The Nobel Prize in Physics 1998

Robert B. Laughlin, Horst L. Störmer, Daniel C. Tsui

The Nobel Prize in Physics 1998

Nobel Prize Award Ceremony

Robert B. Laughlin

Horst L. Störmer

Daniel C. Tsui



Robert B. Laughlin



Horst L. Störmer



Daniel C. Tsui

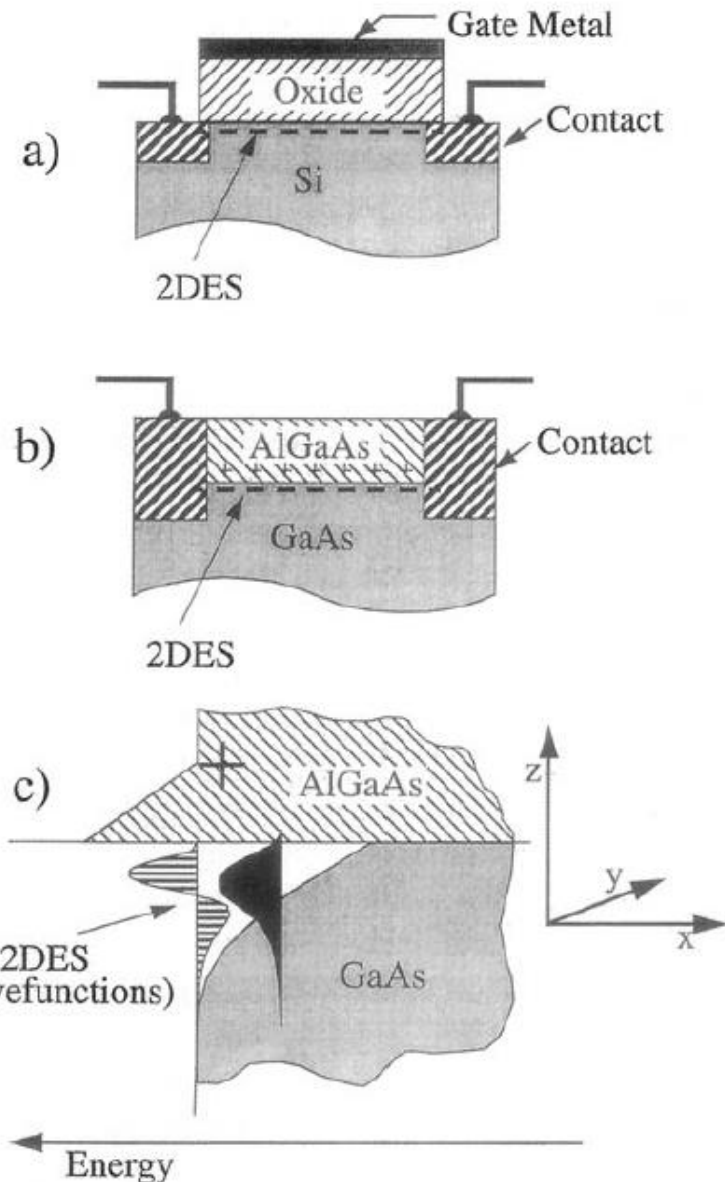
The Nobel Prize in Physics 1998 was awarded jointly to Robert B. Laughlin, Horst L. Störmer and Daniel C. Tsui *"for their discovery of a new form of quantum fluid with fractionally charged excitations"*.



# Quantum Hall Effect

## Integer Quantum Hall effect (IQHE)

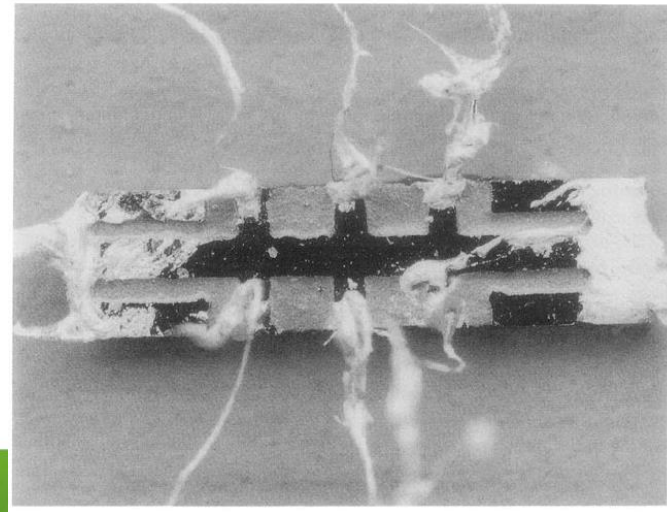
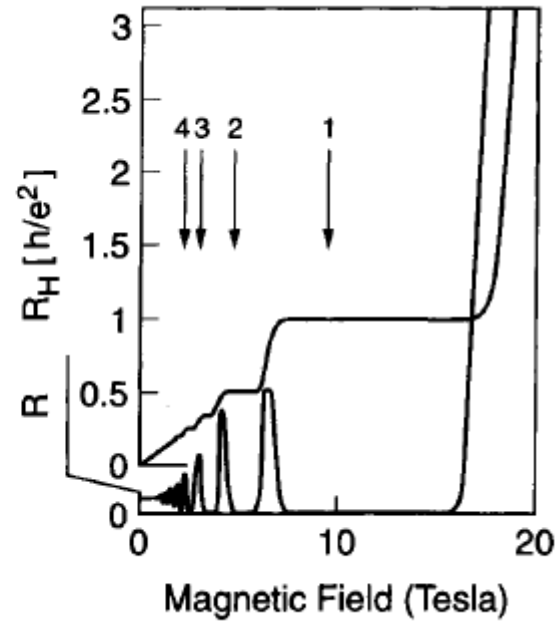
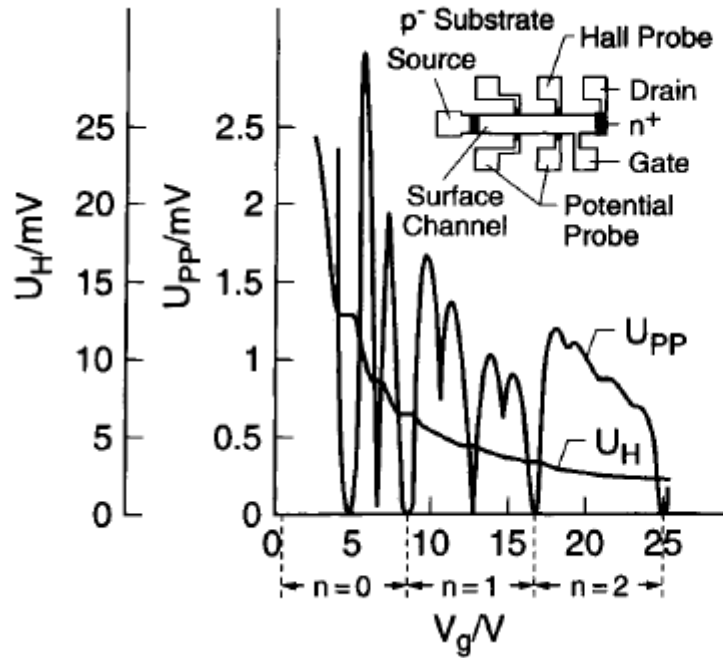
Figure 1 a). Schematic drawings of a silicon Metal Oxide Semiconductor Field Effect Transistor (MOSFET). The two-dimensional electron system (2DES) resides at the interface between silicon and silicon oxide. Electrons are held against the oxide by the electric field from the gate metal. b) Schematic drawings of a modulation-doped gallium arsenide/aluminum gallium arsenide (GaAs/AlGaAs) heterojunction. The 2DES resides at the interface between GaAs and AlGaAs. Electrons are held against the AlGaAs by the electric field from the charged silicon dopants (+) in the AlGaAs. c). Energetic condition in the modulation-doped structure (very similar to the condition in the MOSFET). Energy increases to the left. Electrons are trapped in the triangular-shaped quantum-well at the interface. They assume discrete energy states in the z-direction (black and horizontally striped). At low temperatures and low electron concentration only the lowest (black) electron state is occupied. The electrons are totally confined in the z-direction but can move freely in the x-y-plane.



Horst Stormer, *Nobel Lecture*



# Quantum Hall Effect



Horst Stormer, *Nobel Lecture*

# Quantum Hall Effect

VOLUME 45, NUMBER 6

PHYSICAL REVIEW LETTERS

11 AUGUST 1980

## New Method for High-Accuracy Determination of the Fine-Structure Constant Based on Quantized Hall Resistance

K. v. Klitzing

Physikalisches Institut der Universität Würzburg, D-8700 Würzburg, Federal Republic of Germany, and  
Hochfeld-Magnetlabor des Max-Planck-Instituts für Festkörperforschung, F-38042 Grenoble, France

and

G. Dorda

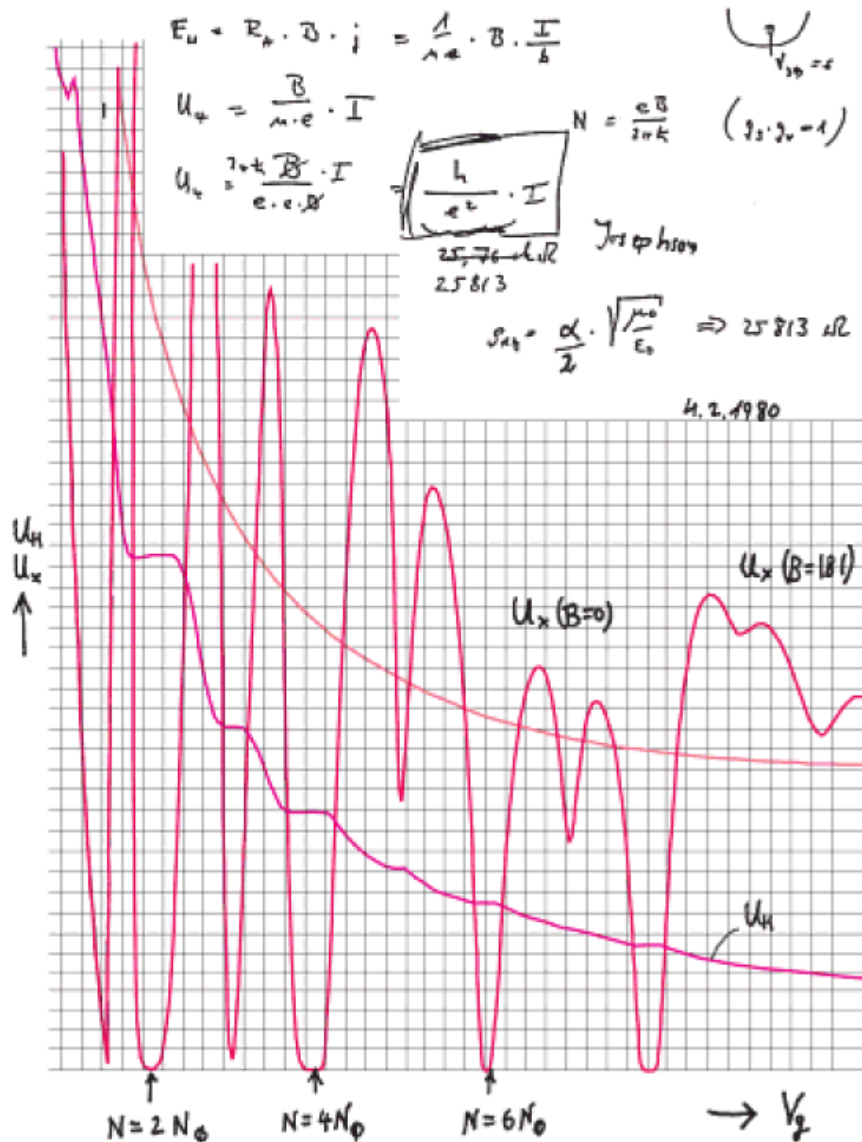
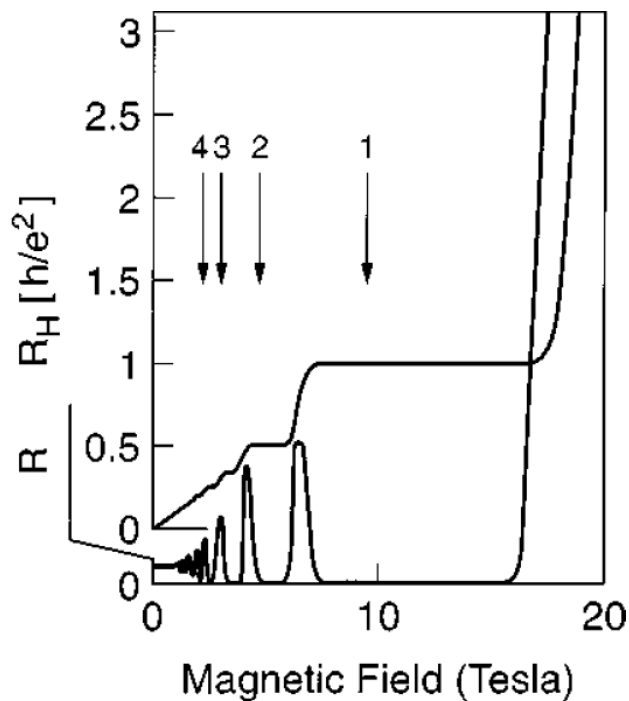
Forschungslaboratorien der Siemens AG, D-8000 München, Federal Republic of Germany

and

M. Pepper

Cavendish Laboratory, Cambridge CB3 0HE, United Kingdom

(Received 30 May 1980)



# Quantum Hall Effect

VOLUME 45, NUMBER 6

PHYSICAL REVIEW LETTERS

11 AUGUST 1980

## New Method for High-Accuracy Determination of the Fine-Structure Constant Based on Quantized Hall Resistance

K. v. Klitzing

*Physikalisches Institut der Universität Würzburg, D-8700 Würzburg, Federal Republic of Germany, and  
Hochfeld-Magnetlabor des Max-Planck-Instituts für Festkörperforschung, F-38042 Grenoble, France*

and

G. Dorda

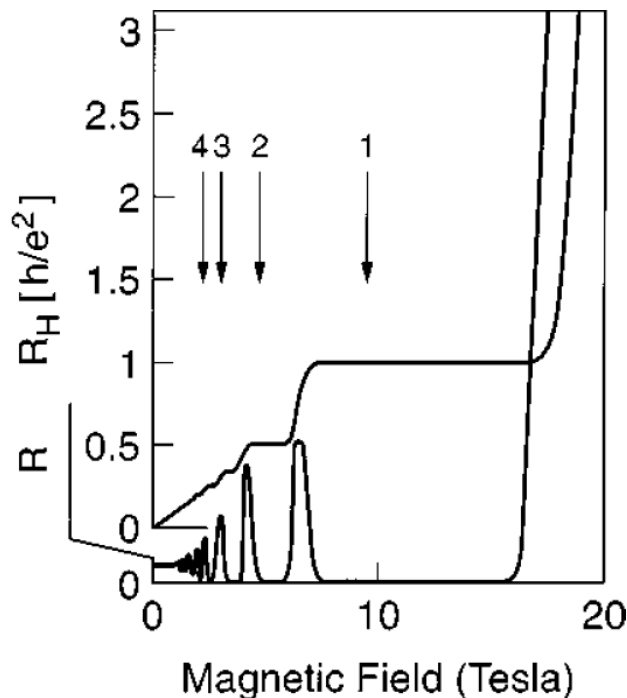
*Forschungslaboratorien der Siemens AG, D-8000 München, Federal Republic of Germany*

and

M. Pepper

*Cavendish Laboratory, Cambridge CB3 0HE, United Kingdom*

(Received 30 May 1980)



## Conductivity tensor

$$\sigma = \begin{pmatrix} \sigma_L & -\sigma_T \\ \sigma_T & \sigma_L \end{pmatrix} = \frac{\sigma_0}{1 + \omega_c^2 \tau^2} \begin{pmatrix} 1 & \omega_c \tau \\ -\omega_c \tau & 1 \end{pmatrix}$$

## Full resistivity tensor

$$\rho = \sigma^{-1} = \frac{1}{ne\mu} \begin{pmatrix} 1 & -s & 0 \\ s & 1 & 0 \\ 0 & 0 & 1 \end{pmatrix}$$

$$\rho = \frac{1}{\sigma_L^2 + \sigma_T^2} \begin{pmatrix} \sigma_L & -\sigma_T \\ \sigma_T & \sigma_L \end{pmatrix} = \frac{1}{\sigma_0} \begin{pmatrix} 1 & -\omega_c \tau \\ \omega_c \tau & 1 \end{pmatrix}$$

For large magnetic fields  $|\sigma_T| \gg \sigma_L$

$$\rho = \frac{1}{\sigma_L^2 + \sigma_T^2} \begin{pmatrix} \sigma_L & -\sigma_T \\ \sigma_T & \sigma_L \end{pmatrix} \approx \begin{pmatrix} \sigma_L/\sigma_T^2 & -1/\sigma_T \\ 1/\sigma_T & \sigma_L/\sigma_T^2 \end{pmatrix}$$

thus  $\rho \sim \sigma_L$  !

# Hall Effect

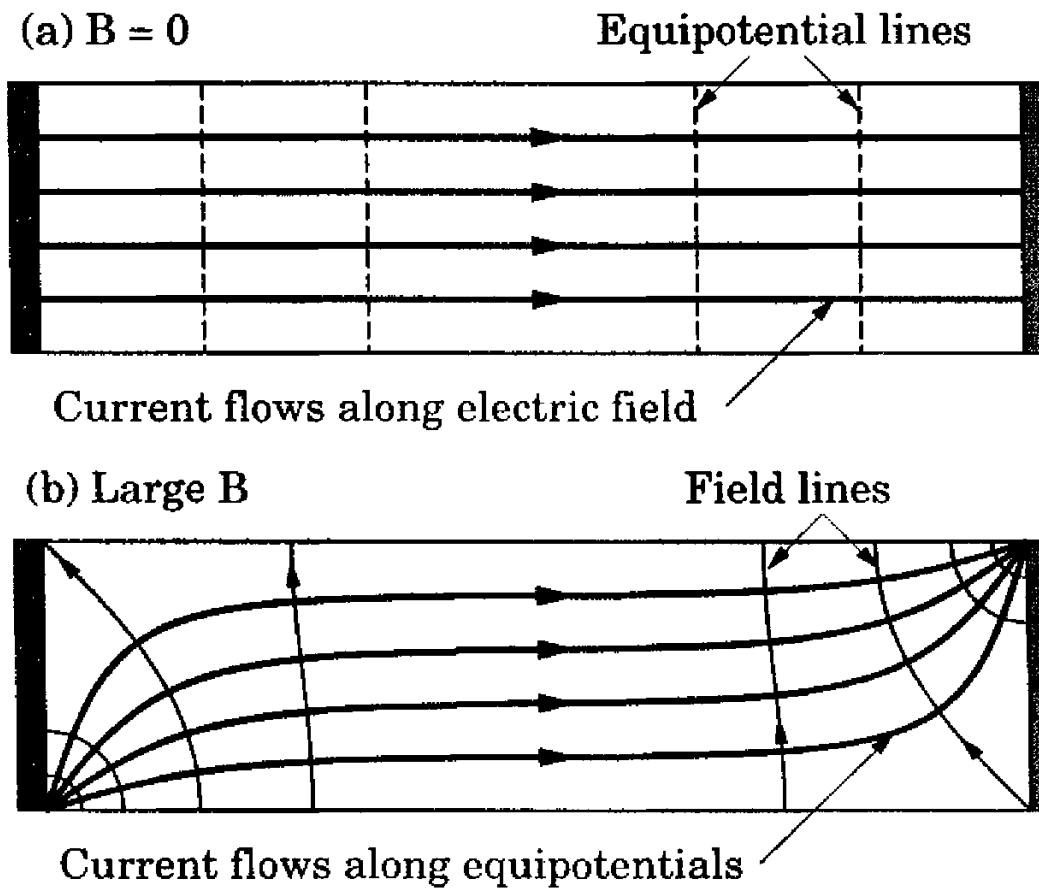


**FIGURE 6.6.** Electric field, current flow, and equipotentials inside a long rectangular sample with contacts across each end. (a) In the absence of an electric field the current is uniform throughout the sample and runs along the electric field. (b) In a strong magnetic field, where  $|\sigma_T| \gg \sigma_L$ , the current runs along equipotentials.



# Quantized conductance

$$G = \frac{dI}{dU} = \frac{2e^2}{h} \int_{E_L}^{\infty} \frac{\partial f(E, \mu)}{\partial E} T(E) dE \approx \frac{2e^2}{h} T(\mu) = G_0 T(\mu)$$

$$\frac{e^2}{h} = 38,7 \mu S$$

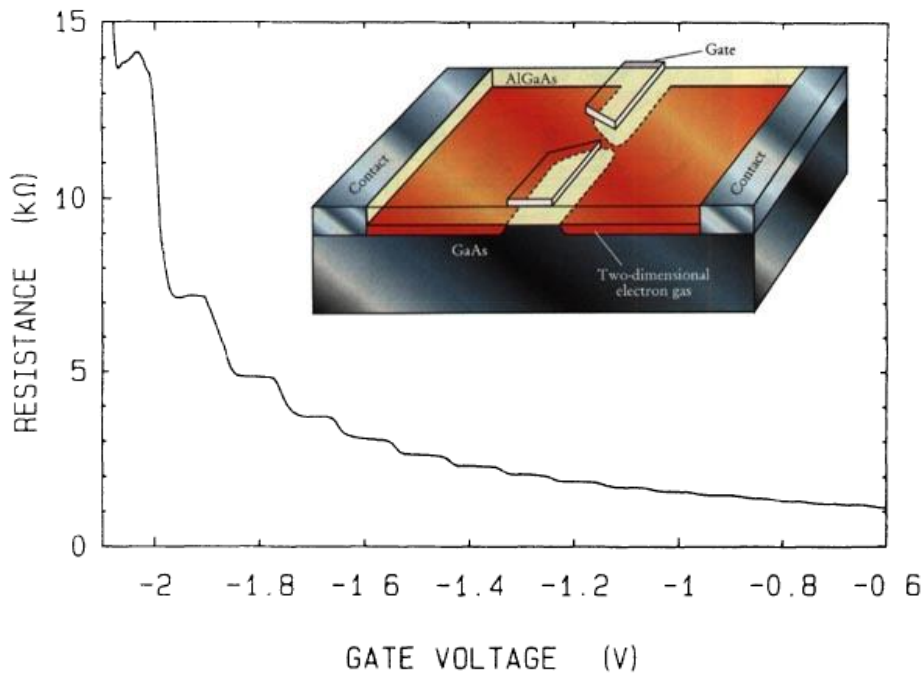


FIG. 1. Point-contact resistance as a function of gate voltage at 0.6 K. Inset: Point-contact layout.

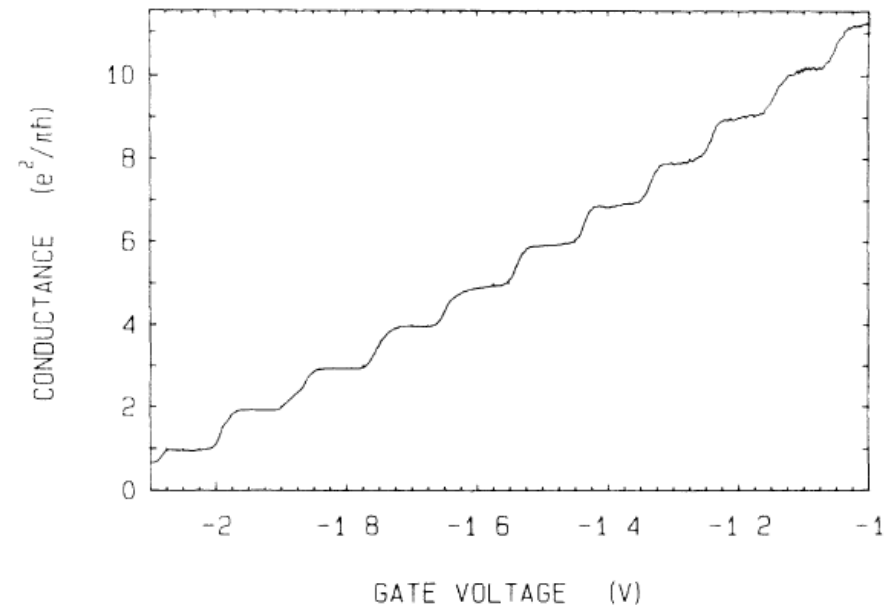


FIG. 2. Point-contact conductance as a function of gate voltage, obtained from the data of Fig. 1. The conductance is a function of the lead resistance. The plateaus are at multiples of  $e^2/\pi h$ .

**Reminder**

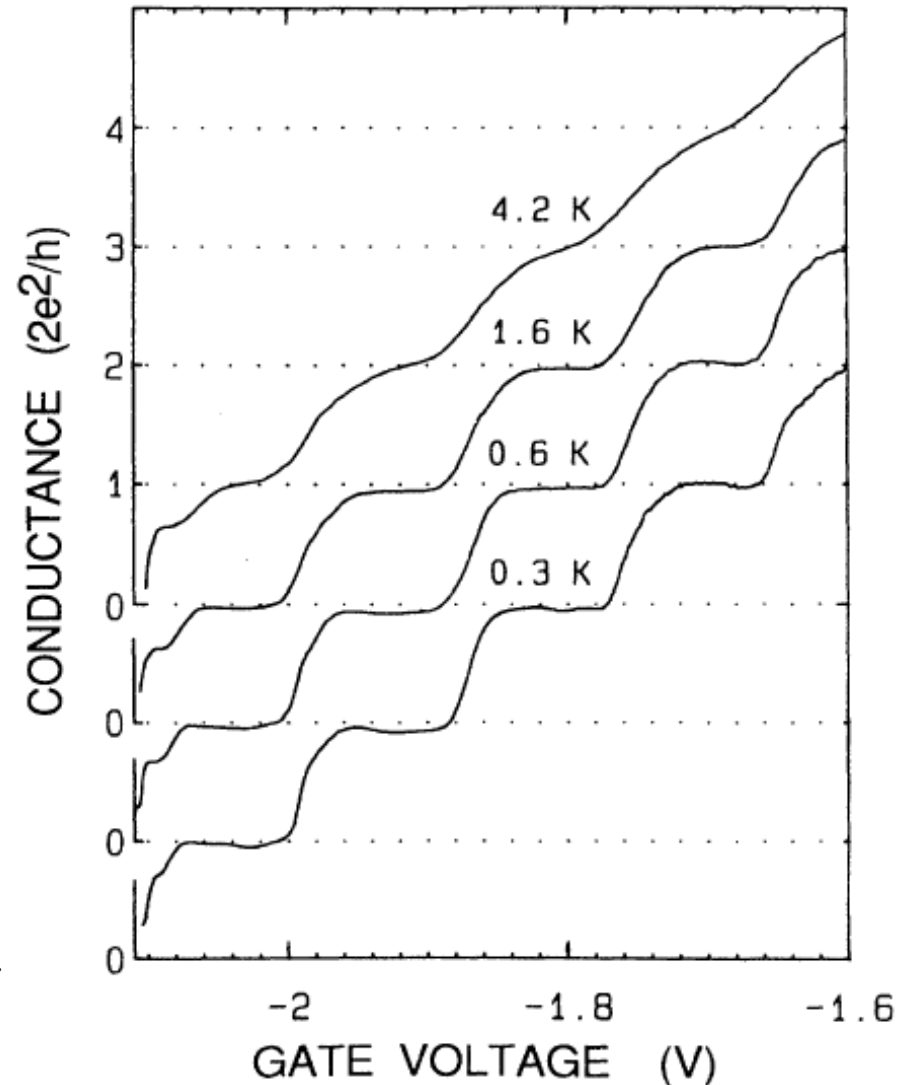
B. J. van Wees et al. *Quantized conductance of point contacts in a two-dimensional electron gas*. Phys. Rev. Lett. **60**, 848–850 (1988)



# Quantized conductance

$$G = \frac{2e^2}{h} T(\mu) = G_0 T(\mu)$$

Reminder



B. J. van Wees et al. *Quantum ballistic and adiabatic electron transport studied with quantum point contacts* Phys. Rev. B 43, 12431–12453 (1991)

FIG. 6. Breakdown of the conductance quantization due to temperature averaging. The curves have been offset for clarity.

# Electric and magnetic fields

Motion of the electron in crossed fields: electric  $\vec{E} = (E, 0, 0)$  and magnetic  $\vec{B} = (0, 0, B)$  is encircled by cycloid :

$$x(t) = -\frac{mE}{eB^2} (1 - \cos \omega_c t)$$

$$y(t) = -\frac{mE}{eB^2} (\omega_c t - \sin \omega_c t)$$

Details of the movement depends on the initial conditions

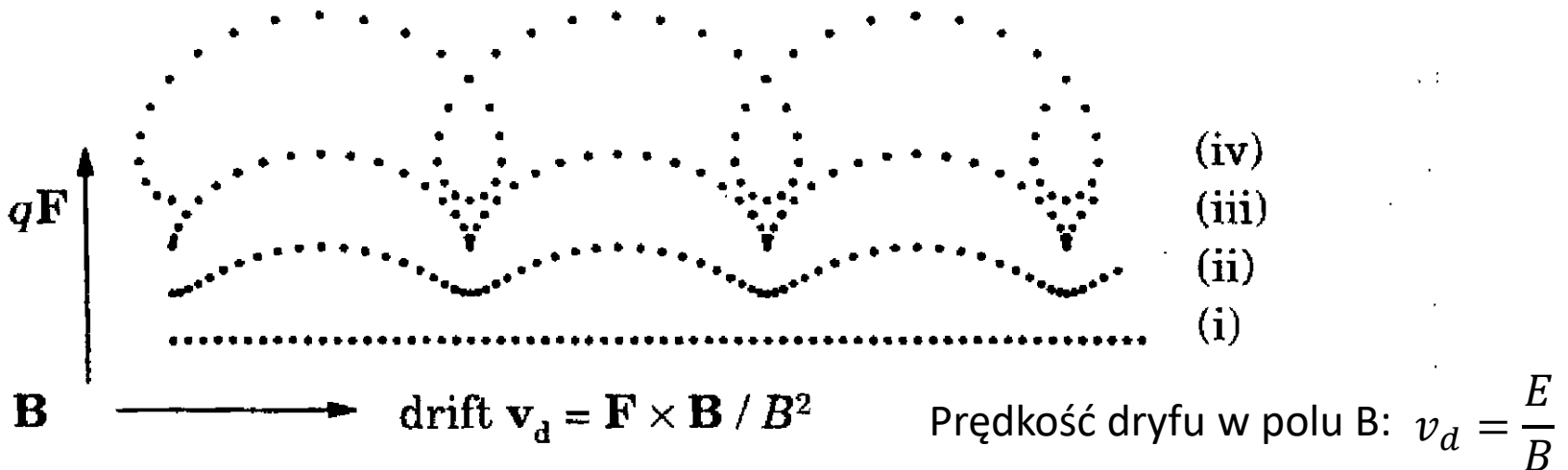


**FIGURE 6.11.** Classical motion of a charged particle in crossed electric and magnetic fields, with  $\mathbf{B}$  normal to the page and equal intervals of time between the symbols. The curves correspond to different initial velocities and energies, with (iii) showing the cycloid for a particle initially at rest.

# Homogenous magnetic field

$$\left[ -\frac{\hbar^2}{2m} \nabla^2 - \frac{ie\hbar}{m} Bx \frac{\partial}{\partial y} + \frac{(eBx)^2}{2m} + U(z) \right] \psi(\vec{r}) = E\psi(\vec{r})$$

Vector potential does not depend on  $y$ , we can assume the function of the form:

$$\psi(\vec{r}) = w(z)u(x) \exp(ik_y y)$$

$$\left[ -\frac{\hbar^2}{2m} \frac{d^2}{dx^2} + \frac{1}{2} m \omega_c^2 \left( x + \frac{\hbar k_y}{eB} \right)^2 \right] u(x) = \varepsilon u(x)$$

$$\omega_c = \left| \frac{eB}{m} \right|$$

$$R_c = \frac{v}{\omega_c} = \frac{\sqrt{2mE}}{|eB|}$$

Cyclotron frequency

Cyclotron radius (*gyroradius*)

$k_y$  wave vector. What interesting in  $\varepsilon$  THERE IS NO  $k_y$ .

The parabolic potential of the form of  $x_k = -\hbar k_y / eB$

**Reminder**

# Electric and magnetic fields

$$\left[ -\frac{\hbar^2}{2m} \nabla^2 - \frac{ie\hbar}{m} Bx \frac{\partial}{\partial y} + \frac{(eBx)^2}{2m} + eEx \right] \psi(\vec{r}) = E\psi(\vec{r})$$

Vector potential does not depend on  $y$ , we can assume:  $\psi(\vec{r}) = w(z)u(x) \exp(ik_y y)$

$$\left[ -\frac{\hbar^2}{2m} \frac{d^2}{dx^2} + \frac{1}{2} m \omega_c^2 \left( x + \frac{\hbar k_y}{eB} + \frac{Ee}{m\omega_c^2} \right)^2 - \frac{\hbar k E}{B} - \frac{mE^2}{2B^2} \right] u(x) = \varepsilon u(x)$$

Factors „added” in order to get  $eE$  after expanding  $(\dots)^2$

Parabolic potential shifted by

$$x_k = - \left( \frac{\hbar k_y}{eB} + \frac{Ee}{m\omega_c^2} \right) = \frac{mv_d - \hbar k}{eB}$$

$$v_d = \frac{E_x}{B_z}$$

$$\begin{aligned} \varepsilon_{nk} &= \left( n - \frac{1}{2} \right) \hbar \omega_c - \frac{\hbar k E}{B} - \frac{mE^2}{2B^2} = \\ &= \left( n - \frac{1}{2} \right) \hbar \omega_c - eE x_k - \frac{1}{2} m v_D^2 \end{aligned}$$

$$J_y = -en_{2D} v_D = en_{2D} \frac{E_x}{B_z} \Rightarrow \sigma_{xx} = \sigma_L = 0$$

$$\rho_T = 1/\sigma_T = B_z/en_{2D} \quad (\text{classical Hall effect})$$

# Electric and magnetic fields

Parabolic potential depends on magnetic field and  $k_y$

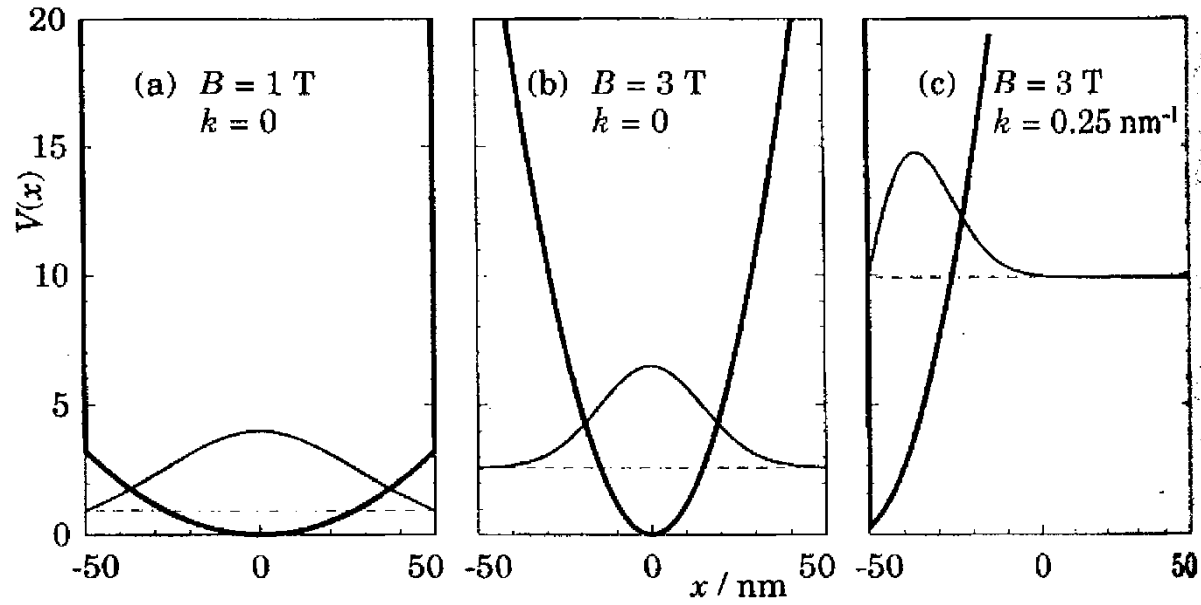
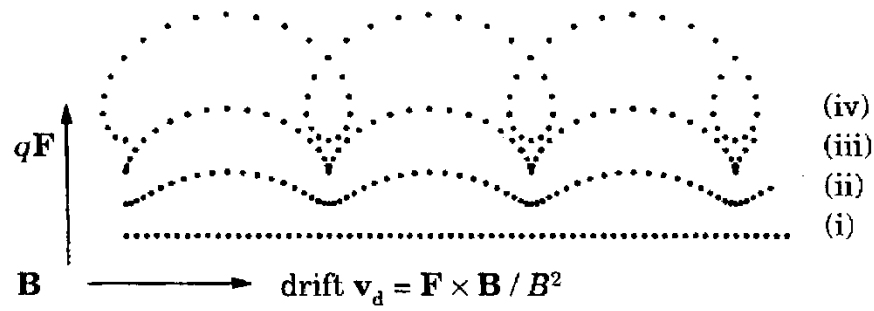


FIGURE 6.13. Potential energy and lowest eigenstate in a magnetic field for an electron with wave number  $k$  in a hard-walled wire of width  $0.1 \mu\text{m}$  in GaAs.



$$v_d = \frac{E}{B}$$

FIGURE 6.11. Classical motion of a charged particle in crossed electric and magnetic fields, with  $\mathbf{B}$  normal to the page and equal intervals of time between the symbols. The curves correspond to different initial velocities and energies, with (iii) showing the cycloid for a particle initially at rest.



# Electric and magnetic fields

Parabolic potential depends on magnetic field and  $k_y$

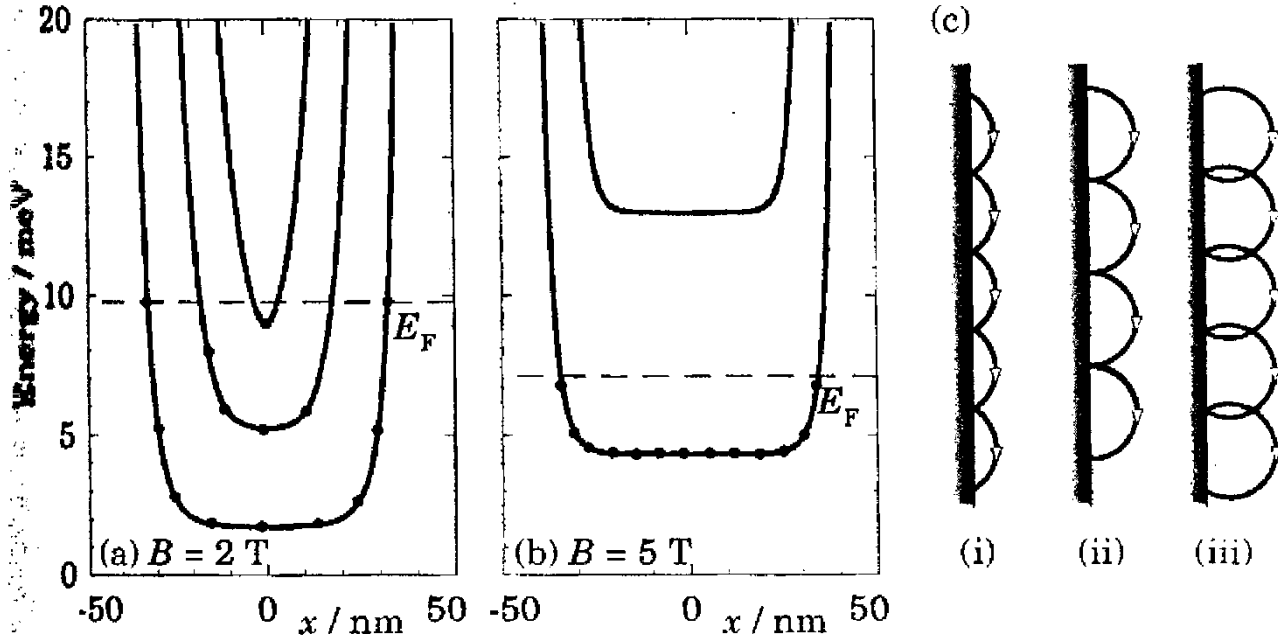
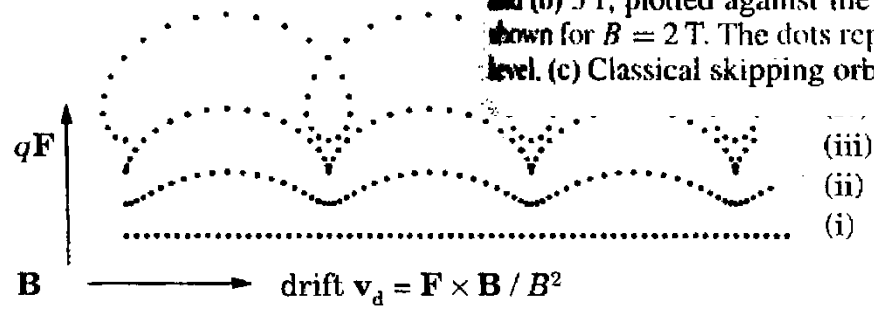


FIGURE 6.14. Energies  $\epsilon_{nk}(B)$  of electrons in a hard-walled wire in a magnetic field of (a) 2 T and (b) 5 T, plotted against the guiding centre  $\langle x_{nk} \rangle$ . For clarity, only the lowest three bands are shown for  $B = 2$  T. The dots represent some of the occupied states and the dashed line is the Fermi level. (c) Classical skipping orbits along the edge of a wire.



$$v_d = \frac{E}{B}$$

FIGURE 6.11. Classical motion of a charged particle in crossed electric and magnetic fields, with  $\mathbf{B}$  normal to the page and equal intervals of time between the symbols. The curves correspond to different initial velocities and energies, with (iii) showing the cycloid for a particle initially at rest.

# Electric and magnetic fields

Parabolic potential depends on magnetic field and  $k_y$

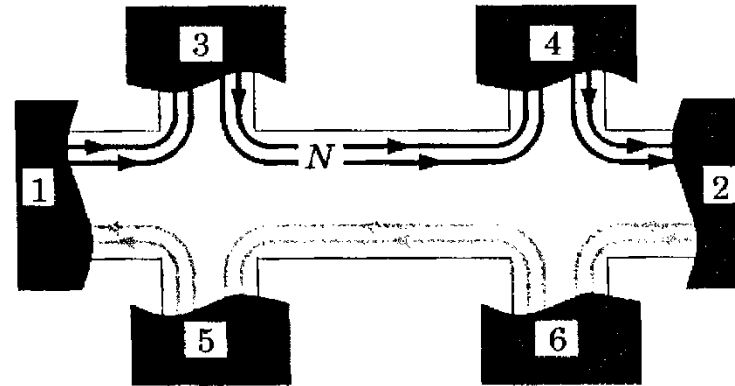


**FIGURE 6.18.** A Hall bar in a strong magnetic field, showing the propagation of edge states. A negative bias on contact 1 injects extra electrons into the  $N$  edge states that leave it (only two of which are drawn); the electrons depart through the other current probe (2).

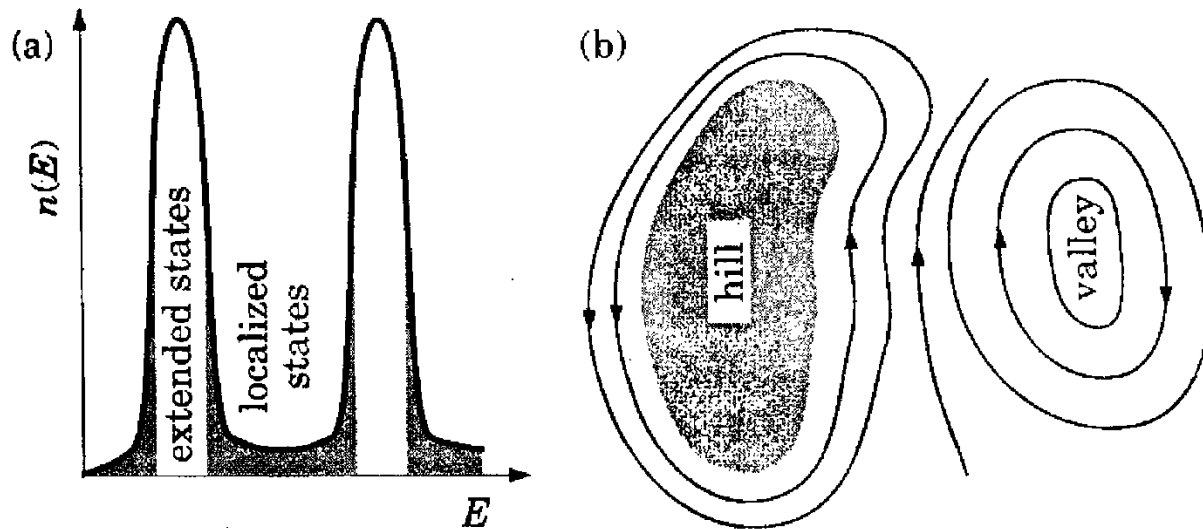


**FIGURE 6.19.** (a) Density of states of a Landau level in a disordered system showing a band of extended states in the centre of each level with localized states in between. (b) Edge states localized in a slowly varying potential, with a hill on the left and a hollow on the right.

# Electric and magnetic fields

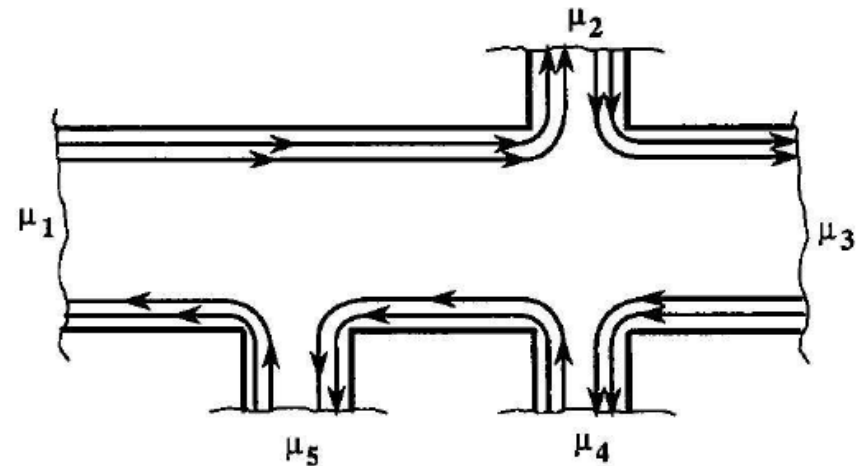
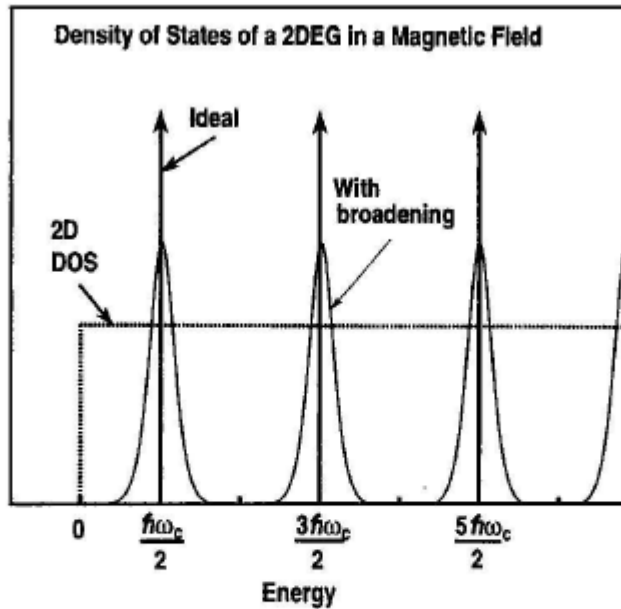


Figure 5.5: Hall bar with five terminals each with chemical potential  $\mu_i$ . The Fermi energy is set in the Quantum Hall regime such that there are two edge-channels connecting the terminals. Picture from Ferry & Goodnick.

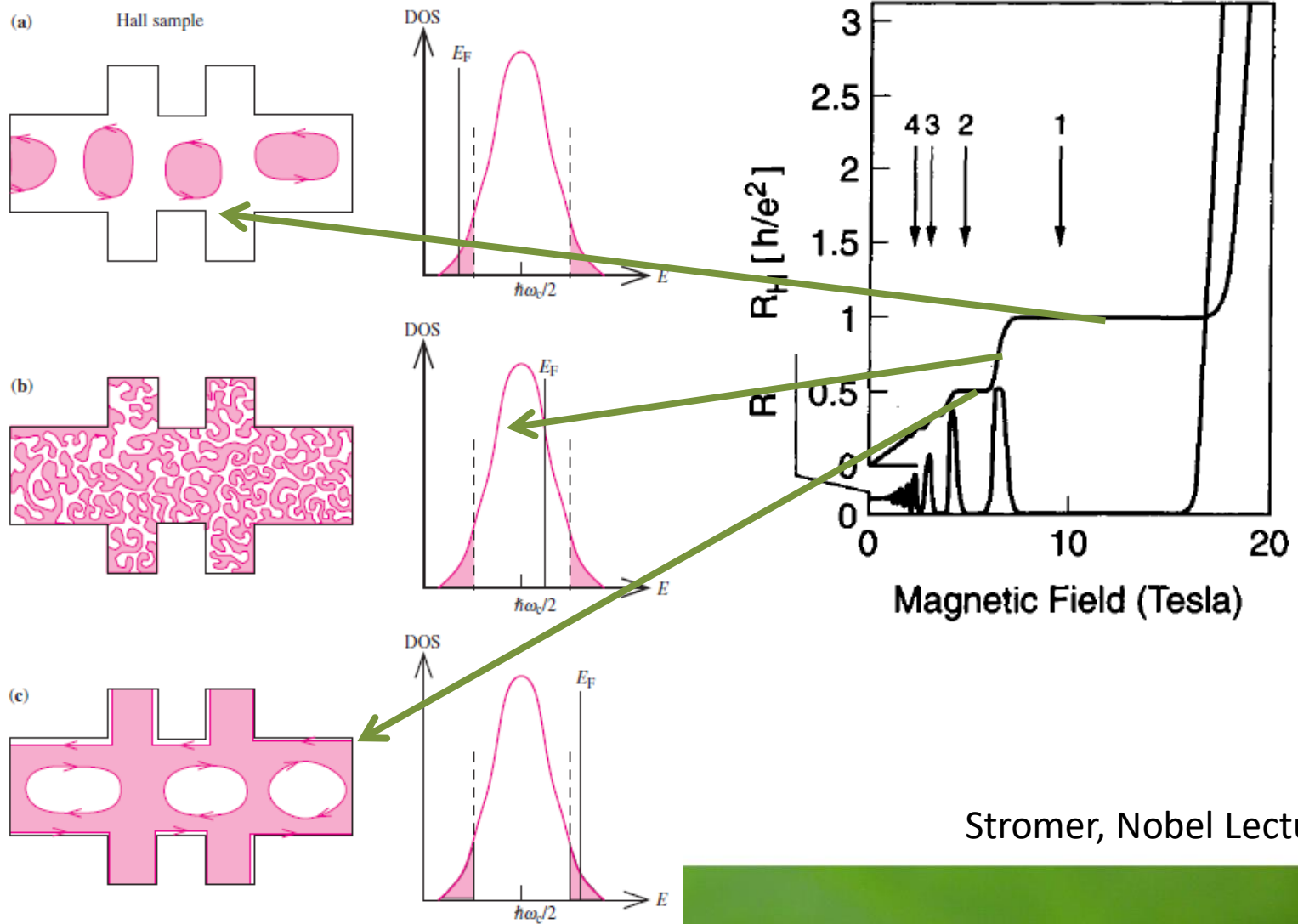
Figure 5.2: Density of states of a 2DEG in magnetic field. By comparing the DOS with and without magnetic field, we can calculate the number of states within each Landau level. From Ferry & Goodnick.

Clive Emary  
Theory of Nanostructures nanoskript.pdf

# Integer Quantum Hall Effect (IQHE)

Integer Quantum Hall effect (IQHE) – for 2D gas: if the Fermi level is located in localized states the Hall resistance (*opór hallowski*) is quantized

$$R_H = \frac{1}{\nu} \frac{h}{e^2}$$



Yu, Cardona

Stromer, Nobel Lecture

# Fractional Quantum Hall Effect (FQHE)

Fractional Quantum Hall Effect (FQHE) – for 2D gas  $\nu \leq 1$ : if the Fermi level is located in localized states the Hall resistance (*opór hallowski*) is quantized

$$R_H = \frac{1}{\nu^*} \frac{h}{e^2}$$

Stromer, Nobel Lecture



# Fractional Quantum Hall Effect (FQHE)

Fractional Quantum Hall Effect (FQHE)  
 Fractional Quantum Hall Effect (FQHE)  
 localized state

$$R_H = \frac{1}{\nu} \frac{h}{e^2}$$

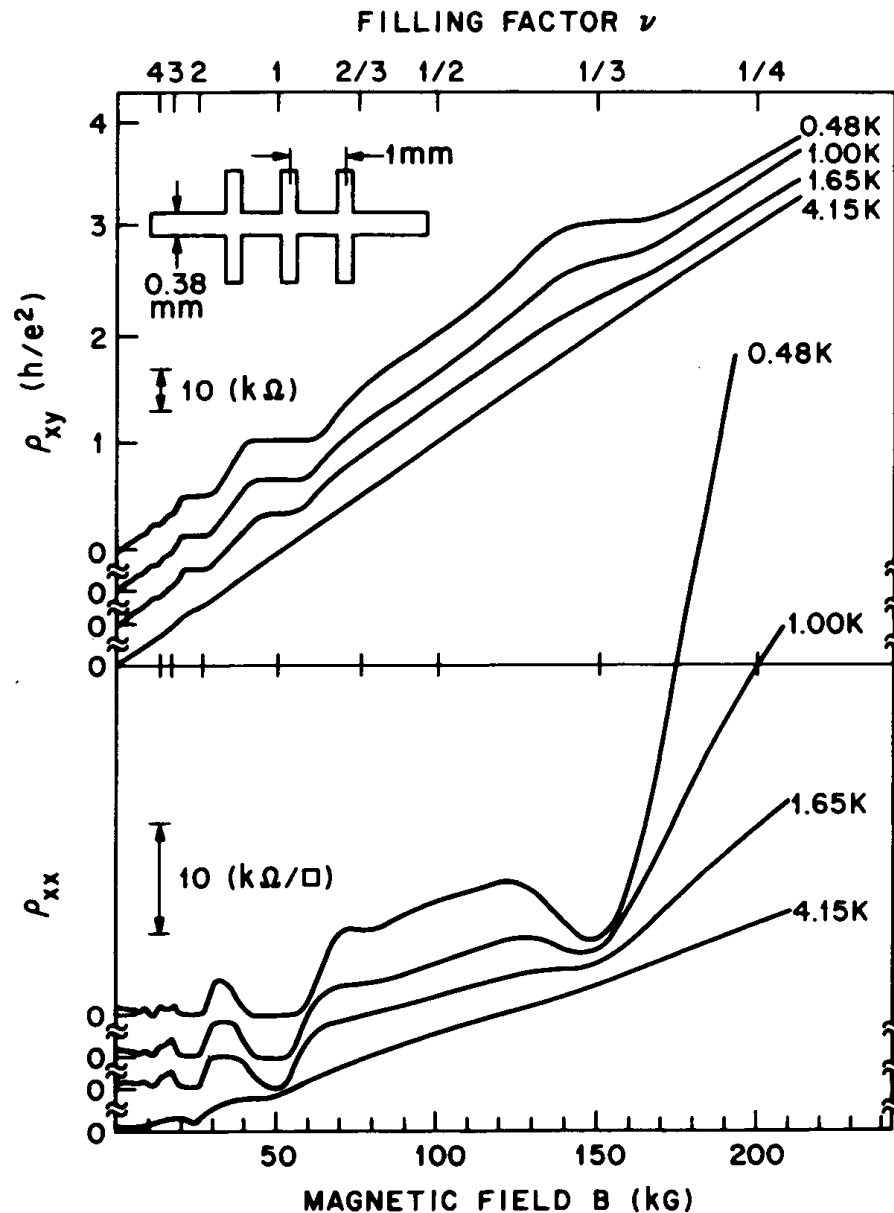


Figure 10. First publication on the FQHE. Hall resistance data (here  $\rho_{xy}$ ) and magneto-resistance data (here  $\rho_{xx}$ ) are from the same specimen as in Fig. 9. The filling factor,  $\nu$ , of the Landau level is indicated on the top. The features at  $\nu=1,2,3..$  are due to the IQHE. The features at  $\nu=1/3$  are due to the FQHE. Sample dimensions and sample temperatures are indicated.

# Stromer (FQHE)

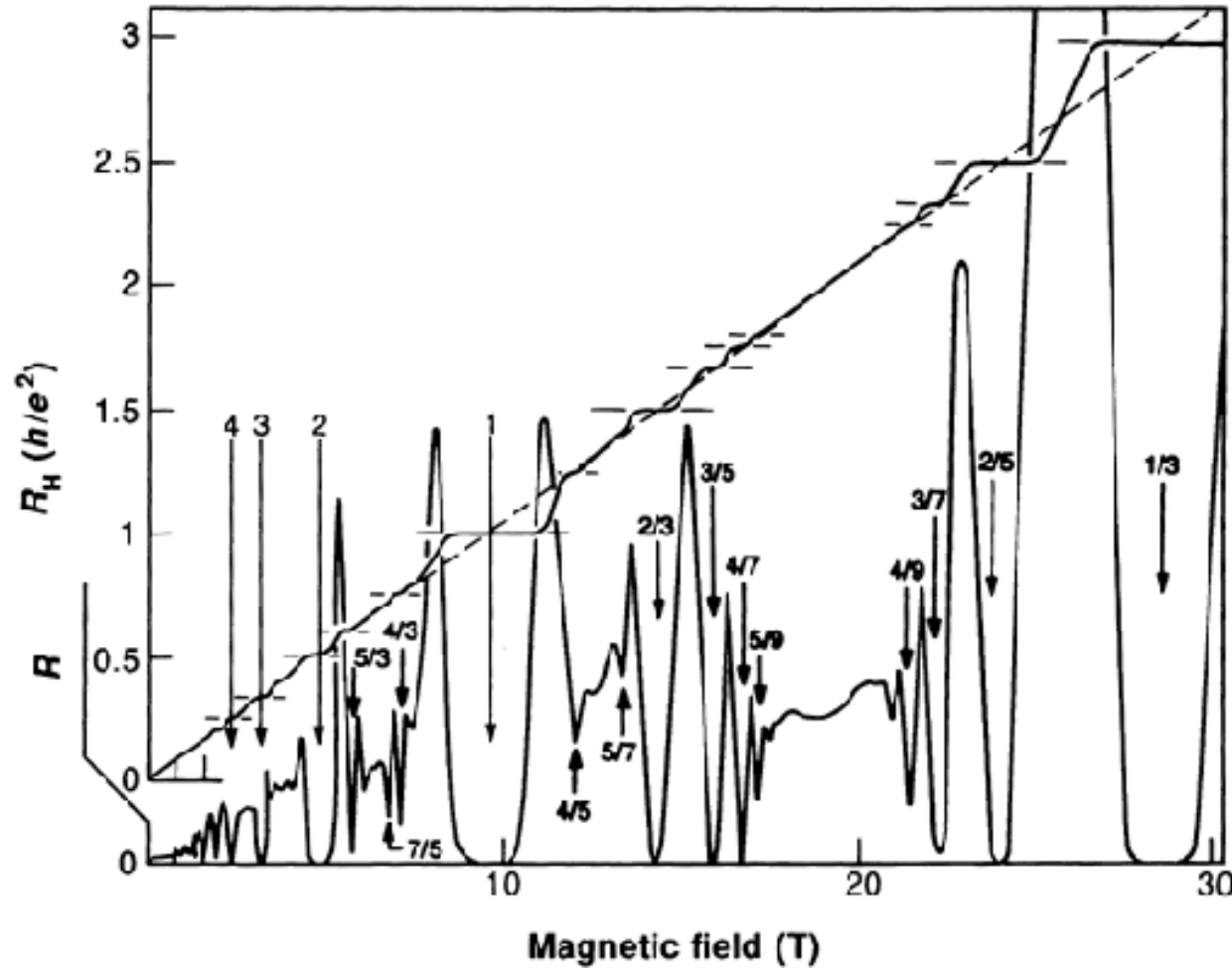
level is located in

Stromer, Nobel Lecture

# Fractional Quantum Hall Effect (FQHE)

Fractional Quantum Hall Effect (FQHE) – for 2D gas  $\nu \leq 1$ : if the Fermi level is located in localized states the Hall resistance (*opór hallowski*) is quantized

$$R_H = \frac{1}{\nu} \frac{h}{e^2}$$



# Fractional Quantum Hall Effect (FQHE)

Fractional Quantum Hall Effect (FQHE) – for 2D gas  $\nu \leq 1$ : if the Fermi level is located in localized states the Hall resistance (*opór hallowski*) is quantized

$$R_H = \frac{1}{\nu^*} \frac{h}{e^2}$$

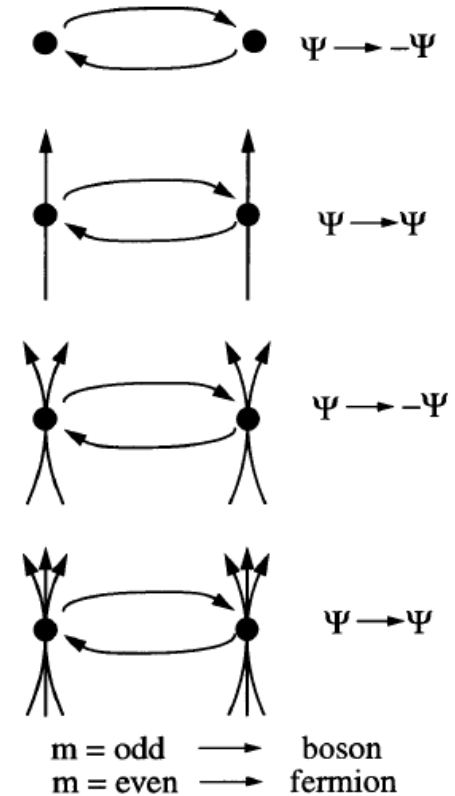
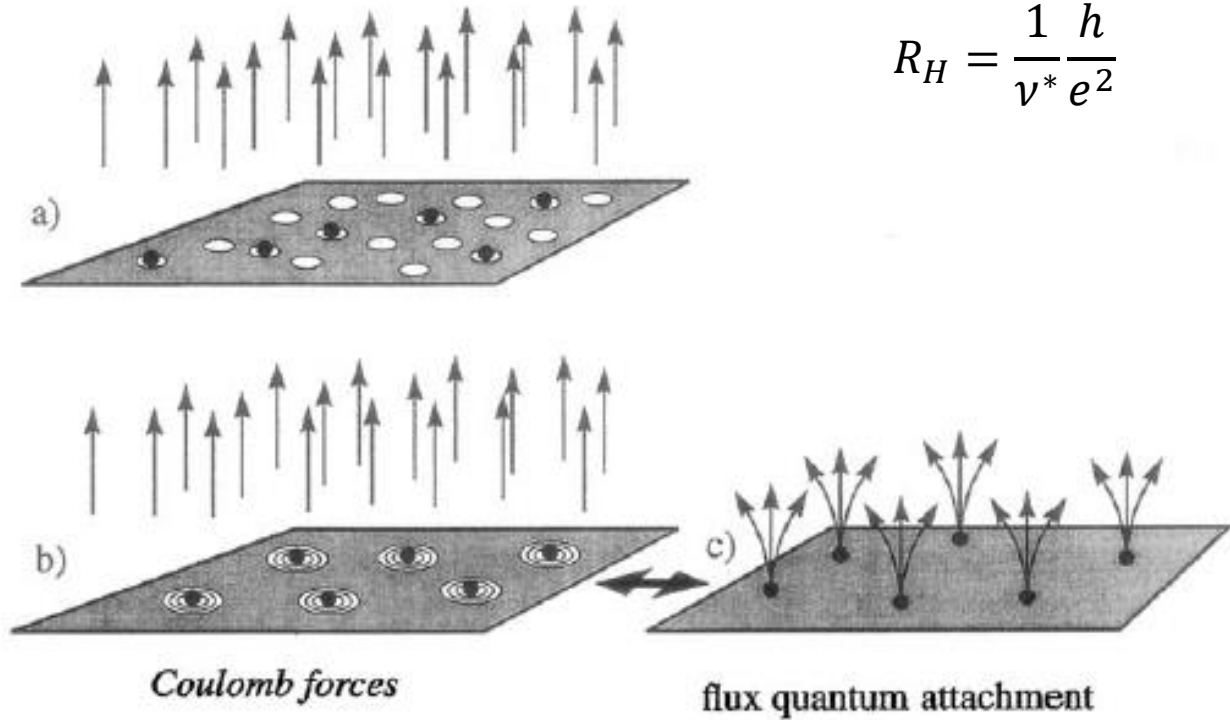


Figure 14. Schematic drawing of electron vortex attraction at fractional Landau level filling,  $\nu=1/3$ . Now there are three times as many vortices as there are electrons. The Pauli principle is satisfied by placing one vortex onto each electron (a). Placing three vortices onto each electron reduces electron-electron (Coulomb) repulsion (b). Vortex attachment can be viewed as the attachment of magnetic flux quanta to the electrons transforming them to composite particles (c).

of electrons and composite particles. Exchange of two particles affects the wavefunction  $\Psi$  which described the quantum-mechanical behavior of the system. For electrons, exchange is multiplied by  $-1$ , identifying the particles as fermions. With the attachment of an odd number of flux quanta, the wavefunction  $\Psi$  remains unchanged under exchange (multiplication by  $+1$ ), identifying the particles as bosons. Attachment of an even number of flux quanta returns the particles to fermions.

Stromer, Nobel Lecture

# Composite fermions

Fractional Quantum Hall Effect (FQHE) – composite fermions, fractionally charged quasiparticles

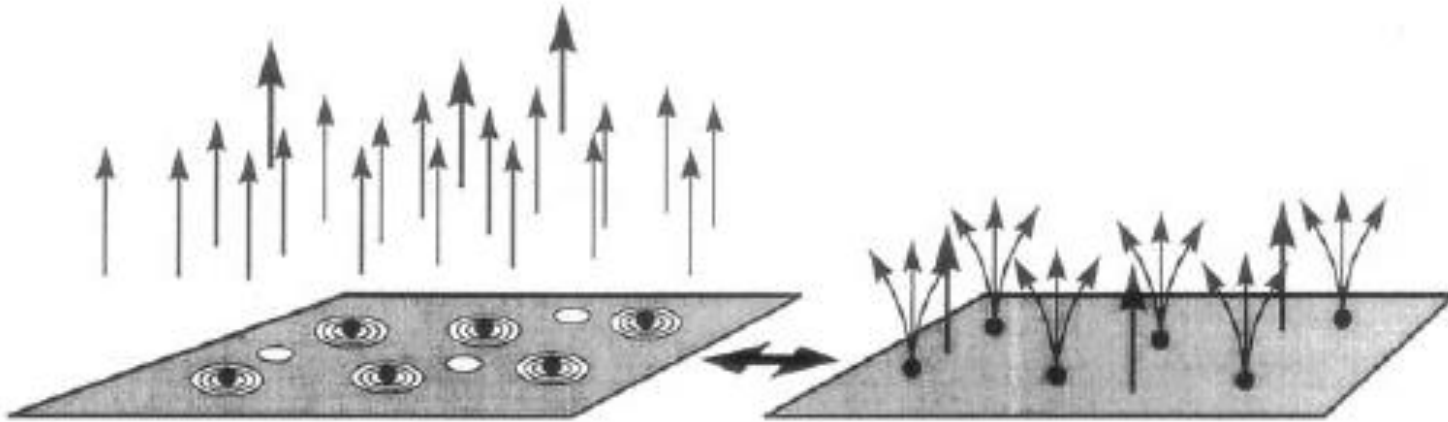
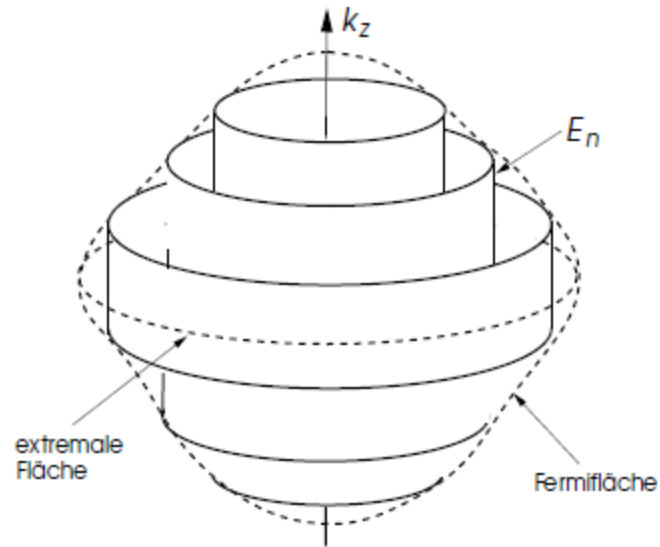


Figure 16. Schematic representation of  $1/3$  charged quasiparticles. At slightly higher B fields than at  $\nu=1/3$  additional vortices are created. They represent dimples in the electron lake. In the dimples exactly  $1/3$  of an electron charge is missing. These are the fractionally charged quasiparticles of the FQHE.

Stromer, Nobel Lecture

# De Haas – van Asphen



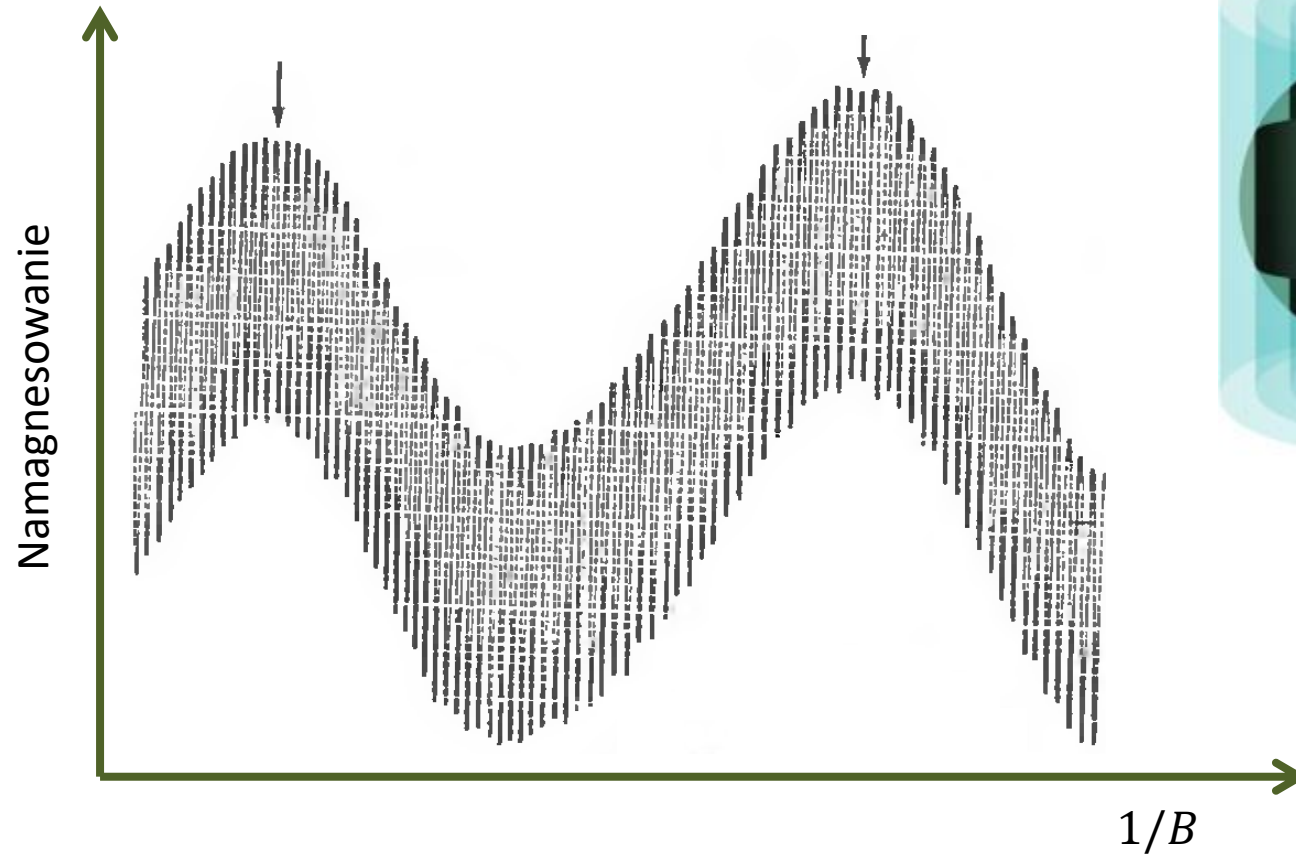
*Fig. 3.12: Tubes of quantized electronic states in a magnetic field along the  $z$ -axis. A maximum of the magnetization occurs every time a tube crosses the extremal Fermi surface area as the magnetic field is increased.*

[www.itp.phys.ethz.ch/education/lectures\\_fs10/Solid/Notes.pdf](http://www.itp.phys.ethz.ch/education/lectures_fs10/Solid/Notes.pdf)



# De Haas – van Asphen

Moment magnetyczny czystego monokryształu metalu oscyluje w zmiennym polu magnetycznym



Ashcroft, Mermin

# De Haas – van Asphen

Moment magnetyczny czystego monokryształu metalu oscyluje w zmiennym polu magnetycznym

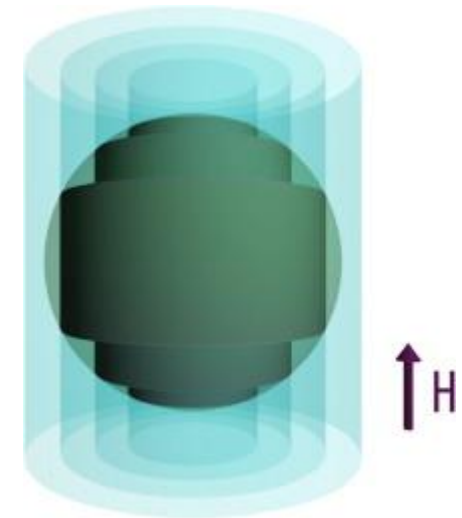
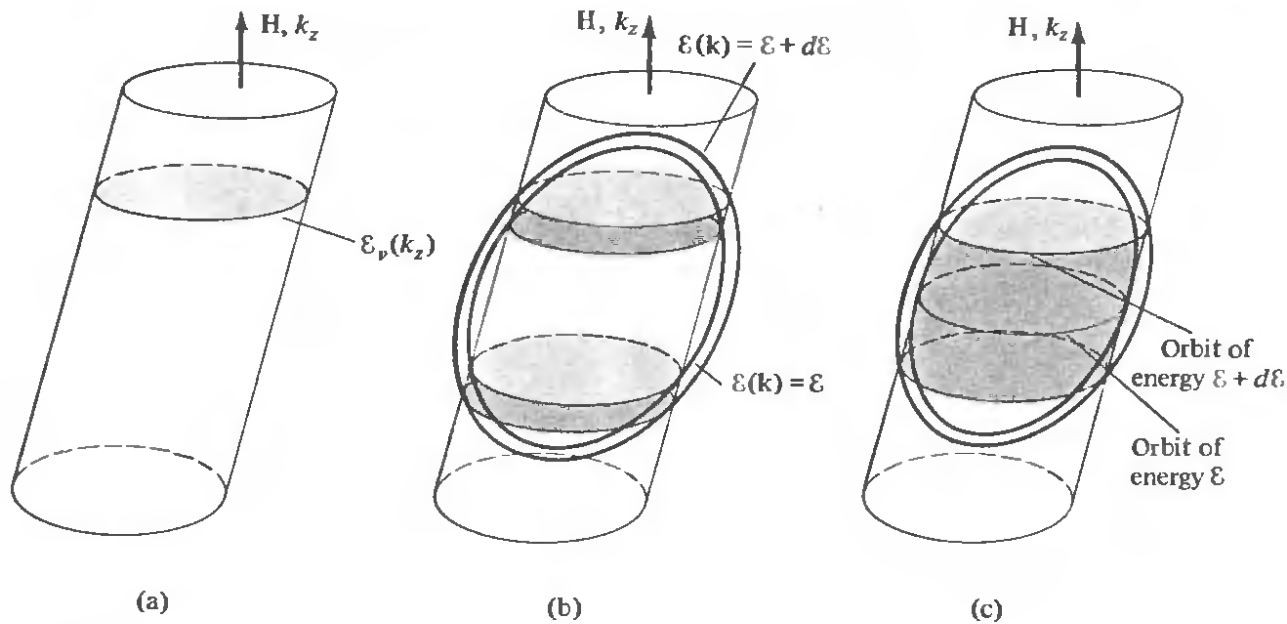


**Figure 14.5**

(a) A Landau tube. Its cross sections by planes perpendicular to  $\mathbf{H}$  have the same area— $(v + \lambda) \Delta A$  for the  $v$ th tube—and are bounded by curves of constant energy  $\epsilon_v(k_z)$  at height  $k_z$ . (b) The portion of the tube containing orbits in the energy range from  $\epsilon$  to  $\epsilon + d\epsilon$  when none of the orbits in that range occupy extremal positions on their constant-energy surfaces. (c) Same construction as in (b), except that  $\epsilon$  is now the energy of an extremal orbit. Note the great enhancement in the range of  $k_z$  for which the tube is contained between the constant-energy surfaces at  $\epsilon$  and  $\epsilon + d\epsilon$ .

Ashcroft, Mermin

# De Haas – van Asphen

**Figure 15.7**  
 Indicating only a few of the surprisingly many types of orbits an electron can pursue in  $k$ -space when a uniform magnetic field is applied to a noble metal. (Recall that the orbits are given by slicing the Fermi surface with planes perpendicular to the field.) The figure displays (a) a closed particle orbit; (b) a closed hole orbit; (c) an open orbit, which continues in the same general direction indefinitely in the repeated-zone scheme.

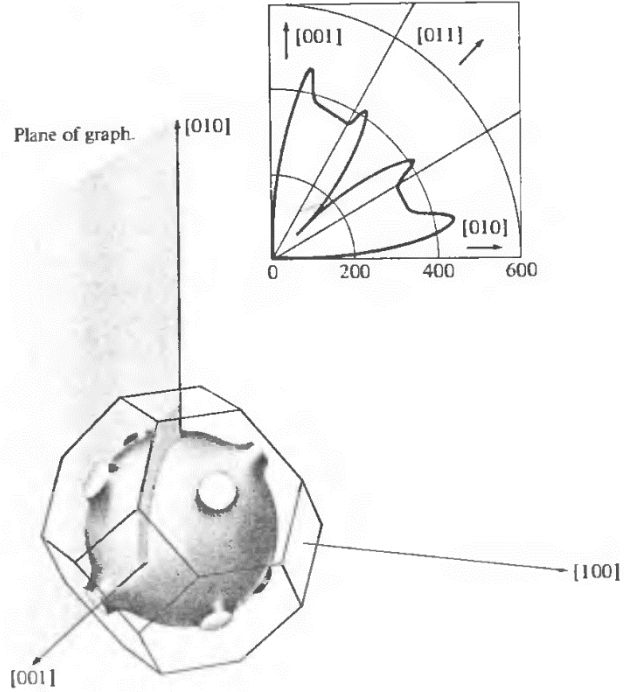
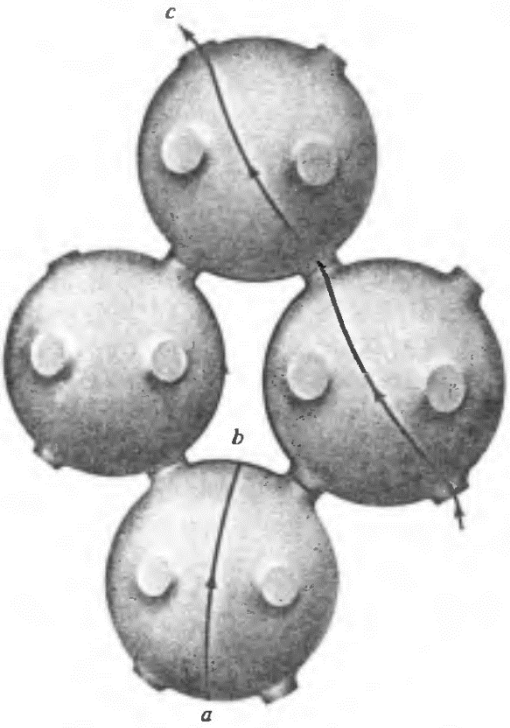


**Figure 15.8**  
 The spectacular direction dependence of the high-field magnetoresistance in copper that is characteristic of a Fermi surface supporting open orbits. The [001] and [010] directions of the copper crystal are as indicated in the figure, and the current flows in the [100] direction perpendicular to the graph. The magnetic field is in the plane of the graph. Its magnitude is fixed at 18 kilogauss, and its direction varied continuously from [001] to [010]. The graph is a polar plot of

$$\frac{\rho(H) - \rho(0)}{\rho(0)}$$

vs. orientation of the field. The sample is very pure and the temperature very low (4.2 K—the temperature of liquid helium) to insure the highest possible value for  $\omega_c\tau$ . (J. R. Klauder and J. E. Kunzler, *The Fermi Surface*, Harrison and Webb eds., Wiley, New York, 1960.)



# De Haas – van Asphen

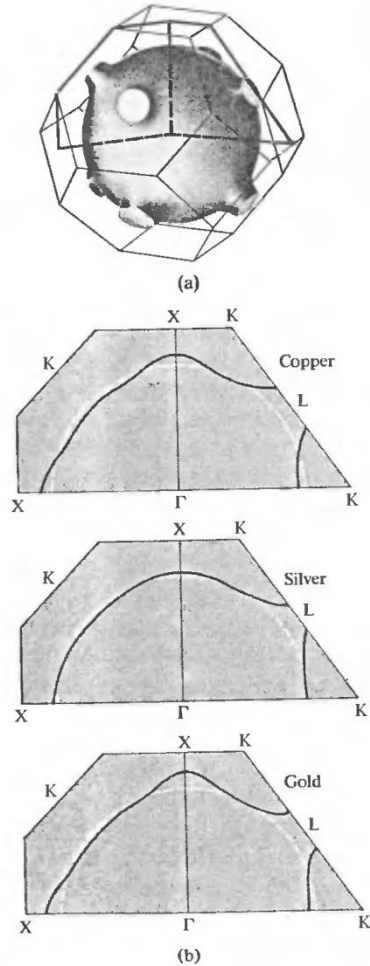


**Figure 15.5**  
 (a) In the three noble metals the free electron sphere bulges out in the  $\langle 111 \rangle$  directions to make contact with the hexagonal zone faces. (b) Detailed cross sections of the surface for the separate metals. (D. Shoenberg and D. J. Roaf, *Phil. Trans. Roy. Soc.* 255, 85 (1962).) The cross sections may be identified by a comparison with (a).

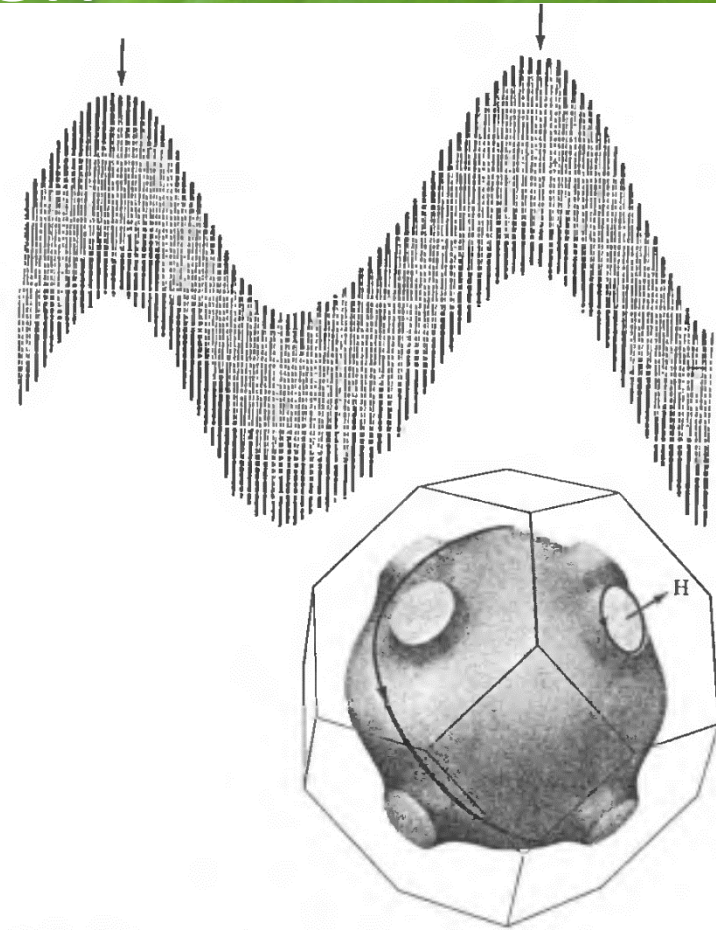


**Figure 15.6**  
 De Haas-van Alphen oscillations in silver. (Courtesy of A. S. Joseph.) The magnetic field is along a  $\langle 111 \rangle$  direction. The two distinct periods are due to the neck and belly orbits indicated in the inset, the high-frequency oscillations coming from the larger belly orbit. By merely counting the number of high-frequency periods in a single low-frequency period (i.e., between the two arrows) one deduces directly that  $A_{111}(\text{belly})/A_{111}(\text{neck}) = 51$ . (Note that it is not necessary to know either the vertical or horizontal scales of the graph to determine this fundamental piece of geometrical information!)



fot. AcidCow.com